Institute for Water
and Energy Sciences
(incl. Climate Change)

PAN-AFRICAN UNIVERSITY
INSTITUTE FOR WATER AND ENERGY SCIENCES
(including CLIMATE CHANGE)

Master Dissertation

Submitted in partial fulfillment of the requirements for the Master degree in

CLIMATE CHANGE ENGINEERING

Presented by

Jones Mayamiko PATEL

ASSESSING THE FUTURE SPATIAL-TEMPORAL CHARACTERISTICS OF METEOROLOGICAL DROUGHT IN NORTHERN MALAWI, UNDER SHARED SOCIO-ECONOMIC PATHWAY SCENARIOS

Defended on 13/04/2025 Before the Following Committee:

Chair	Bernhard Tischbein	Dr	Affiliation (Institution only)
Supervisor	Isaac Tchuwa	Dr.	Malawi University of Science and Technology
External Examiner	Antònio Bento Gonçalves	Pr	Affiliation (Institution only)
Internal Examiner	Ghenim Abderrahmane	Pr	Affiliation (Institution only)

PAN AFRICAN UNIVERSITY

Assessing The Future Spatial-Temporal Characteristics of Meteorological Drought in Northern Malawi, Under Shared Socio-Economic Pathway Scenarios

Master of Science Degree in Climate Change Engineering

Jones Mayamiko Patel

(Bachelor of Science in Meteorology and Climate Science)

Supervisor:

Dr Isaac Tchuwa

This thesis is submitted for the partial fulfillment of requirements for the Master of Science degree at the Pan African University - Institute for Water and Energy Sciences, Tlemcen, Algeria

March 2025

Approval Sheet

The undersigned approves that they have read and hereby recommend for submission to Pan African University of Water and Energy Sciences including Climate Change (PAUWES) a research thesis entitled: **Assessing the Future Spatial-Temporal Characteristics of Meteorological Drought in Northern Malawi, Under Shared Socio-Economic Pathway Scenarios**, in partial fulfilment of the requirements for the award of **Master of Science in Climate Change (Engineering Option)**.

Supervisor: Dr Isaac Tchuwa Signature:

Date: 24-03-2025

STATEMENT OF AUTHOR

By virtue of my signature below, I, **Jones Mayamiko Patel**, herewith declare that this thesis is my work. I have followed all ethical principles of scholarship in preparation, data collection, data analysis, and completion of this thesis. I have given all scholarly matter recognition through accurate citations and references. I affirm that I have cited and referenced all sources used in this document. I have made every effort to avoid plagiarism.

I submit this document in partial fulfilment of the requirements for a degree from Pan African University. I declare that I have not submitted this document to any other institution for the award of an academic degree, diploma, or certificate

Scholars may use brief quotations from this thesis or dissertation without special permission if they make an accurate and complete acknowledgment of the source. The dean of the academic unit may grant permission for extended quotations or reproduction of this document. In all other instances, however, the author must grant permission

.

Name: Jones Mayamiko Patel Signature: j.patel _______

Date: 24th March 2024

Academic Unit: Master of Science in Climate Change (Engineering Option)

Institute: Pan African University - Institute of Water and Energy Sciences (including Climate Change

ACKNOWLEDGEMENTS

I would like to thank the African Union through Pan African University Institute of Water and Energy Science (Including Climate Change) for financing my postgraduate studies. Their research grant was helpful towards the completion of this research.

Special thanks to my supervisor, Dr. Isaac Tchuwa, whose academic guidance and motivation proved vital towards the successful write-up and completion of the thesis. Your inspiration was the fuel towards transforming this dream into a reality.

To the Department of Meteorology and Climate Change Services, thank you for the meteorological data. Thank you, the National Meteorological Center team, for your help in data analysis and keeping me motivated.

My sincere gratitude extends to my friends and family for their essential support and belief during the times when I grew weary. Patricia Chisanje Patel, Patrick Patel, Kantibhai Patel, Hannah Mngoli, Christopher Padi Tuwor, Abdulai Osman Koroma, Peace Attah, Francis Okwatch, Mervis Namakhwa, Maxwell Likhule, and all friends too numerous to mention, thank you!

Abbreviations and Acronyms

ACCESS-CM	Australian Community Climate and Earth System Coupled Model
CMIP	Coupled Model Intercomparison Project
CoV	Coefficient of Variation
DMAP	Drought Mapping and Prediction Software
ENSO	El Nino Southern Oscillation
FIOESM	First Institute of Oceanography-Earth System Model
GCM	Global Circulation Model
GWP	Global Water Partnership
IDMP	Integrated Drought Management Program
INM-CM	Institute for Numerical Mathematics Coupled Model
IPCC	Intergovernmental Panel on Climate Change
Pr	Precipitation
RCP	Radiative Concentration Pathways
SDG	Sustainable Development Goals
SPEI	Standard Evapotranspiration Index
SRES	Special Report on Emissions Scenarios
SSP	Shared Socio-economic Pathways
Std	Standard Deviation
Tasmax	Maximum Temperature
Tasmin	Minimum Temperature
USAID	United States Agency for International Development
Var(S)	Variance of S
WMO	World Meteorological Organization
UNDRR	United National Disaster Risk Reduction

Table of Contents

List of Tables

List of Figures

List of Tables in the Appendix

List of Figures in the Appendix

ABTRAIT

La survenue de sécheresses majeures dans le nord du Malawi, exacerbée par le changement climatique, a causé des dommages importants aux moyens de subsistance et une dégradation de l'environnement. De plus, le changement climatique d'origine humaine souligne l'importance d'examiner comment les comportements socio-économiques peuvent influencer les caractéristiques spatio-temporelles des futures sécheresses météorologiques dans le nord du Malawi. Cette étude modélise la sécheresse future dans le nord du Malawi à l'aide de deux scénarios de trajectoires socio-économiques partagées (SSP) et de l'indice standard d'évapotranspiration des précipitations (SPEI). L'analyse des données climatiques historiques (1991-2020) et futures (2021-2080) révèle des changements dans les tendances des précipitations et des températures, avec une baisse des précipitations annuelles sous SSP2-4,5 et une augmentation sous SSP5-8,5. De plus, les températures annuelles minimales et maximales devraient augmenter de plus de 1 °C d'ici le milieu du siècle par rapport aux valeurs de 1991-2020. Les projections suggèrent une augmentation des épisodes de sécheresse extrême à court et à long terme, entraînant des impacts négatifs sur l'équilibre hydrologique de la région. Plus précisément, la durée et l'intensité des sécheresses devraient augmenter dans des zones comme Bolero et Mzuzu, tandis que certaines régions pourraient connaître une réduction de leur gravité. Cependant, les sécheresses extrêmes devraient devenir plus fréquentes à long terme, en particulier sous la SSP5 que sous la SSP2. L'étude recommande de promouvoir des stratégies de développement sobres en carbone et d'étendre les mesures d'adaptation à la sécheresse à l'échelle régionale afin d'atténuer la fréquence croissante des sécheresses.

ABSTRACT

The occurrence of major droughts in Northern Malawi, exacerbated by climate change, has caused significant damage to livelihoods, and environment degradation. Furthermore, human-induced climate change highlights the importance of examining how socio-economic behaviors may influence spatio-temporal characteristics of future meteorological droughts over Northern Malawi. This study models future drought in Northern Malawi using two shared socio-economic pathways (SSP) scenarios and the Standard Precipitation Evapotranspiration Index (SPEI). Analysis of historical (1991-2020) and future (2021-2080) climate data reveals shifts in rainfall and temperature trends with a decline in annual rainfall under SSP2-4.5 and an increase under SSP5-8.5. Moreover, annual minimum and maximum temperatures are projected to rise by more than 1°C by mid-century compared to 1991-2020 values. The projections suggest an increase in extreme drought events both in the near and far future, leading to negative impacts on the region's hydrological balance. Specifically, the drought duration and intensity are expected to increase in areas such as Bolero and Mzuzu while some regions may experience a reduction in severity. However, extreme droughts are projected to become more frequent in the far future, particularly under the SSP5 than SSP2. The study recommends promoting low carbon development strategies and upscaling of drought adaptation measures to regional level to mitigate the increasing frequency of drought.

1 INTRODUCTION

1.1 Background

Although drought is one of the major hydrometeorological hazard across the globe, its creeping nature makes its onset and cessation hard to detect and monitor (UNDRR, 2021). In recent years, as a resolution to the difficulty, drought has usually been categorized into meteorological, hydrological, agricultural, and socio-economic drought, depending on its characteristics and impacts (UNDRR, 2021; IDMP, 2022). Furthermore, to quantify drought intensity severity, and occurrence, parameters such as temperature, precipitation, and soil moisture have been used as inputs in numerous drought indices. Interestingly, temperature and precipitation have proven to be important parameters in understanding the observed characteristics of drought, especially with meteorological drought. According to WMO (2022), when precipitation is below the normal threshold that an area receives, a meteorological drought occurs. For instance, in Malawi, drought is reported when the precipitation is less than 75% of the ‘normal’ precipitation (Ministry of Natural Resources and Climate Change, 2023). The combination of reduced precipitation and increased temperature intensify the duration, magnitude, spatial extent, and severity of meteorological drought (Mtilatila, Bronstert, Bürgera, & Vormoora, 2020; Zuzani, 2019).

Changes in temperature and precipitation due to global warming, have been observed which have led to an increment in the number of drought cases over the Africa region, especially Malawi, since 1960s (World Meteorological Organization , 2021; Mtilatila, Bronstert, Bürgera, & Vormoora, 2020). For instance, the drought frequency and severity over Northern Malawi has been noted to increase under the influence of the temperature shift and rainfall decline under global warming (Likoya, Birch, Chapman, & Dougill, 2023; Dai, 2013), even though the influence tends to be exacerbated by major climate drivers such as the El-Nino Southern Oscillation (ENSO). Considering the growing concern of further global warming and its potential impacts on altering climate-related hazards, the impacts of climate change on drought have received growing attention (Salah, Mourst, Soliman, & Gamal, 2023; Collados-Lara, Gómez-Gómez, Pulido-Velazquez, & Pardo-Igúzquiza, 2022; Ayugi, et al., 2022; Gizaw & Gan, 2017). Studies reveal that future climate change alterations on the meteorological drought vary greatly, globally and locally (Price, et al., 2022; Wang, Tu, Singh, Chen, & Lun, 2021). Climate model projections reveal an increase in drought severity and intensity in some locales with a possible decrease in the far future whilst a different scenario of overall increasing severity is observed under some climate scenarios (Su, et al., 2021). This hints at varying future drought scenarios, which adds uncertainty in selection and implementation of drought risk reduction strategies.

Projections over Northern Malawi reveal an increase in drought severity and intensity under RCP global warming effect but there is a lack of consideration towards socio-economic factors (Kumwenda, et al., 2024; Lu, Carbone, & Grego, 2019; Lehner, et al., 2017; Gan, et al., 2016). For example, Kumwenda observed the increase in drought frequency in Lufilya catchment, Northern Malawi whilst focusing only on RCP4.5 and RCP8.5. Similarly, Lehner, et al (2017) observed the increment in drought risk under RCP8.5 over Northern Malawi but from a global perceptive using Community Earth System Model (CESM). Existing literature on drought across Malawi places much emphasis on historical climatic trends to observe the meteorological drought characteristics over different areas in the country such as Lake Chilwa, and Lake Malawi basin, (Chabvungma, Mawenda, & Kambauwa, 2014; Chitedze & Chikabvumbwa, 2021). They concluded that decreasing rainfall and increasing temperature are causing the drought duration and intensity over Malawi to increase, reducing the drought frequency but the change is not homogenous. However, there is no consideration towards predicting future drought occurrence over the Northern Malawi.

Although Global Circulation Models (GCMs) project severe drought cases across the southern Africa region, the shifts in drought in response to future climate change over Malawi are less understood (IPCC, 2023b). Studies have looked at drought changes in relation to Representative concentration pathways using GCMs (Spinoni, et al., 2020; Lehner, et al., 2017) but the coarse spatial resolution of Global Circulation Models(>250km) fails to capture the impacts of climate change on drought that are occurring at local scale(<100km). Although downscaling techniques have been applied to reduce this bias (Naik & J., 2020), the utilisation of re-analysis data as opposed to ground station data introduces additional spatial biases in results. Regional scale consideration of climate change over Northern Malawi have focused on Representative Concentration pathways without highlighting the effects of socio-economic shifts on meteorological drought. Even though, analysis of the characteristics of future hydro-meteorological drought conditions using bias-corrected Global Circulation Models and Regional Climate Models has been conducted over different areas of Malawi (Chikabvumbwa, et al., 2024), no comprehensive analysis of the impacts of climate change on the spatial characteristics of drought over Northern Malawi under socio-economic scenarios-climate projections has been conducted. Thus, this research seeks to provide insight the changes in drought conditions over the Northern region of Malawi in relation to the climate projections under the socio-economic pathways as undertaking drought projections at a local level is crucial for implementation of sufficient disaster risk management strategies (Dione, Faye, & Sadio, 2023).

1.2 Problem statement

Malawi, being a developing country, is highly dependent on the agricultural sector for 29% of its Gross Domestic Product, and 80% of the population's livelihood is related to farming (GFDRR, 2019). Northern Malawi is highly dependent on rainfed agricultural production making the area particularly vulnerable to the consequences of meteorological drought such as reduced effective rainfall and reduced groundwater. The impacts are observable in the reduction of agricultural yields which increases the risk of famine and hunger in the area and creates a hinderance towards achieving the Sustainable Development Goals (SDG) 2030 such as SDG 2(zero hunger). Furthermore, farming is the major source of income for over 70% of households as many practice subsidence farming via rice, cassava and maize cultivation or commercial farming of tobacco. Increasing cases of erratic rainfall, temperature changes and drought have impacted this livelihood negatively. According to Kamanga *et al* (2020), there is high susceptibility and exposure to drought in Northern Malawi that contributes to increased drought risk to its various sectors, especially agriculture. Recently, droughts have become more frequent during the 21st century with 3 major droughts been recorded between 2005-2016 that led to major losses in livelihood across the region. Additionally, longer dry-spells during the start and middle of the 2013-17 rainy seasons led to moderate-severe drought across Rumphi and Chitipa that heavily impacted food security as agricultural yields have seen reduction.

With the recent changes in precipitation and temperature across the region being attributed as the causal factors for the changing occurrence and impacts of drought, there is a need to understand their plausible future direction and magnitude of change to understand upcoming drought conditions. Moreover, human socio-economic actions have been highlighted as the driving force for ongoing climate change, leading to uncertainty in future climate conditions as these actions are not homogeneous. Inadequate understanding of the changes in drought characteristics combined with the uncertainty of future climate creates a hurdle in disaster risk management and planning and sustainable development of the community, thus needing closer scrutiny. Although studies at country and local level portray increasing drought frequency, less studies have been done with particular focus on drought and climate change over Northern Malawi with no studies present that account for socio-economic pathway in future drought projections even though the region contains areas such as Chitipa and Karonga that are highly susceptible and vulnerable to hydro-meteorological hazards including meteorological drought. Shared Socio-economic Pathways (SSPs) have been assessed to better quantify the impact of human actions on the climatic system leading to robust climate projections (Su, et al., 2021). This robustness helps in reducing inadequate adaptation and maladaptation towards climatic extremes such as drought as it improves disaster risk planning process. Likewise, Tamura, et al (2019) demonstrates that the choice of SSPs scenario for development and adaptation strategies can reduce the economic damages and population losses driven by climate change Thus, necessitates the need for a robust future meteorological drought hazard identification over Northern Malawi for proper drought risk planning strategies to be undertaken and implemented.

1.3 Objectives

The main objective is to assess the future drought characteristics of Northern Malawi under SSP scenarios.

i. Analyze the rainfall and temperature trends of Northern Malawi from 1991-2020.
ii. Model the spatio-temporal characteristics of drought in Northern Malawi through climate scenario- drought modelling.
iii. Contrast future drought characteristics against historical drought.

1.4 Research Questions

Questions:

i. What are the rainfall and temperature trends for Northern Malawi from 1991-2020?
ii. Based on simulations, what are the future meteorological drought conditions under various SSPs?
iii. How do the future spatio-temporal characteristics of meteorological drought over the area differ from observed cases?
iv. What is the effectiveness of the current strategies enough towards reducing the possible impacts?

1.5 Justification of study

This study will help in advancing scientific knowledge in the growing sector of climate change impacts on meteorological extremes and provide valuable information for future drought studies in Northern Malawi and the world. The findings from this study can also be used by policymakers to prepare sustainable drought risk management strategies. The spatial extent and temporal characteristics of drought can help local communities and the world in assessing drought exposure and allow them to adequately reduce future drought risk as generalized strategies sometimes lead to wasted resources or inadequate preparedness due to the impacts of drought not being homogenous on a temporal and spatial scale. Secondly, hazard identification is an integral part of disaster risk assessment as it influences the degree of preparation and mitigation strategies are implemented. Even though drought, and climate studies have been conducted across the region (Kumwenda, et al., 2024; Demissie & Gebrechorkos, 2024; Gama, et al., 2014), there is a lack of knowledge on how climate change is influencing hazards resulting in less ineffective disaster risk mitigation and adaptation strategies, a gap which this study seeks to address. Closing this gap effectively reduces the cases of maladaptation and coping strategies that occur due to lack of knowledge on drought severity and intensity, which diminishes the development process. Understanding meteorological drought also indirectly benefits the agricultural and hydrological sectors as they are highly reliant on precipitation and thus, inform their strategies on achieving goals 2 and 6 of the 2030 Sustainable Development Goals.

1.6 Limitations of the study

The study is limited by the lack of evaporation data over the area and thus, assumptions were made using other climatic information. This combined with time limitation led to the study only focusing on meteorological drought, precipitation and temperature whilst assuming stationarity in their relationship. Meanwhile, the distribution of stations in the area varies with elevation and may introduce biases when looking at spatial characteristics due to their sparseness. This sparse distribution of ground weather stations in the study area led to assumptions towards spatial heterogeneity of drought and climate. Additionally, the study does not focus on the changes in other factors that might have an effect on drought such as land use, land cover change, water management and urbanization. There were some data gaps where estimation was conducted using statistical methods. Inaccessibility of daily values restricted the choice and selection of temporal and spatial techniques utilized in the study.

2 LITERATURE REVIEW

This chapter seeks to present insight into the existing literature in the field of drought and climate change as this help provides an emphasis on existing gaps and how this study seeks to close them. The chapter delves into the key concepts in drought, such as categorization, computation methods and characterization theory of foci. It also looks into the existing research in climate change, its relation to drought shifts, and climate and drought modelling, especially under differing socio-economic factors. The present gaps in studies in drought and climate change over the Northern Malawi are also highlighted.

2.1 Concepts of drought

2.1.1 Drought

There is a lack of a universally agreed term for drought due to the different onset, duration, triggers and impacts of drought. In the meteorological field, the World Meteorological Organization (WMO) defines drought as the occurrence of below-normal precipitation that is accompanied by a period of uncharacteristically dry weather that results in results in a hydrological imbalance (WMO, 2023). Wang *et al* (2021) report that such definition of drought is lacking when analyzing from a spatial-temporal scale as drought can also be triggered by shifts in the normal precipitation intensity and frequency of a region. Thus, the sum of days with precipitation within a given threshold, and certain concentration are key to drought process definition and quantification (Wang, Zhang, Wang, Liu, & Zhang, 2021).

However, the National Drought Mitigation Center (USA) emphasizes that such a definition is best applicable to humid regions, which tend to have precipitation throughout the year, and inapplicable to climatic regions that experience seasonal rainfall such as the tropics, due to the influence of seasonality on the region's water balance (National Drought Mitigation Center, n.d.). Likewise, IDMP (2022) places emphasis on the temporary nature of drought and warns of possible confusions of the term with water scarcity and aridity that occur due to normal climatic conditions and/or human interactions with the natural environment. Drought is, therefore, regional and climate specific with underlying topography of regions also influencing the definition of drought. This study utilizes the definition devised by the Department of Climate Change and Meteorological Services that defines drought as the occurrence of total precipitation below a given threshold (Chabvungma, Mawenda, & Kambauwa, 2014).

Based upon the impacts of drought on the environment and/or society, WMO (2023), IDMP (2022) and UNDRR (2015) categorized drought into four main classes, namely:

- Meteorological drought: occurrence of rainfall below the normal range for the given climatic zone.
- Hydrological drought: lower water table levels and decrease in streamflow in rivers and lakes resulting from changes in water recharge levels.
- Agricultural drought: presence of inadequate soil moisture and water availability to facilitate vegetation growth and animal husbandry.
- Socio-economic drought: the lack of water to meet the need of social and economic activities of a society leading to shortfalls in goods and service provision.

Meteorological drought precedes the occurrence of the other droughts as reduced rainfall affects the hydrological balance of a watershed/ given area causing the drought to propagate into the agricultural and/or hydrological droughts (IDMP, 2022; Caretta, et al., 2022). Mtilatila *et al* (2020) reported that meteorological and hydrological drought show a strong correlation when meteorological drought is observed at a higher timescale than hydrological drought. The occurrence and duration of meteorological, agricultural, and hydrological droughts can lead into socio-economic drought as resources availability is negatively impacted (WMO, 2023).

2.1.2 Drought indices and indicators

Whilst identifying and quantifying drought can be challenging and confusing due to its nature, scholars have developed different methods to identify drought but also describe its features (WMO & Global Water Partnership(GWP), 2016). This is achieved through using various variables such as temperature, vegetative cover, streamflow, precipitation as drought indicators. Drought indicators are assessed and computed into mathematical descriptions of drought severity using drought indices, which provides the qualitative nature of drought over any given location. The indices can range from physical data models such as SPI, to remote sensing techniques such as Vegetative Drought Response Index. In meteorological drought, indices that use precipitation as the only indicator, such as Standard Precipitation Index (SPI) and Percent of Normal Index (PN), have been utilized to calculate the meteorological drought properties in various areas (Onyeuwaoma, Sivakumar, & Bade, 2024; Kubiak-Wójcicka, Owczarek, Chlost, Olszewska, & Nagy, 2023). Single and multiple parameter drought indices have also been used to observe the spatial and temporal changes of meteorological drought (Choudhury, Dutta, Bera, & Kundu, 2021). Most multiple-parameter indices are usually overly complex, require high computing power and data than single-parameter drought indices. Nonetheless, (Ukkola, Kauwe, Roderick, Abramowitz, & Pitman, 2020) argues that multiple parameter drought indicators perform better in characterizing meteorological drought than single variables, and that the inclusion of temperature and evapotranspiration provides more robust results.

2.1.3 Drought characterization

The run theory is the frequently used concept when characterizing drought using the drought indices (Choudhury, Dutta, Bera, & Kundu, 2021). According to the run theory, every drought event has a definite starting point and cessation point based upon a preset threshold of severity (Figure 2.1). Thus, each drought has a duration, which is usually referred to in terms of months. Drought severity is measured by how much the indices' values have departed from the normal conditions whilst drought intensity is the average severity for a given drought duration (Muthiah, Sivarajan, Madasamy, Natarajan, & Ayyavoo, 2024). In the study by (Kumalioglu, 2020) using runtime theory with drought indices, they considered negative runs to be the negative values of the meteorological indices SPI and SPEI as they symbolize the dry periods. The lower the values of a particular dry period, the higher the severity of the drought and the cessation point was where a positive value occurred. Similarly, (Salimi, Asadi, & Darbandi, 2021; Hadri, et al., 2024) used a similar principle in accessing for meteorological drought conditions over Iran and Morocco, respectively. They classified drought into three classes based on dryness, namely, moderate, severe and extreme based on the distance of the value from the threshold.

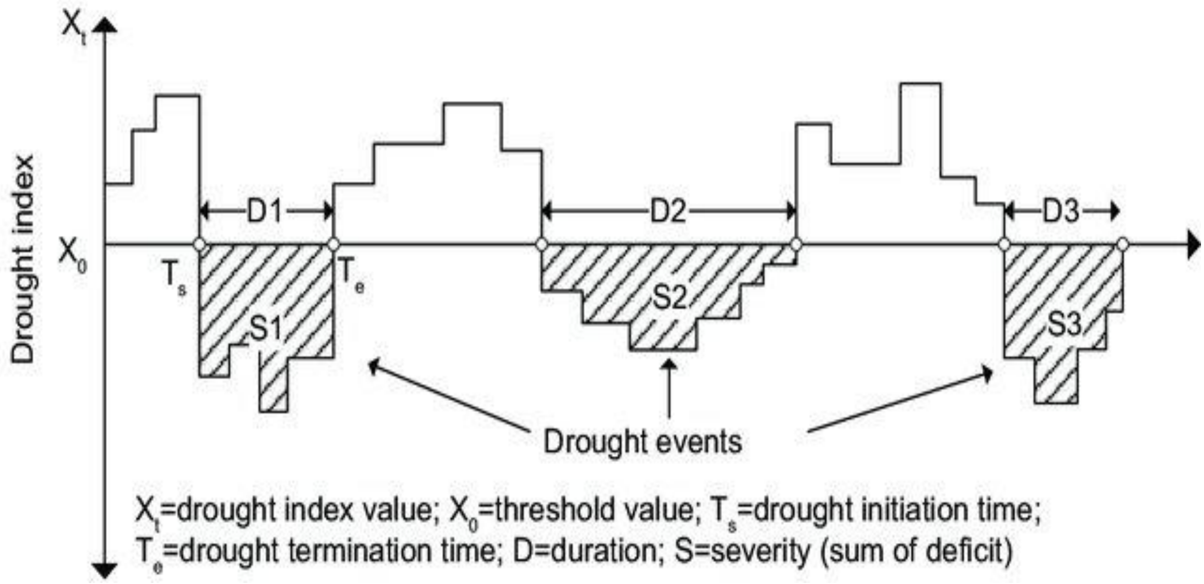

Figure 2.1: Drought identification under run theory.

However, (Wang, Zhang, Wang, Salahou, & Fang, 2020) highlights that not every dry period leads to drought especially in regions of uneven and variable rainfall and thus, considers a certain threshold of dry values under SPI to be normal conditions. Hence, the choice of threshold becomes pivotal to reducing analysis bias due to the climatic tendency of the locale. Different from the three-threshold method applied by (Huang, et al., 2024) to reject dry periods that are non-drought months, this study utilizes a two-threshold approach whereby the first threshold(0) denotes a dry episode whilst the second threshold(-1) denotes a drought occurrence. Furthermore, the study seeks to utilize drought frequency as the number of observable drought events under a monthly timescale as opposed by yearly. In addition, the timeframe for observed and projected drought events is split evenly to reduce temporal biases on shifts in drought duration, intensity and frequency.

2.2 Climate change and drought overview in Africa

Globally, there has been an observed increasing trend in the damages and costs associated with drought. Between 1970-2019, even though drought accounted for 6% of occurring disasters, it caused a third of disaster related deaths and $20 billion in economic losses (World Meteorological Organization , 2021). Furthermore, drought tends to have adverse effects on the availability of food and water resources, leading to negative impacts on Africa’s food security (Lombe, Carvalho, & Rosa-Santos, 2024). In an effort to understand the underlying causes of drought, Henchiri *et al* (2021) analyzed the interlinkage between meteorological drought and the climate drivers over North and East Africa. They concluded that drought severity and intensity shifted in response to changes in climate due to large-scale atmospheric circulation such as El Nino Southern Oscillation (ENSO) and the North Atlantic Oscillation (NAO). Indeed, ENSO does have an effect on meteorological drought, as it suppresses and/or enhances rainfall leading to spatiotemporal variations in monthly rainfall across Africa (Hoell, Gaughan, Magadzire, & Harrison, 2021; Gizaw & Gan, 2017). Although climatic drivers cause such climate variability, Trisos *et al* (2022) concluded that ongoing long-term shifts in climate have been induced by human actions. This anthropogenic influence on climate is due to the ongoing increase in greenhouse gas (GHG) emissions associated with industrial development and urbanization.

Even though Africa is responsible for around 3-5% of the global GHG emissions, making it one of the lowest emitters, it is inversely one of the most impacted regions by climate change (Trisos, et al., 2022). Bedair *et al* (2023) investigated the future magnitude and direction of climate change over Africa and found that there was irregularity in the changes on a spatial scale, particularly in reference to precipitation. It was observed that some countries would experience a decline in precipitation whilst other areas were projected to have greater than 25% increment in annual precipitation. In addition, shifts in evapotranspiration are causing changes in Africa's climate water balance, a phenomenon which is projected to continue as temperature continues to rise and are estimated to increase by more than 2°C by 2040 if the greenhouse gases emissions are left unchecked (Bedair, et al., 2023). A similar conclusion was reached in an analysis of temperature and rainfall projections over Africa under Shared Socio-economic pathways by (Almazroui, et al., 2020) but the study only focused on boreal winter and summer seasons. Likewise, (Umwali, et al., 2024) used gridded data and globally downscaled CMIP6 models and found that May-April-May rainfall will decrease in the near-term but increases as the end of the century approaches during the rainy season over East Africa. However, the lack of ground observation data and consideration of a singular particular season fails to highlight the overall monthly shifts in rainfall and temperature due to global warming trends.

2.3 Impacts of climate change on meteorological drought

Changes in climate have been observed to have varying impacts on the occurring meteorological drought. This section gives a little insight into the varying relationship between climate variables such as temperature and precipitation, with meteorological drought, and how their changes are influencing its characteristics.

2.3.1 Changes in intensity and severity

Investigations have been conducted to understand the role precipitation characteristics such as precipitation distribution, intensity and volume plays in influencing observed meteorological drought conditions with varying impacts. For instance, Wang *et al* (2021) investigated the influence of precipitation intensity on drought intensity in China and found that decrement of precipitation intensity causes higher drought intensity. In their findings, they also suggested that cumulative precipitation plays a major role in influencing the drought intensity values as wet autumn precipitation-drought intensity correlation values were lower than for dry winter months. Under the theme of accumulative precipitation, Onyeuwaoma *et al* (2024) modelled the meteorological drought of 4 selected areas in South Africa using 3-months, and 6-months standard precipitation index (SPI). They found that during 2000-2021, Cape town experienced higher drought severity than the other zones even though it received more rainfall (Onyeuwaoma, Sivakumar, & Bade, 2024). They underscored that there must be other factors at play in the relationship between climate and meteorological drought. Interestingly, Behrangi *et al* (2015) argued that precipitation alone cannot be the factor responsible for the shifting drought conditions, and other climatic variable such as temperature, also play a role. The level of temperature rise with global warming has been noted to influence the drought severity with projections revealing that 0.5°C increase in drought-prone zones above the 1.5°C baseline would lead to a 30% increment in the observed cases of extreme drought especially in the tropical region (Kamal, Hossain, & Shahid, 2021).

2.3.2 Deviations in duration and frequency

A study by (Gizaw & Gan, 2017) investigated the changes in drought frequency over Africa in response to future climatic scenarios and found that 6–12-month drought will on average occur 5% in the mid and late twenty-first century as the climate gets drier. They argued that the increase in occurrence of extreme precipitation events might reduce long-term drought duration leading to shorter timespans of drought events greater than 12 months. Remarkably, a recent study in India revealed that the future climatic conditions portray a higher increase in occurrence of long-term drought events (≥6-month timescale) as compared to short term drought events (Samantaray, Ramadas, & Panda, 2020). However, a study by Collados-Lara *et al* (2022) assessed changes in drought using Regional Climate Models(RCMs) and found that 31.6%-44% decrease in average precipitation combined with a mean 29.1% increase in mean temperature leads to an average of 200% and 400% increase in extreme drought duration and frequency. But the study did not assess the changes in length and occurrence of moderate and severe droughts.

2.3.3 Shifts in spatial extent

The range of drought and the location of predominant drought occurrence has been found to shift with ongoing climate change. Kamal *et al* (2021) projected using Coupled Model Intercomparison Project 6 (CMIP-6) models that under the same temperature shifts of 1.5°C and 2°C, drought-prone locations within the tropics are shifting from regions of mainly low rainfall to regions of high humidity and rainfall as drought occurrence reduces in the low rainfall regions due to an increase in the precipitation over those areas. Similarly, Samantaray *et al* (2020) investigated the effects of potential precipitation change over tropical Eastern India's meteorological drought using SPI, k-means clustering and bivariate copula. They found that compared to 1971-2003, severe drought hotspots will shift from scattered across the whole Eastern India to being heavily situated in the eastern side. The study, however, failed to quantify the influence of precipitation and temperature shift on the drought.

Oguntundea *et al* (2017) observed that looking at mid-late 21st century drought coverage from a precipitation perceptive against a temperature and precipitation change yields varying results. They found that under the former, the drought area decreases as precipitation increases whilst in the latter, changes in evapotranspiration due to temperature rise lead to an increase in drought extent. Remarkably, Yang *et al* (2023) assessed the magnitude of the climatic forces that drive meteorological drought over North China plain, finding that precipitation and temperature have the strongest influence on drought. During 1970-2020, precipitation (1.57%-2.69%) had the strongest influence on drought throughout the year, only being second to temperature (-3.64%) during the winter period. Whilst warming temperatures and decreasing precipitation increase drought occurrence, and alter spatial distribution of drought, the impacts are exacerbated by altitude differences within the regions (Yang, Liu, Wang, Gu, & Ma, 2023).

2.4 Drought and Climate Modelling

With meteorological drought indicators utilizing climatic parameters and recent development of climatic models leading to growing interest in climate change, there has been shift from merely understanding meteorological drought properties to using climate models to predict and quantify meteorological drought and climate change interactions (Ngwenya & Simatele, 2024; Sreeparvathy & Srinivas, 2022). Climate models are mathematical descriptions of the climate system based on the biological, chemical, and physical properties of its components and their interconnections (IPCC, 2022). The atmosphere, hydrosphere, biosphere, lithosphere and cryosphere are key elements of the climate system, with their interactions and feedback processes influencing the climatic conditions of any given location. Ngwenya & Simatele (2024) sucessfully modelled the meteorological drought over South Africa using Global Circulation Models(GCMs). Correspondingly, Sreeparvathy & Srinivas (2022) also used GCMs to model and project meteorological drought over India. However, GCMs have large grid sizes leading to low spatial resolution which can induce biases in their representations of mesoscale-microscale climate. According to Hellwig *et al* (2018) investigation of spatial resolution and precipitation bias, the bigger the size of the grid, the higher the bias in representing areal precipitation as the resolution decreases. Their study focused on biases of using gridded meteorological data for drought research.

En-Nagre et al (2024) also modelled and predicted the meteorological drought over Morocco using climate prediction with machine learning algorithms. However, climate prediction assumes stationarity in the parameters and feedback processes that can influence climate such as land-use and socio-environmental factors. Modelling shifts in spatio-temporal shifts in socio-economic and environmental factors such as population growth, deforestation and rapid urbanization have been identified to affect the rate of change in climate conditions (Ebedi-Nding, Tamoffo, & Mouassom, 2024). Similarly, studies into human-induced landscape change impacts on temperature have found that loss of vegetation leads to increased air temperature, evapotranspiration and affects precipitation leading to changes in drought conditions (Li, et al., 2024; Zhang & Zhou, 2021). Interestingly, these investigations have been vital towards guiding future meteorological drought studies from focusing solely on predictions to utilizing climate scenarios. This is because climate scenarios differ from climate predictions as they consider changes in human activities as a driving force for possible changes in climate.

Various scenarios have been developed that have been used project plausible climate conditions, such as Representative Concentration Pathways (RCPs), Shared Socio-economic Pathways (SSPs) and Special Report of Emissions Scenarios (SRES). Newly developed SSPs capture the anthropogenic forcing of climate, and link that to the considerations of adaptation and mitigation strategies implemented more robustly than previous climate scenarios such as RCPs (Lee, et al., 2021).The SSPs consist of five pathways, namely:

i. SSP1: human development focusing on sustainable development with rapid economic growth, and investment in education and health.
ii. SSP2: a center of the road scenario with moderate challenges to both mitigation and adaptation strategies.
iii. SSP3: a regional security foci scenario with little investment in education and health, and equality whilst the population grows rapidly.
iv. SSP4: similar to SSP3 but with inequalities being dominant both inside and across the country.
v. SSP5: human development focusing on rapid economic development, investment in health and education but with a focus on fossil fuel- energy intensive economy.

These pathways have been linked to different radiative forcing levels (W/m^2), resulting in the formulation of SSP1-1.9, SSP1-2.6, SSP4-3.4, SSP5-3.4OS, SSP2-4.5, SSP4-6.0, SSP3-7.0, and SSP5-8.5, wherein the suffix is the radiative level (IPCC, 2023a; O'Neill, et al., 2016).

2.5 Existing meteorological drought and climate change studies

The impacts of climate change on future meteorological drought have been analyzed using various global circulation models and regional climate models to simulate changes in drought characteristics. This section aims to highlight the context of these studies, and their arguments, findings and methodologies. According to scholars (Sidiqi, Kasiviswanathan, Scheytt, & Devaraj, 2023; Mehr, Sorman, Kahya, & Afshar, 2020; Price, et al., 2022), observed and future climate change has increased the number of recorded meteorological drought events in the last 50 years and is projected to double in duration and severity by the end of the century.

Spinoni *et al* (2020) utilized sixteen global circulation models and twenty regional circulation models to examine the future spatio-temporal characteristics of extreme drought in relation to the changes in temperature and precipitation under RCP8.5 and RCP 4.5 scenarios to discover future global meteorological drought hotspots. The research is interesting as it provides a comprehensive overview of the influence of spatial resolution when using regional circulation models and global circulation models for drought analysis. They found that the global temperature rise of 2.6°C-4.8°C, and precipitation decline by 2071-2100 would lead to half of Sub-Sahara Africa, the Mediterranean and central Asia regions experiencing a significant increase in extreme drought events with drought frequency and severity than 1981-2010. Though, regions in the northern hemisphere such as Northeast Asia and Canada would experience a decline in such drought characteristics due to the 10% increase in precipitation (Spinoni, et al., 2020).

Using delta downscaling and thirty-nine climate models, Zhang *et al* (2023) investigated the alterations in the spatio-temporal characteristics of drought under different timescales over Yellow River Basin, China, in relation to four different Shared Socio-economic Pathway scenarios (SSP), taking 1901-2014 and 2022-2100 as historical and future periods, respectively. They reported that the time of occurrence of the most severe drought is dependent upon the climate scenario, as severe droughts were highest in 2060s, 2087, 2023, and 2040s, 2064 and 2080s under SSP1-2.6, SSP2-4.5, SSP3-7.0, and SSP5-8.5, respectively. Arguing that the climate change impacts under SSP5-8.5 and SSP3-7.0 result in severe droughts occurring sooner and for longer durations. Meteorological drought severity over the area would decrease across all timescales and scenarios except for the timescales of SSP1-2.6 across the middle region of the basin, although there was increased probability of droughts of weak severity, and low duration and intensity under SSP2-4.5 and SSP 8.5. However, the northern and central-western regions of the basin are projected to experience an increase in drought severity and duration.

In the Middle East, Behzadi *et al* (2022) assessment of 2022-2100 future meteorological drought over Iran using from the Coupled Model Intercomparison Project 6(CMIP-6) and two scenarios (SSP1-2.6 and SSP5-8.5) in comparison to 1990-2018, found that Iran will experience a significant increase in drought duration of 5-30 months under SSP5-8.5 with a 20-year severe drought occurring in south Iran from 2080-2100. Intriguingly, the study highlighted the importance of inclusion of temperature in drought analysis because utilizing only precipitation (SPI) led to projection of the most severe drought occurring within 2022-2032 instead over the same region, neglecting the influence of higher future evapotranspiration, projected to occur during 2051-2100, on meteorological drought severity and intensity. Projected decrease in precipitation in the near-term (2022-2050) with an increase in precipitation in far-future (2051-2100) in Iran with reference to the same scenario highlighted that influence of climate change on future precipitation is highly uncertainty. Thus, care must be taken when using precipitation alone as a drought indicator.

To study the impacts of temperature and precipitation changes on future drought occurrence, Abiodu *et al* (2018) analyzed 20 regional climate simulations of Representative Concentration Pathway-8.5 scenario from 6 CORDEX RCMs over the major river basins of Southern Africa under 4 different Global warming levels (1.5°C-3.0°C) above the pre-industrial level (1861-1890). The study discovered a robust increase in drought intensity of 0.9 and severe drought frequency of 2 more events per decade across the Southwestern coast than the north tropical areas of Southern Africa at GWL 2.0 with GWL 3.0 turning a large area of South Africa and Namibia into meteorological drought hotspots due to decreasing precipitation and increasing temperature (Abiodu, Makhanya, Petja, Abatan, & Oguntunde, 2018). Interestingly, a study over the same area conducted by Maure *et al* (2018), using 25 Coordinated Regional Downscaling Experiment Africa (CORDEX-Africa) regional climate model simulations and future global warming levels (1.5°C and 2.0°C), found that Southern Africa would experience above global mean temperature rise, especially during the onset of rainy season, September-October, with 10-15% decrease in December-January precipitation (Maure, et al., 2018).

Moreover, according to (Ayugi, et al., 2022), the East Africa is affected differently by future climate change with highlands and coastal areas projected to experience increasing precipitation as opposed to the arid and semi-arid regions, which will experience less precipitation. In their study of the projected meteorological characteristics under 4 SSP (SSP1, SSP2-4.5, SSP3-7.0 and SSP58.5) using a bias-corrected multi-model ensemble of 16 CIMP6

Global Circulation Models to reduce single model bias, they found that spatio-temporal variations existing in the magnitude and intensity of drought is influenced by the effort placed on climate change mitigation. High drought intensity (10-25%) was projected to occur in the region during in the near-future before subsequently reducing to 4-8% in the far-future as increased precipitation would occur in comparison with 1901-2020 and 2020-2050 period.

Spatially, a homogeneous increase in drought severity was noted throughout the region in all scenarios, whilst drought frequency showed high variations under SSP3-7.0 and SSP8.5, with a decrease in the central and north countries of East Africa, such as Ethiopia, and 2-16% increase over the southern areas of Tanzania that border Northern Malawi. The research by (Ayugi, et al., 2022), however, just focused on the precipitation over the area which is projected to decrease in the near-future and increase in the latter half of this century leading to more wetter conditions, without looking at the temperature anomalies, arguing that temperature's influence on the hydrological balance is already accounted for by the climate model. This contrasts with the study by (Behzadi, et al., 2024) who emphasized the underlying issue of utilizing precipitation as a stand-alone drought indicator.

2.6 Drought and Climate over Malawi

Drought in the Malawi is influenced by the El-Nino Southern Oscillation (ENSO) which suppresses or enhances precipitation across the country. La Nina phenomena increases rainfall over the Southern region and suppresses the rainfall over the northern parts of Malawi, with the vice-versa observed during El Nino (Ministry of Natural Resources and Climate Change, 2023). Since 2000, severe drought has been recorded in 2005, 2012 and 2016/17, with the recent one being exacerbated by ENSO resulting in the need of outsourcing basic needs for 6 million people (GFDRR, 2019; Chabvungma, Mawenda, & Kambauwa, 2014). According to (GFDRR, 2019), high agricultural drought risk is observed over the Southern and Central regions due to high vulnerability (product of high population density), although districts such as Karonga and Salima have high drought hazard score.

Studies by (Kambombe, Ngongondo, Eneya, Monjerezi, & Boyce, 2021; Chabvungma, Mawenda, & Kambauwa, 2014) have agreed that the climate change is having an influence on the meteorological drought experienced in Malawi. These studies, which utilized historical climatic datasets and drought indices, all agree that the average temperature increment of 0.5°C/decade since the 1970s combined with precipitation decline in most parts of the country, have increased the occurrence of drought events. Additionally, the changes in spatio-temporal distribution of precipitation are found to be heterogeneous as some areas in the central Malawi experiencing an insignificant increase in precipitation. Although the precipitation over the region have found the decrease to be insignificant, Kambombe *et al* (2021) argued that decreased precipitation has more significant impact on drought across the Lake Chirwa, Malawi, than air temperature. Changes in precipitation by 5% can lead to an 8% decrease in drought intensity across the Lake Malawi basin as the increased precipitation corrects the negative hydrological imbalance (Mtilatila, Bronstert, & Vormoor, 2022). Mtilatila *et al* (2020) found that although the drought hazard identification from drought indices such as SPEI and SPI, show different drought characteristics over Malawi, such as spatial extent, they agree that there has been an increase in frequency of meteorological drought across the area from 1970-2013. Highlighting the influence of evapotranspiration and temperature on meteorological drought characteristics over Malawi (Spinoni, et al., 2020).

Future projections of drought in Malawi using multi-model ensemble of CMIP5 models show that the drought duration will increase by 7 and 8 months during 2071-2100 under RCP 8.5, 2 months more than under the RCP 4.5 scenario (Mtilatila, Bronstert, & Vormoor, 2022). Longer drought duration affects the return period by reducing the frequency of drought whilst increasing the magnitude and impacts. The research focused only on the temporal changes without investigating the spatial shifts of drought due to climate change across Northern Malawi. Apart from this study that highlights changes in temporal drought characteristics over Northern Malawi, research focusing on drought projection in Northern Malawi, particularly, with climate scenarios as foci is minute. Previous studies across the area have focused on historical drought, drought impact assessment, and climate change impacts on temperature and precipitation without integrating the shifts in drought characteristics.

For example, (Amosi & Anyah, 2024) assessed the tendency of drought over Malawi and Mozambique and analyzed the future climate projections under SSP2-4.5 and SSP5-8.5 till 2050 with particular focus on the decadal changes in historical drought from 1981-2020 from observational data and only went as far as assessing future temperature changes till 2050 but not drought projections. The study, which used simulation from 4 NASA-NEX-GDPP-Coupled Intercomparison Model Project, concluded that there was agreement in that temperature over the Northern Malawi will increase by a mean of 1.2°C which could exacerbate the prominent drying conditions observed over the area as compared to 1981-2020. Similarly, a study by (Demissie & Gebrechorkos, 2024) only focused on observing the temperature and rainfall over

Northern Malawi finding a significant increase in the summer and winter temperatures of 0.4°C and insignificant decrease in precipitation of -4.5mm/year during the rainy season since 1981.

Even the analysis of the future weather patterns by Gama, et al. (2014) over Mzimba, Northern Malawi, only modelled the impacts of temperature and rainfall projections on the maize cultivation over the area. Using 20 Global circulation models under the Representative Concentration Pathway 8.5 and Crop APSIM software, they found that the 1-3°C temperature increase and 1.1% decrease in October-April rainfall between 2040-70 will reduce the yields. Additionally, even though Kumwendaet al (2024) assessed the future meteorological drought from 2025-2100 over Northern Malawi's Lufilya catchment using RCPs and portayed plausible increase in drought frequency over the area, their study only focused on rainfall as a meteorological drought indicator and did not capture how the different increment in temperature over the period would affect drought prevalence. Their study found that during 2025-69 and 2070-2100, the area would experience a 1%, 3.7%, 6% and 12.7% increase in average temperatures under RCP4.5 and RCP8.5 respectively. Thus, the study seeks to bridge this existing gap on analysis of drought characteristics using the shared socioeconomic pathway scenarios over the terrain of Northern Malawi.

2.7 Theoretical Concerns / Situating the Study in the Field

In the area of drought studies and climate change, various methods and theories have been used to investigate the influence of climate change on drought characteristics such as duration, intensity and severity. Looking into existing literature, a vivid debate is found pertaining the role of temperature in assessing future meteorological drought condition but analyzing drought with only precipitation as a drought indicator presents a source of uncertainty as the relationship of climate change and rainfall variability is fluctuates greatly in terms of spatial-temporal characteristics (Warnatzsch & Reay, 2019). Thus, proper assessment of drought indices and parameters needs to be undertaken to reduce the uncertainties induced by either future temperature and precipitation, which can be observed by comparison with observed climatic datasets and drought records.

In terms of drought indices, (Sidiqi, Kasiviswanathan, Scheytt, & Devaraj, 2023) concluded that choice of meteorological drought index and timescale influences the observed future drought trends and drought characteristics. In the area of meteorological drought assessment, SPEI has more robustness in terms of presenting changes of future drought trends than other meteorological drought indices, such as Palmer Drought Severity Index (PDSI) and

Standardized Precipitation Index (SPI) (Abiodu, Makhanya, Petja, Abatan, & Oguntunde, 2018; Ukkola, Kauwe, Roderick, Abramowitz, & Pitman, 2020). This was attributed to the use of potential evapotranspiration in combination with precipitation. Arguably usage of potential evapotranspiration sometimes leads to overestimation of drought but nonetheless provides a good basis for the highest limit for meteorological drought which is critical for drought management (Mohammed, Yimer, Tadesse, & Tesfaye, 2018). Whilst choice of parameters is vital, the timescale used for selected drought indicators has also an influence on the intensity, duration and severity of observed meteorological drought conditions as well as area impacted by specific classes of meteorological drought (Muthiah, Sivarajan, Madasamy, Natarajan, & Ayyavoo, 2024; Kubiak-Wójcicka, Owczarek, Chlost, Olszewska, & Nagy, 2023). Short timescale of 1 month or 3 months are unsuitable for the analysis of meteorological drought over a long period as they are highly sensitive to short term shifts of precipitation and temperature and fail to represent the actual drought conditions, especially in climate zones with extended dry seasons (Zhang, Zhang, Li, Zheng, & Zhang, 2023). Thus, this study will utilize 6- and 12-month timescales in combination with SPEI for the drought analysis.

The most prominent tool in assessment of future drought conditions under climate change is global climate models and scenario-based approach such as RCPs and SSPs. The shared socio-economic scenarios (SSPs) provide a more comprehensive approach for assessing climate change and drought than RCPs as they capture the complex interactions of anthropogenic actions with climate allowing for more realistic presentation of future drought conditions. According to Spinoni (2020), Southern Africa is prone to increased meteorological drought severity and intensity under climate change but the impacts of climate change on a regional and local scale portray different relations as climate change impacts especially on precipitation are not homogenous in terms of time and space. Even under the same locality, areas are projected to experience different levels of meteorological drought severity and intensity in response to climate change (Promping & Tingsanchali, 2020). Thus, although studies by using CMIP6 and SSPs have shown that there will be an increase in drought severity across Southern Africa including Malawi, there is a need to understand the drought characteristics from a local perceptive across the Northern Malawi. In the terms of climate models, the new generation CMIP6 models show robustness in predicting future climate characteristics and high correlation with historical climate over the Northern Malawi in comparison to previous CMIP5 and CIMP3 models (Mmame & Ngongodo, 2024; Ukkola, Kauwe, Roderick, Abramowitz, & Pitman, 2020; Libanda & Nkolola, 2019). However, bias-correction of the GCM and RCM models is still required to improve the reproduction of the local and regional climate variability and change. Hence, this study seeks to bridge this gap existing in Northern Malawi drought studies by utilizing downscaling methods, historical climate data, CIMP6 models and climate scenarios to investigate the future meteorological drought conditions.

2.8 Chapter conclusion

In conclusion, literature pertaining to meteorological drought has been assessed with the interconnections of climate and drought being highlighted. The influence of temperature and rainfall over drought characteristics over meteorological drought characteristics has been supported by existing literature but differing results can be observed. Moreover, the impacts of climate scenarios on drought show that higher temperature shifts combined with reduced rainfall, leading to more severe droughts, are expected under fossil-fuel intensive scenarios such as RCP-8.5 and SSP5-8.5, although the exact magnitude of change is location and scenario dependent. Furthermore, the different drought shifts under each scenario validate spatio-temporal, and scenario biases that require a more localized approach for better preparedness. The observable gap in meteorological drought projections under Shared Socio-economic scenarios over Northern Malawi requires a methodological approach using downscaled CMIP6 models. The subsequent chapters describe this approach, and statistical techniques used in the study before discussing the significant findings and recommendations.

3 METHODOLOGY

This methodology chapter delves into the techniques and methods utilized in the study to obtain results that answer the research questions. A description of the study area is provided in terms of the area's topography, climatic and socio-economic conditions to highlight its suitability and need for this specific meteorological drought research. Furthermore, there is a section on data acquisition and processing that portrays the reasoning behind the historical and future data choice and their availability. The statistical techniques used for trend analysis, drought modelling, statistical downscaling and spatial analysis are presented, in addition to their formulas. A figure containing the flow design of the methodology is presented at the end of the chapter to give the overall outlook of the methodology (Figure 3.2).

3.1 Study area

3.1.1 Topography and Location

The Northern region of Malawi is one of the three main regions of Malawi, which is a country found in the Sothern-eastern part of Africa. Northern Malawi is situated between 32°48'E and 34°34'E longitudes and 9°15'S to 12°15'S latitudes, and bordered by Lake Malawi to the east, Tanzania in the north, central Malawi to the south, and Zambia to the west.

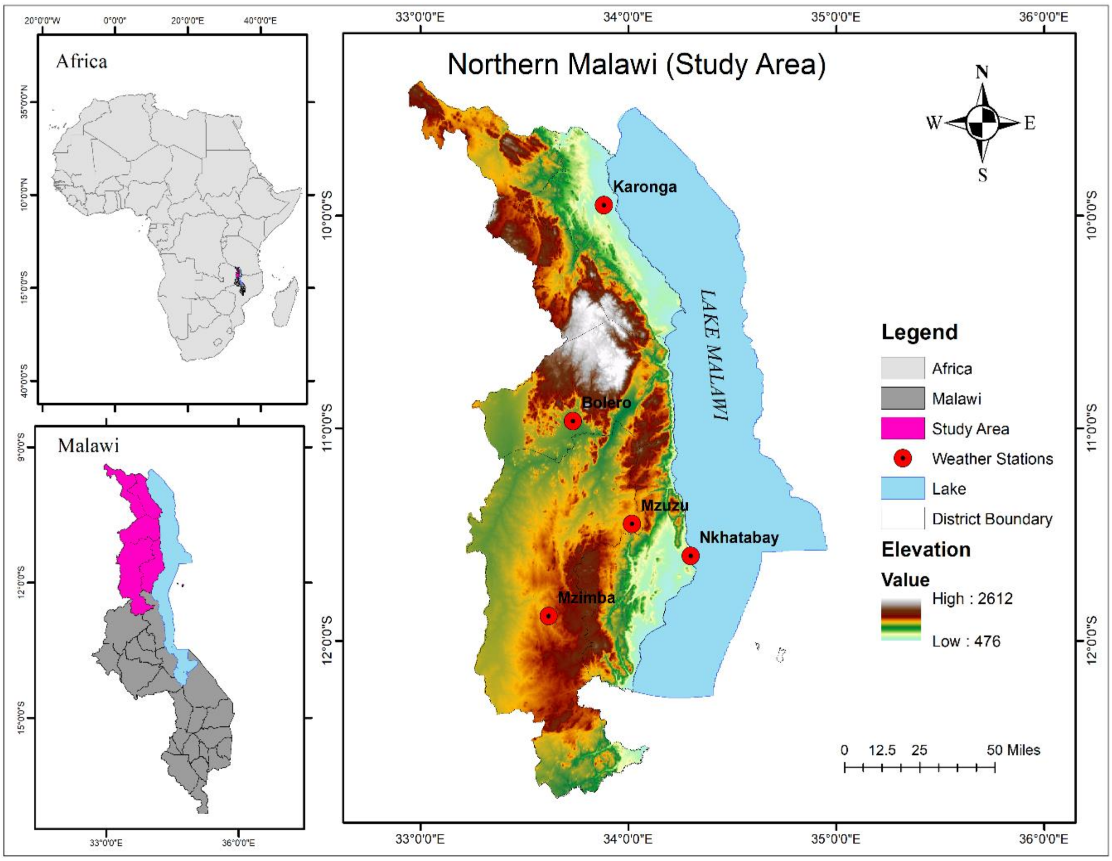

Figure 3.1: Map of the Northern Malawi (source: Author,2024)

It is a highly mountainous area with an elevation of 476m, along the lakeshore areas of Nkhatabay and Karonga to 2612m at Nyika plateau(Figure 3.1 above). With an area of 27131km^2, covering only 29% of Malawi, Northern Malawi is the most forested area in the country. Most of its forests are found in the form of woodlands and grasslands but recent trend portrays that agricultural and settlement expansions have led to significant losses in forest area (Gondwe, Chirwa, & Geldenhuys, 2019).

3.1.2 Climate

As the northern region is within the tropics, it experiences equatorial savanna and humid subtropical climate (Beck, et al., 2023). The area has two distinct seasons, a rainy summer season that starts from November-April, that is driven by the Intertropical Convergence Zone and the El Nino Southern Oscillation, and a dry season from May-October. Under the influence of these atmospheric drivers and underlying topography, the average annual rainfall ranges vary from 700mm to 2400mm (Ministry of Natural Resources and Climate Change, 2023). Additionally, there are cool winter conditions from May-August with average temperatures of 15-19°C whilst the summer months of September- December bring warm to hot daily temperatures of 22-30°C. According to (Irish Aid, 2017), there has been an increase in mean annual temperature by 0.21°C per decade since 1960 whilst the rainfall has declined by -4.5mm/year since early 1980s which has increased the frequency and magnitude of drought. Interestingly, nine major drought cases have been documented since 1961 with four occurring recently between 2000 and 2017.

3.1.3 Socio-economic factors

Northern Malawi consists of six districts and has a total population of less than 4 million (Government of Malawi, 2019).Even though it has the smallest population region wise, its population growth rate is one of the highest per district level. Salaries account for 20% of economic activity as a large percentage of this population practices agriculture as a livelihood option, especially in the rural areas. The major crops grown are tobacco, maize, cassava and rice whilst sorghum, soya beans and coffee are minor field crops. Recurring drought cases in the 2000s have impacted this livelihood practice with the National Gross Domestic Product contribution of the agricultural sector dropping by 14% in 2017 from 40% of GDP due to the impacts of the 2015-17 droughts on crop yield and livestock production (USAID, 2019; GFDRR, 2019).

3.2 Research Design

The study follows a quasi-experimental quantitative research design to assess for the future meteorological drought conditions over Northern Malawi. It undertakes a scenario-based approach of integrating historical data, climate projections, drought modelling and statistical downscaling. A systematic process of data collection, processing and analysis was followed to ensure that the results were scientifically sound. Due to the focus on climate, the historical data was obtained as a basis for the evaluation of current climate and drought trends over the study area. Modelling selection for climate model projection was conducted through literature assessment and the four CMIP6 models (Table 3.3) found to accurately represent the rainfall and temperature over Northern Malawi were selected (Mmame & Ngongodo, 2024). The climate scenarios of focus were SSP2- 4.5(balanced adaptation and mitigation) and SSP5-8.5(high challenge to mitigation, high emissions). Prior to further analysis, evaluation of the statistical downscaling techniques in their performance in downscaling each parameter was conducted to further refine the model results. This was done using Root Mean Square Error, (RMSE), Normalized Root Mean Square Error (NRMSE) Nash Sutcliffe coefficient, Pearson's correlation, Spearman's correlation, Index of Agreement, Mean Bias error (MBE), and Mean Absolute Error (MAE). The downscaling was conducted on the models to refine the climate projections into local high-resolution datasets by decreasing the coarseness.

The Standardized Precipitation Evapotranspiration Index (SPEI) index was the chosen drought index for its capability to capture the interaction between precipitation and potential evapotranspiration (PET) over drought occurrence. PET was calculated using the Hargreaves method due to its simplicity and low data requirements, particularly in regions of sparse climate records. To represent the seasonal and long-term trends, SPEI was calculated at 6-month and 12-month timescales. The run-time theory was applied to the results to obtain the drought intensity, severity and duration. Modelling of both historical and future drought conditions helps in validating the projected shifts and visualization of shifts in meteorological drought hotspots. The spatial characteristics of Northern Malawi's climate and drought were visualized using Inverse Distance Weight (IDW) spatial interpolation. The spatial analysis helps to better understand the spatial shifts in climate and drought patterns resulting in effective and more localized strategies towards drought risk management and climate change adaptation

3.3 Data acquisition and processing

3.3.1 Historical Data

In terms of historical climate data, station observed data was selected as opposed to satellite or reanalysis data as station data provides on ground truth and reduces satellite or reanalysis biases in meteorological analysis (Zhan, Guan, Sheffield, & Wood, 2016). The datasets, namely, monthly maximum and minimum temperature, and precipitation, were collected from the Department of Meteorology and Climate Services. There are several meteorological weather stations that record both temperature and rainfall parameters within northern Malawi but only stations that have been observing the climatic conditions for over 30 years were considered in this study (Table 3.1). The focus was mainly on 1991-2020 as these years help to capture the current climate trend in terms of rainfall, temperature and drought.

Table 3.1: Stations in Northern Malawi

Name	**Latitude**	**Longitude**	**Elevation ()**	**Date of operation**
Bolero	-10.966	33.733	1100	1961-current
Karonga	-9.95	33.883	529	1952-current
Mzimba	-11.883	33.616	1349	1946-current
Mzuzu	-11.45	34.017	1254	1961-current
Nkhatabay	-11.6	34.3	500	1961-current

3.3.1.1 Quality control and assessment

High quality data is vital in climatic research as there are many sources of error that can hinder the applicability and validity of the results obtained. Thus, any climatic data needs to go through screening for missing data points and homogeneity testing to reduce the impacts of human or equipment error on the obtained data. As such, the 5 synoptic stations present in the Northern region were crosschecked for data completeness using R-Instat software (a software specially built for climatic analysis) with a condition that stations with more than ten percent data missing will be discarded. All stations were found to have data completeness above 90% as in Table 3.2. Missing data values were filled in using CHIRPS data obtained from NASA power and the arithmetic average of the stations.

Table 3.2: Data quality check for station rainfall and temperature

Name	**Latitude**	**Longitude**	**Elevation(m)**	**Data Completeness (%)**
Bolero	-10.966	33.733	1100	99.91

Karonga	-9.95	33.883	529	100
Mzimba	-11.883	33.616	1349	100
Mzuzu	-11.45	34.017	1254	99.89
Nkhatabay	-11.6	34.3	500	99.72

Homogeneous of data helps quantify the usefulness of the data as heterogeneous data sets can highlight non-existent relationships and affect the accuracy of the research results (Mohammed & Scholz, 2023). Heterogeneity in datasets can occur due, but not limited to, broken equipment, human interferences, changes in station location and changes in equipment. Furthermore, shifts in climate drivers, and anthropogenic interaction such as urbanization can create environmental changes that significantly alter climate characteristics. Thus, a statistical analysis of homogeneity using Pettit's test was conducted to highlight any departures in the data distribution.

3.3.1.1.1 Pettit test:

The Pettit's test is non-parametric statistical test that utilized the null hypothesis of Y_i is homogeneous and alternative hypothesis that there is a break/ a change point in the dataset (Kocsis, Kovács-Székely, & Anda, 2020). The advantage of this test is based on not requiring the data to have normality or any specific data distribution as it ranks the variables (Y_i) using their ranking order in ascending order. The equation of Pettit's test is as follows:

$$U_{t,T} = \sum_{i=1}^{t} \sum_{j=i+1}^{T} sgn(x_i - x_j)$$

Whereby

$$sgn(x_i - x_j) = \begin{cases} 1 & if\ (x_i - x_j) > 0 \\ 0 & if\ (x_i - x_j) = 0 \\ -1 & if\ (x_i - x_j) < 0 \end{cases}$$

$U_{t,T}$ is the number of years for record, T is the length of the dataset, x_i and x_j are the values of the variable being assessed. Additionally, the two-tailed K_T or the Pettitt's statistic was found via:

$$K_T = max_{1 \le t < T} |U_{t,T}|$$

The results (see Appendix7.1) highlight that there exist significant change points in the maximum and minimum temperatures but a similar conjecture, found by (Chauluka, Singh, & Kumar, 2020), of change points coinciding with climatic extremes is observed here. Thus, no application of homogenization techniques was conducted to prevent distortion of climatic truth due to type II error.

3.3.1.2 Trend analysis

In analyzing the time series of climatic data such as precipitation, it is important to understand whether there is a decline, an incline in the values or the values are staying the same. Thus, in this study, the obtained historical climate parameters were assessed using trend tests to determine the existing trends. There are two ways in which a trend occurs; a steady change over time(monotonic) or a sudden shift at a particular point in time (step trend). Trend analysis tests used in this study were Mann-Kendall and Theil Sens's slope estimator.

3.3.1.2.1 Mann-Kendall

The Mann-Kendall is an important statistical tool for assessing trends in meteorological parameters such as temperature and precipitation as it is not influenced by the need for the data to be a specific distribution (Chauluka, Singh, & Kumar, 2020). This not only reduces the complexity of the calculation but also allows for accuracy in the results as no transformation of obtained data is conducted. The Mann-Kendall test assumes data independence and only compares the current variable with the previous variables in the datasets whilst keeping the data in its original distribution. Mann-Kendall test is also insensitive to missing data and vital in determining the monotonic trend in hydro-climatic data. The test uses a null hypothesis, H_0, of that the data values are identically distributed and have independent realizations. The alternative hypothesis, H_A, is that the data follows a gradual change in time (monotonic trend) by either decreasing or increasing with time. The Mann-Kendall test is calculated using the following equations:

$$S = \sum_{k=1}^{n-1} \sum_{j=k+1}^{n} sgn(X_j - X_k)$$

With

$$sgn(X_j - X_k) = \begin{cases} 1 & if\ (X_j - X_k) > 0 \\ 0 & if\ (X_j - X_k) = 0 \\ -1 & if\ (X_j - X_k) < 0 \end{cases}$$

In the equation above, n is the length of the time series, the X_j and X_k represent sequential data values in the years, j and k, and j > k, and sgn (X_j – X_k) is the sign function. The starting value of S is zero (no trend present) and increments or decrements occur to this value in accordance to results of the sign function as shown in equation 2 and 3. Thus, if the value of X_k is greater than X_j, there will be a reduction in S highlighting a possible declining trend and the vice versa is true. When n is greater than 10, the variance of S, which takes account the ties that occur in the calculation, is calculated for the dataset. The variance is found by:

$$Var(S) = \frac{1}{18}\left((n-1)(2n-5) - \sum_{j=1}^{p} t_j(t_j - 1)(2t_j + 5) \right)$$

Whereby p is the number of tied groups and t_j is the number of data values within the j_{th} tied group. The value of S is approximately normally distributed by using the following Z transformation equations if n is larger than 10, using:

$$Z = \begin{cases} \frac{S-1}{Var(S)} & if\ S > 0 \\ 0 & if\ S = 0 \\ \frac{S+1}{Var(S)} & if\ S < 0 \end{cases}$$

A positive Z value represents a positive trend, and a negative value represents a decreasing monotonic trend. For testing statistical significance of the trend, the Z value is checked by comparing it to the standard normal distribution table with two-tailed confidence levels, based on significance level, α. When Z is greater than $Z_{1-\alpha/2}$, there is a significant trend present, and the null hypothesis is rejected whilst the alternative is accepted. Else, the null is accepted, and the trend is not statistically significant.

3.3.1.2.2 Sen's Slope estimator

The Sen's slope estimator, also referred to as the Theil Sen's slope estimator, is a non-parametric trend test that is used to measure the magnitude of an existing trend. It helps to calculate the change per unit time of any given variable using a linear model and is suitable for accessing meteorological variables such as precipitation and temperature (Muse, Tayfur, & Safari, 2023). It divides the dataset into data pairs and considers the median from all the possible combinations of these data pairs. The advantage of this test is that it limits the impact of outliers on the trend and is free from statistical constraints. The mathematical equation for this is:

$$Q_k = \frac{X_j - X_i}{j - i} \quad , j > i$$

whereby Q_k is the slope estimate, X_j and X_i are data values at time j and i respectively. Once n values of Q_k have been computed, the median is the slope estimator. A positive estimator signifies an increasing trend, and a negative signifies a decreasing trend in the analyzed variable.

3.3.2 Future climate data

For future rainfall and temperature datasets, four climate models from the Coupled Model Intercomparison Project-6(Table 3.3) were considered and their data obtained from the

Copernicus website. These models, namely ACCESS-CM2, FIOESM-2-0, INM-CM5-0 and MIROC6, were identified through studies that assessed the model's accuracy in representing the climate parameters (Mmame & Ngongodo, 2024). The selected timeframe for the historical run of each model was 1991-2020 in agreement with the historical data obtained from DCCMS. In terms of future climate, 2020-2080 was the selected timeframe for the study which was further segmented into 2021-50 as near-term to mid-century and 2051-80 as the far future period. Two climate scenarios, representing the plausible emissions and socio-economic conditions over northern Malawi, were selected for the study, namely Shared Socio-economic Pathway2-4.5(SSP2-4.5) and Shared Socio-economic Pathway5-8.5. These scenarios present the middle of a road scenario focusing on both climate adaptation and mitigation whilst SSP5-8.5 is a high challenge to mitigation and low challenge to adaptation. In SSP-8.5, the use of fossil fuel technologies results in higher greenhouse gas levels than the SSP2-45 scenario. There were no temporal resolution differences between modelled and historical observed data as the data was also obtained in a monthly timestep.

Table 3.3: CMIP-6 models used in the study.

Model	**Institute**	**Resolution (lat. x lon.)**	**Reference**
ACCESS-CM2	Commonwealth Scientific and Industrial Research Organization (CSIRO), Australia	1.875°× 1.25°	(Dix, et al., 2019)
FIO-ESM-2-0	The First Institute of Oceanography (FIO), China	1.25°x0.9°	(Song, et al., 2019)
INM-CM5_0	Institute for Numerical Mathematics (INM), Russia	2° × 1.5°	(Volodin, et al.)
MIROC6	Japan Agency for Marine-Earth Science and Technology (JAMSTEC)	1.4°×1.4°	(Shiogama, Abe, & Tatebe, 2019)

3.3.2.1 Statistical downscaling and Bias correction

As earlier discussed in chapter 2, biases in global climate models due to spatial and temporal resolution need to be smoothened out prior to undertaking any analysis on a local level. Thus, downscaling was conducted on the obtained modelled data to gain station level projected rainfall and temperature datasets for each selected model. The choice of downscaling method was the statistical downscaling method due to its low computer requirement and presence of high-quality station data. Although various statistical methods exist, delta, quantile mapping and empirical quantile mapping were the methods used in this study. Whilst studies by (Dinku & Gibre, 2024; Mendez, Maathuis, Hein-Griggs, & Alvarado-Gamboa, 2020; Feyissa, Zeleke, Bewket, & Gebremariam, 2018) have commented on each method's effectiveness in downscaling rainfall and temperature, an evaluation was conducted on the selected climate models to find the best performing method for each station per climate parameter. This evaluation used root mean square error (RMSE),normalized root mean square error(NRMSE) Nash Sutcliffe coefficient, Pearson's correlation, Spearman's correlation, Index of Agreement, Mean Bias error(MBE), and Mean absolute error(MAE)(Table 3.4). For RMSE, NRMSE, MBE and MAE, the closer to zero the better the performance of that downscaling method (Mahesh & Shahapure, 2023). Meanwhile, the values closest to -1 or 1 in Pearson's and Spearman coefficient, symbolize excellent correlation of the downscaled results. Similarly, 1 in index of agreement means the method results in a good agreement between observed and model simulations while 0 means no agreement exists.

Table 3.4: Metrics used in model evaluation via SD-GCM software.

Error Metric	**Formula**	**Evaluation**
RMSE	$= \sqrt{\frac{\sum_{i=1}^{n}(x_{obs_i} - x_{mod_i})^2}{n}}$	0 to infinity
NRMSE	$= \frac{RMSE}{(x_{obs_{max}} - x_{obs_{min}})}$	0 to 1
Pearson's correlation	$= \frac{\sum_{i=1}^{n}(x_{obs_i} - avg_{obs})(x_{mod_i} - avg_{mod})}{\sqrt{\sum_{i=1}^{n}(x_{obs_i} - avg_{obs})^2}\sqrt{\sum_{i=1}^{n}(x_{mod_i} - avg_{mod})^2}}$	-1 to 1
Spearman's correlation	$= 1 - \frac{\sum_{i=1}^{n} d_i^2}{n(n^2-1)}$	-1 to 1
Mean Absolute Error	$= \frac{\sum_{i=1}^{n} \lvert x_{obs_i} - x_{mod_i} \rvert}{n}$	0 to infinity
Mean Bias Error	$= \frac{\sum_{i=1}^{n}(x_{mod_i} - x_{obs_i})}{n}$	-∞ to -∞
Index of Agreement	$= 1 - \frac{\sum_{i=1}^{n}(x_{obs_i} - x_{mod_i})^2}{\sum_{i=1}^{n}(\lvert x_{mod_i} - avg_{obs}\rvert + \lvert x_{obs_i} - avg_{obs}\rvert)^2}$	0 to 1
Nash-Sutcliffe model efficiency	$= \frac{\sum_{i=1}^{n}(x_{obs_i} - x_{mod_i})^2}{\sum_{i=1}^{n}(x_{obs_i} - avg_{obs})^2}$	-∞ to 1

obs=observed data, *mod*= modelled data, d is the difference in ranks between the datasets.

Based on best of eight, delta was found to be best performing for rainfall in nearly all the models whilst the downscaling of maximum and minimum temperatures was mostly conducted using quantile and empirical quantile mapping (see Appendix 7.2). Furthermore, an ensemble mean of all the models was produced and together with the models compared to the observation to assess their effectiveness in reproducing the climate over Northern Malawi. The analysis was conducted using Taylor's diagram, which utilizes Pearson's coefficient, standard deviation and root mean square error. The ensemble means were constructed using simple mean average and using weighted mean respectively whilst the lowest correlated model was removed in similarly constructed ensembles of only three models. The removal was done as poor correlating models tend to reduce the effectiveness of an ensemble in representing climate over an area (Yılmaz, Aras, & Nacar, 2024).

3.4 Drought calculations

3.4.1 SPEI

The Standard Precipitation Evaporation Index (Vicente-Serrano, Begueria, & López-Moreno, 2010) uses the difference between precipitation and the evapotranspiration to account for the occurrence of drought. Due to the sparseness of data, potential evapotranspiration (PET) for each month was calculated using the Hargreaves method (Hargreaves, 1994) as it is less complex than the Penman-Monteith method. This was completed using the SPEI package in R which uses the formula below:

$$PET_i = 0.0023 \times Ra(T_{max} - T_{min})^{0.5} \times (T_{mean} + 17.8)$$

Where T_{max}, T_{min} and T_{mean} are the maximum, minimum, and average monthly temperatures, respectively whilst Ra is the extraterrestrial radiation. The PET obtained was then used to calculate the water balance for each month over the study area via:

$$CWB_i = P_i - (PET)_i$$

$(PET)_i$ is the potential evapotranspiration(mm), CWB is the water balance, and P is the precipitation for month i. While SPEI can be used to compute for 1-48 months, the focus of this study was on 6- and 12-months timescales, namely, SPEI6 and SPEI12.These two timescales are referenced as seasonal and long-term conditions, respectively. Thus, accumulation of CWB_i for each timescale was undertaken before a log-logistic distribution was applied to the water balance of the study area. SPEI values were computed via:

$$w_i = \begin{cases} \sqrt{-2\ln(p)} & ,p \leq 0.5 \\ \sqrt{-2\ln(1-p)} & ,p > 0.5 \end{cases}$$

$$SPEI_i = w_i - \frac{c_0 + c_1 w_i + c_2 w_i^2}{1 + d_1 w_i + d_2 w_i^2 + d_3 w_i^3}$$

Where c_o= 2.515517, c_1= 0.802853, c_2=0.010328, d_1=1.432788, d_2=0.189269 and d3 = 0.001308. The values obtained were classified in drought classes based on the Table 3.5.

Table 3.5: Drought classification of SPEI values

SPEI values	Class
SPEI > 1	Very Wet
1 > SPEI > -1	Normal
-1 ≥ SPEI > -1.5	Moderate drought
-1.5 ≥ SPEI > -2	Severe drought
SPEI < -2	Extreme drought

3.4.2 Drought characteristics

The SPEI values computed were used to determine the drought magnitude, duration and intensity based on the runtime theory. The drought duration for each drought was the number of months that a drought event was observed. For drought intensity(I), severity(S) and frequency(F), these were calculated for each drought event based on the formulas below:

$$S_k = \sum_{i=1}^{m} (SPEI_i - SPEI_0$$

$$I_k = \frac{S_k}{m_k}$$

$$F = \frac{n}{N}$$

Where $SPEI_0$ is the threshold value, -1., m is the drought duration for each drought run(k), n is the total number of drought events and N is the total number of months under observation, which was 360 as all the time periods stretched 30 years respectively.

3.5 Spatial interpolation

Interpolation was conducted to help in spatial analysis of the climate and meteorological drought conditions to better understand the spatial shifts over the study area due to sparseness of stations. This was conducted using Inverse Distance Weighted interpolation tool in the ArcGIS software. IDW has been observed to capture the high spatial variability of climatic data due to its ability to capture effect of nearby data point as opposed to other interpolation techniques (Jaya, Ruchjana, Abdullah, & Andriyana, 2021; Chen & Liu, 2012)

IDW estimates the values of unsampled locations (x_0) using the known points nearby using weight distribution based on proximity. The influence exerted by each known point(x_i)is determined by the inverse of its distance to the unknown point. Thus, closer points are assigned to a higher weight in estimation of average. To find the values of unsampled location ($Z(x_0)$), the IDW formula below was utilized:

$$Z(x_0) = \frac{\sum Z(x_i) \times d(x_i, x_0)^{-p}}{\sum d(x_i, x_0)^{-p}}$$

Where d (xi, x0) is the distance between known location(x_i) and unsampled point (x_0), Z(xi)p is a user-defined positive parameter that controls the decay rate, which was set to the standard choice of p=2. This parameter, p, enhances the climatic spatial assumption by reducing the influences of distant points whilst maximizing effect of nearby points. IDW was applied to capture the temperature and precipitation variability over Northern Malawi. The results of SPEI6 and SPEI12 were also interpolated for both historical and future periods to assess the spatial variations in meteorological drought hotspots. The drought and climatic variability observed in both SSP2-4.5 and SSP5-8.5 are vital in assessing the exposure and vulnerability to climatic hazards and ensuring localized and scientifically directed approach to climate risk.

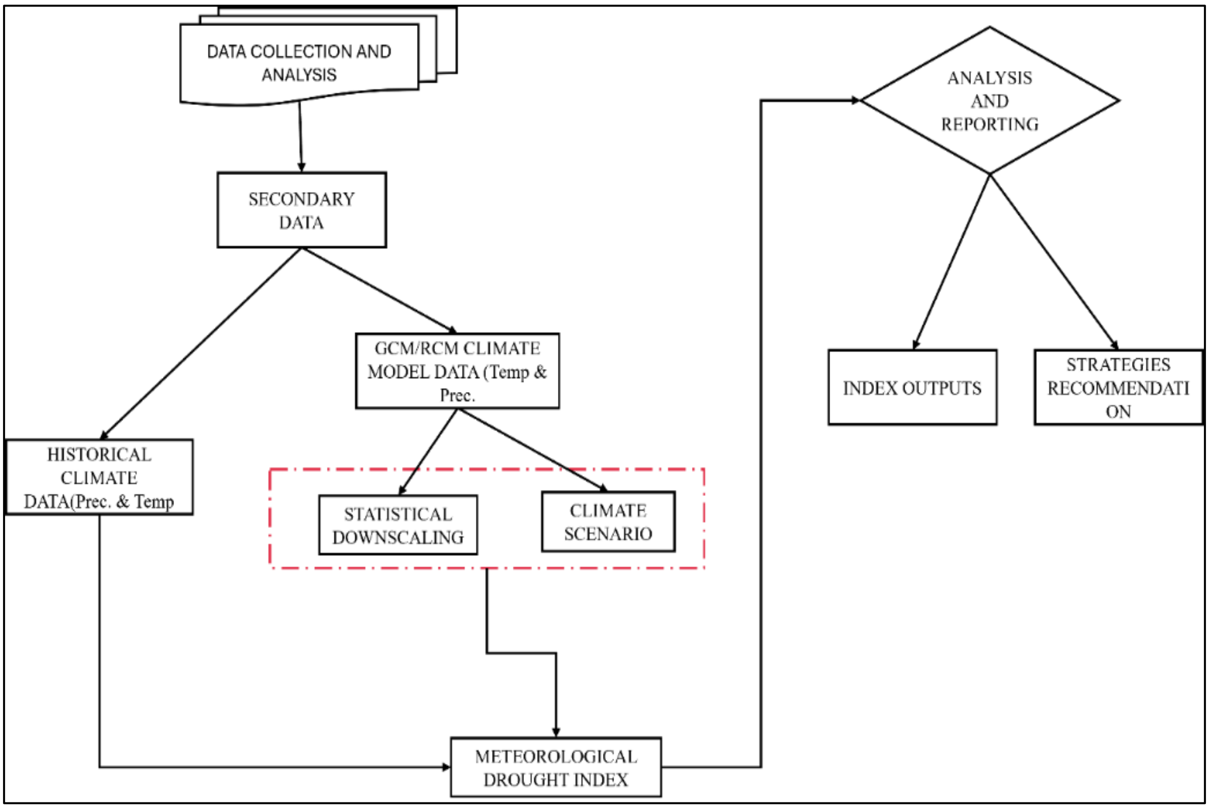

Figure 3.2: Flow design of the methodology.

4 RESULTS AND DISCUSSION

This chapter presents the findings of the study and gives insight into the changing climate and drought conditions over the study area. The early sections describe the historical and projected climatic conditions over the area in terms of trends and distribution. Afterwards, results obtained on the historical and future drought conditions obtained from both SPEI6 and SPEI12 are presented and discussed. Furthermore, the findings of the comparative assessment of future drought conditions against observed drought conditions are presented. A section on the implications of these results and their correlations to the research foci and existing literature is also included.

4.1 Historical Climate Analysis

4.1.1 Temporal distribution

Precipitation

From Table 4.1, values of average monthly precipitation above 50mm were observed in the months of November-April for nearly all the stations with the only outliers being Bolero (November, April), Mzimba (April) and Karonga (November). For Bolero, the highest amount of rainfall occurs in January (208.6) before reducing to 33.6mm in April, May to October are mostly dry months with rainfall being lower than 10mm whilst rainfall. Equally, Mzimba portrays the similar trend of rainfall peaking in January before dropping to 30.1mm in April and rises to 53mm in November and 165mm in December.

Table 4.1: Descriptive Statistics for precipitation at each station

Stat	Jan	Feb	Mar	Apr	May	Jun	Jul	Aug	Sep	Oct	Nov	Dec
Bolero												
Mean	208.6	148.9	115.07	33.66	2.42	1.04	1.5	0.05	0.66	3.17	31.09	142.48
Skew	1.27	1.93	3.79	0.9	2.76	2.11	2.09	3.47	4.65	3.01	2.39	2.93
Karonga												
Mean	180.13	164	248.35	162.94	19.57	0.82	1.09	0.16	0.53	1.45	36.03	153.83
Skew	-0.06	1.11	0.37	1.16	3.29	4.07	5.1	3.35	3.62	3.42	1.93	1.5
Mzimba												
Mean	246.27	184.25	132.64	30.15	5.24	0.6	0.49	0.97	0.42	6.66	53.54	165.35
Skew	0.56	0.34	1.03	0.85	3.81	3.15	1.97	3.76	2.77	1.98	2.29	1.76
Mzuzu												

Mean	253.24	202.69	229.38	210.95	41.69	43.07	20.31	17.06	10.84	34.58	77.69	186.04
Skew	0.39	1.78	1.2	1.19	1.75	2.6	2.15	1.32	1.86	1.73	1.63	1.4
Nkhatabay												
Mean	242.3	196.07	333.85	352.66	93.21	50.47	62.95	18.45	5.58	17.77	74.55	183.14
Skew	0.89	0.18	1.58	0.73	0.58	2.24	1.7	2.9	2.89	1.96	1.52	2.15

The period from May to October is mostly dry with the rainfall being lower than 20mm over most of the stations except for Nkhatabay. Rainfall in Nkhatabay is above 30mm nearly throughout the year with July-August being the only months with rainfall below 21mm. Rainfall over area follows a different trajectory by peaking in April(352mm) and not in January. Interesting, Mzuzu and Nkhatabay are the only stations with the five of months with rainfall above 180mm, signifying a higher annual precipitation as compared to Bolero, Karonga and Mzimba. A study by Kumbuyo, et al (2014) also found similar results when assessing rainfall over Malawi and concluded that the even distribution of topographical and convective rainfall at Nkhatabay induced this phenomenon. The skewness was calculated using Pearson's skewness and results close to zero symbolize symmetric precipitation whilst the positive and negative values represent median is lesser, and greater than the mean, respectively. Thus, Karonga has positive skewness in all the months except for January which has the median and mode slightly higher than the mean as denoted by -0.06. However, for Bolero, Mzuzu, Mzimba and Nkhatabay have median and mode values below the mean dominate across all the months. The largest deviation between median and mean is observed during the dry period of May-October.

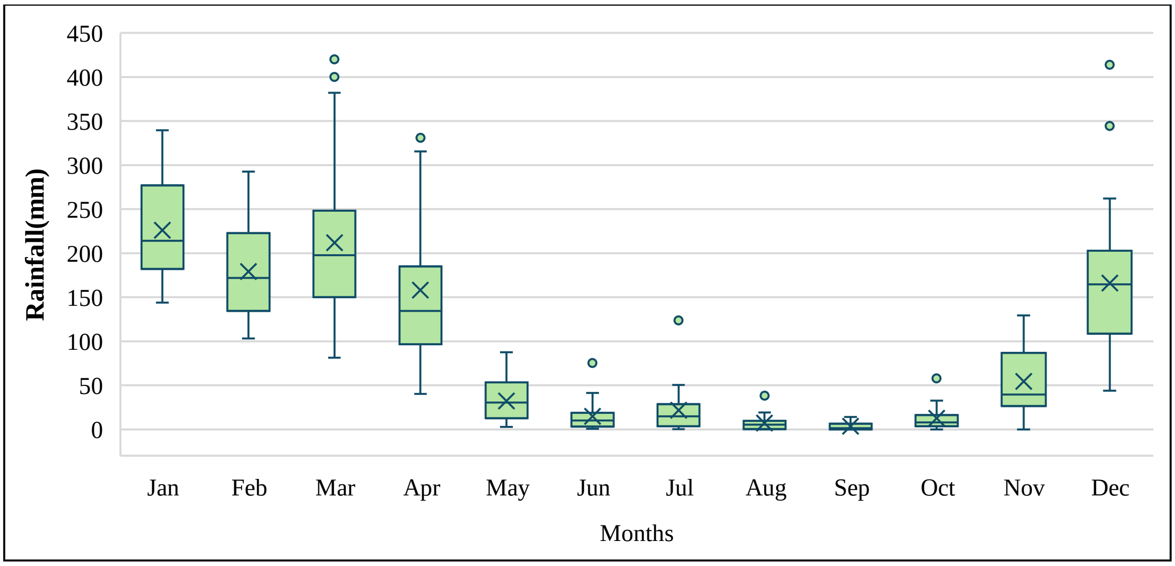

Figure 4.1: Monthly rainfall for Northern Malawi from 1991-2020

Averaging the areal monthly precipitation over the northern region of Malawi during 1991-2020, it was observed that rainfall ranges from 0-420mm with the high amounts being observed during the month of March and January. Figure 4.1 ,above, is a boxplot depicting this statistical observation of monthly rainfall over the Northern region with X symbolizing the average whilst the box represents the interquartile range of 25% and 75% of the values. The study shows that rainfall is high reaching 100m and above during the January – April before declining to below 50mm through the months of May-Oct. The months of June, August, September and October are generally dry with the average rainfall below 20mm in agreement with the dry season expected over this time period. Meanwhile during November, rainfall increases to a mean of 54.58mm and reaches above 100mm in December which is usually when the rainfall season over Malawi begins.

Annually, precipitation over Northern Malawi during 1991-2020 ranged from 384mm in Bolero to 2465.5mm in Nkhatabay (Figure 4.2). The location with the lowest precipitation in the region was Bolero with the mean of 688.63mm whilst Nkhatabay and Mzuzu are the stations that record the highest amount of annual rainfall in the region at 1630.98mm and 1327.54mm respectively. These results are similar to the study by (Tadeyo, Chen, Ayugi, & Yao, 2020) who observed that during 1979-2015, annual rainfall was lowest in Bolero whilst Nkhatabay has the highest precipitation of 1572mm. The difference in the annual rainfall is most likely due to a difference in period of observation. Most of the observed annual rainfall over the region is above 500mm with the lowest 25 quartile value being 583mm for Bolero.

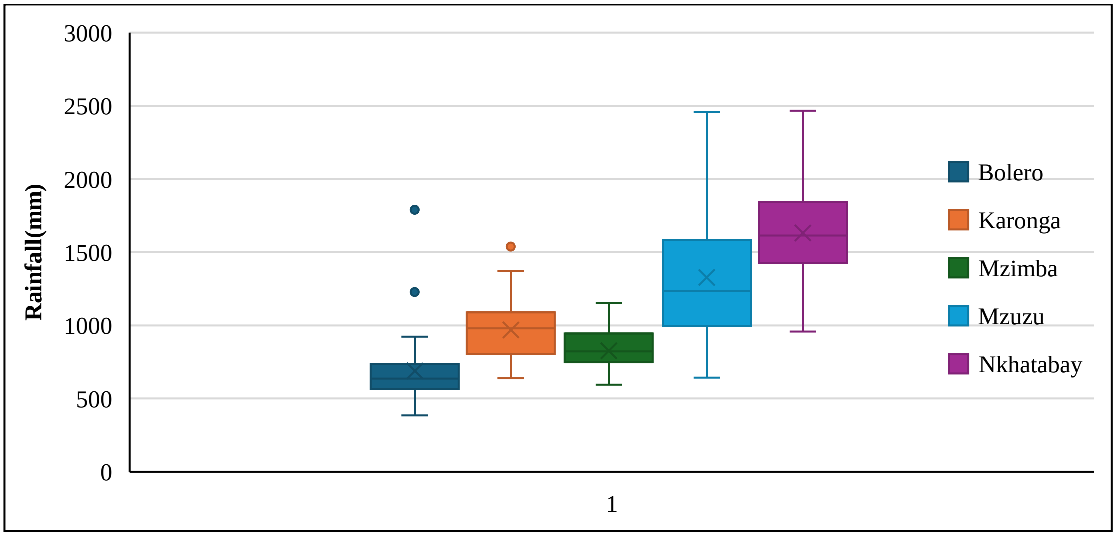

Figure 4.2: Annual precipitation over Northern Malawi from 1991-2020

Temperature

The monthly average temperature was computed to understand the temperature range on the stations. From Table 4.2, it can be observed that the monthly average temperature ranges from as low as 13.49°C in Mzuzu to as high as 29.54°C in Karonga during 1991-2020. The difference between the maximum average temperature and the minimum average temperature is 8-10°C for each station in the study area. The mode and median monthly average temperature values are greater than the mean as shown by the negative skew values whilst the variation of the temperature ranges from 0.074 to 0.143 with Karonga having the lowest variation and skewness.

Table 4.2: Descriptive statistics of average monthly temperature in the study area

Station	Min	Max	Mean	Std	CoV	Skewness	Kurtosis
Bolero	16.340	27.530	22.163	2.847	0.128	-0.270	-0.882
Karonga	21.555	29.530	25.569	1.894	0.074	-0.050	-0.719
Mzimba	15.895	25.230	20.994	2.137	0.102	-0.354	-0.635
Mzuzu	13.490	23.985	19.265	2.748	0.143	-0.504	-1.190
Nkhatabay	18.695	28.405	23.743	2.362	0.099	-0.426	-1.067

The boxplot of the maximum temperature (Figure 4.3) reveals the trend of temperature over the study period. Similar to Warnatzsch & Reay, (2019) analysis of 1961-2005 Malawi temperature, this study found that high average maximum temperature of over 29°C occur during September till November whilst low temperatures below 26C are common in June and August. However, compared to 1961-2005 mean maximum temperatures, the 1991-2020 temperatures are higher by 0.3°C, highlighting the existing climate change. But following the mean values, the study shows monthly maximum temperature exhibits the similar wave-like pattern of a higher value in January at 28.35°C. a reduction in subsequent month until a low of

24.79°C in July and an increment from August with the highest mean temperature occurring in November(31.57°C). The months of November, December, August and February have the highest range between the 25th and 75th percentile. Thus, the temperatures in these months have high variability in terms of spread.

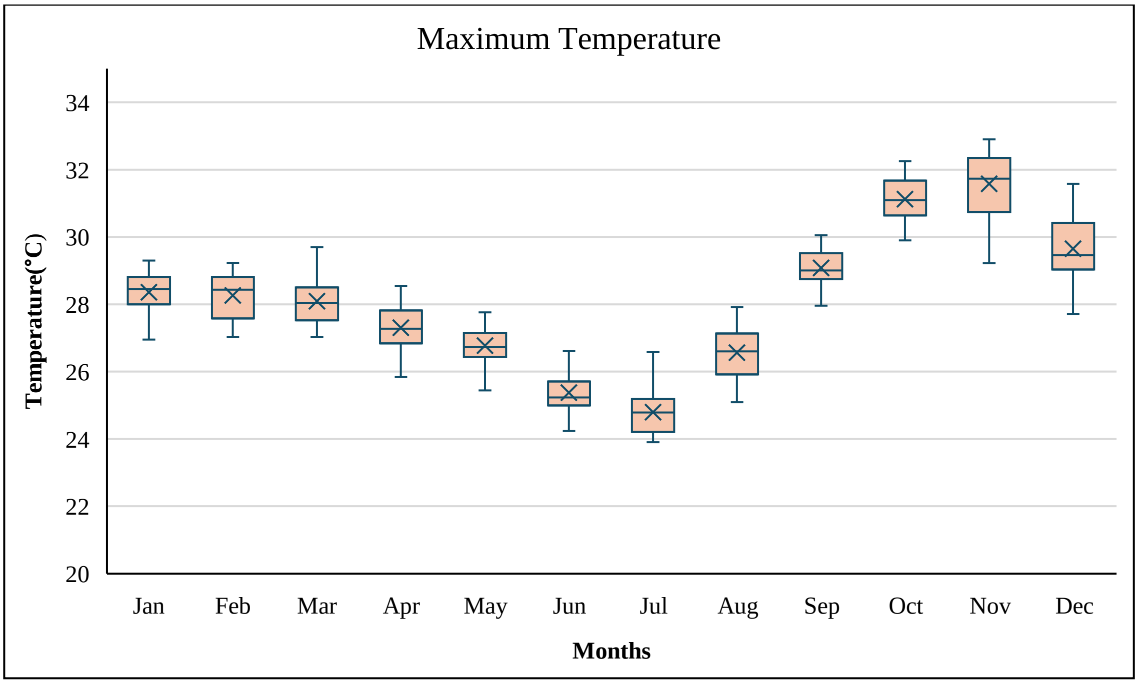

Figure 4.3: 1991-2020 monthly maximum temperature for Northern Malawi

Interestingly, a similar wave pattern in observed maximum temperature is also observed in minimum temperature over the study period (Figure 4.4). The areal minimum temperature over Northern Malawi ranges from 10.71°C in July to 20.46°C. As opposed to maximum temperature, the months of May and June have the biggest difference in interquartile range. The behaviour temperature from November to January showcases the summerly nature over this time as the values are usually 18°-20°C. A swift decline and incline in temperature values are observed between the months of April and May, and August and September, respectively.

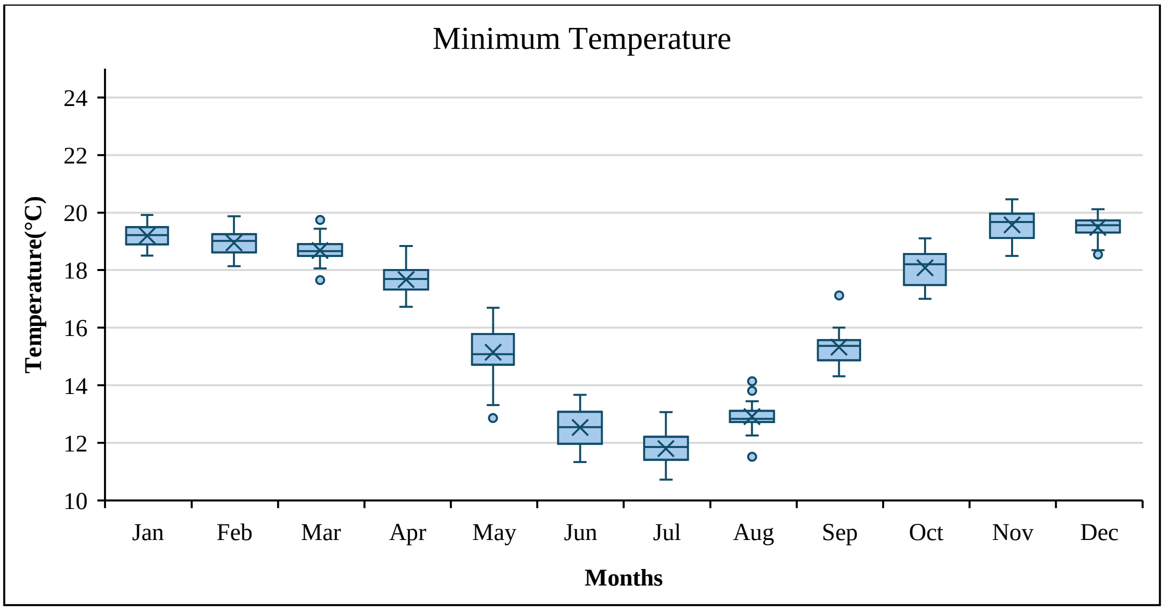

Figure 4.4: Monthly minimum temperature for Northern Malawi from 1991-2020

4.1.2 Spatial distribution

Spatially, the average annual precipitation from 1991-2020 ranges from 688.6 to 1630.9mm with the highest rainfall occurring on the south-eastern side of the region (Figure *4.5*). Light blue represents the lower ranges of rainfall whilst the high rainfall values are represented by darker shades of blue. Most of the area receives rainfall in the ranges of 823.2 -1092.4 mm, with the central area receiving rainfall below 823.2mm. The area experiences a minimum and maximum temperature range of 13.56°C-20.62°C and 24.96°C-30.53°C respectively. The southern regions experience moderate maximum and minimum temperatures of less than16.7°C and 27.44°C individually as seen by the bluish-green color over the area. The minimum and maximum temperatures increase going northward and south-eastward with notably, the northern area experiencing the highest maximum(red) and minimum temperature(red). The central-eastern area receives the lowest maximum and minimum temperatures of 14°C and 24.9-25.59°C. Even though a wide area experiences warm-hot temperatures of above 27.44°C whilst a large expanse receives cool minimum temperatures of below 15.91°C, it can be observed that the temperature parameters follow a similar spatial pattern.

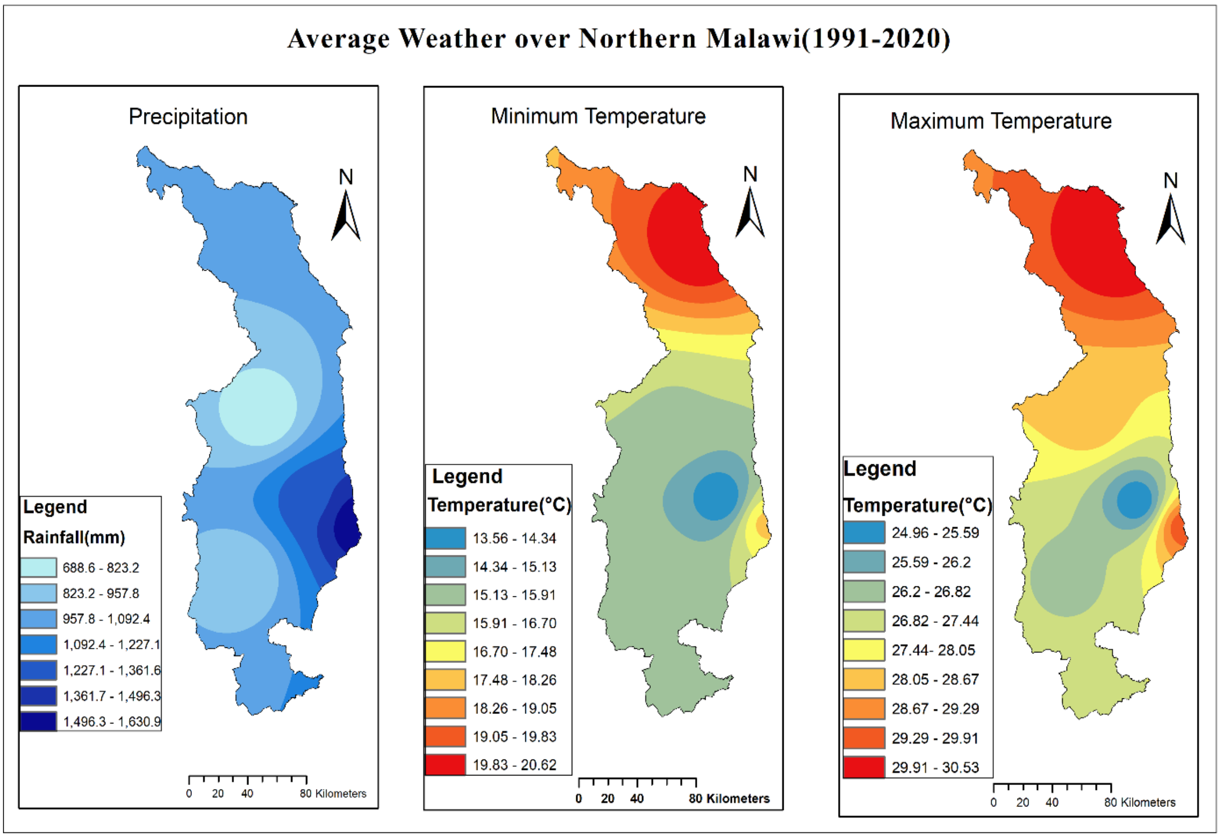

Figure 4.5: Average annual precipitation and temperature over Malawi.

4.1.3 Trend analysis under Mann-Kendall

The trend analysis of annual precipitation over the stations reveals presence of decreasing and increasing trends within the stations, although only two stations have significant trends, namely, Mzuzu and Bolero (Table *4.3*). Interestingly, these stations of significant climate also have the highest levels in annual precipitation change. Bolero has a significant increase in rainfall of 7.25mm per annum whilst Mzuzu has a significant decrease of 16.79mm per annum. Similar to the study by Demissie & Gebrechorkos,(2024), Karonga, Mzimba and Nkhatabay have an insignificant trend of 5.36mm, 2.17mm and -2.14mm, respectively.

Table 4.3: Mann-Kendall and Sen's slope for annual precipitation in Northern Malawi

Station	**Kendall's tau**	**S**	**p-value**	**Sen's slope**
Bolero	0.278	121	**0.032***	7.25
Karonga	0.149	65	0.254	5.36
Mzimba	0.094	41	0.475	2.17
Mzuzu	-0.255	-111	**0.049***	-16.79
Nkhatabay	-0.034	-15	0.803	-2.14

* The data showed a significant trend at 95% confidence interval

In terms of trend for the annual temperature, the region experiences significant increasing trend in temperature for both maximum and minimum temperature across all stations except form Mzuzu and Karonga. Karonga records a significant rising trend of 0.023°C per annum whilst a significant decreasing trend of 0.033°C is observed in its minimum temperature. Notably, this is the only station with a decreasing trend for temperature. The maximum temperature trends across the area ranges from 0.004-0.039°C, with the lowest being an insignificant trend at Mzuzu whilst the increasing minimum temperature trend ranges from 0.037-0.052°C, which are similar to the findings were reported by (Demissie & Gebrechorkos, 2024).

Table 4.4: Sen's slope and Mann-Kendall for annual temperature for Northern Malawi

	Maximum Temperature				**Min Temperature**			
Station	**Kendall's tau**	**S**	**p-value**	**Sen's slope**	**Kendall's tau**	**S**	**p-value**	**Sen's slope**
Bolero	0.490	213	0.0002*	0.026	0.549	239	2.17E-05*	0.037
Karonga	0.423	184	0.001*	0.023	-0.425	-185	0.0010*	-0.033
Mzimba	0.568	247	1.14E-05*	0.038	0.444	193	0.0006*	0.037
Mzuzu	0.078	34	0.556	0.004	0.609	265	2.48E-06*	0.052
Nkhatabay	0.457	199	0.0004*	0.039	0.494	215	0.0001*	0.041

* The data showed a significant trend at 95% confidence interval

4.2 Future Rainfall and temperature Analysis

4.2.1 Model performance evaluation

Figure *4.6* and Figure *4.7* present Taylor diagrams of the model evaluation for precipitation(pr), maximum(tasmax) and minimum temperatures(tasmin). The evaluation utilized Pearson's coefficient, RMSE and Normalized Standard Deviation to find the best performing model to be used for climatic projection over the study area. The ensembles generated were referred to as Ensemble for simple average ensemble whilst coefficient weighted ensemble was coded as Weighted. The climate models were well correlated with temperature than precipitation, with minimum temperature as the best correlation between climate models and observation data. Moreover, MIROC6 was found to be the worst performing model in all climate parameters, particularly when it came to maximum temperature. Hence, two different simple average and weighted ensemble without considering MIROC6 were generated. Notably, for precipitation(Figure *4.6*), FIOESM-2-0 performed better than the ensembles even though ensemble models tend to perform better than individual Global circulation models as found in the study by (Ayugi, et al., 2022). FIOESM was found to have the highest correlation of 0.808

in comparison with the weighted ensemble (0.800) and simple average ensemble (0.800). Compared to other models, FIOESM-2-0 has the highest resolution which could be the factor for its better representation of precipitation over the study area However, both methods of computing ensembles were found to have performed better for maximum (Figure 4.7a) and minimum temperatures (Figure 4.7b), respectively. The weighted ensemble method performed well for maximum temperature after the exclusion of MIROC6 whilst the simple average ensemble containing all models performed best for minimum temperature

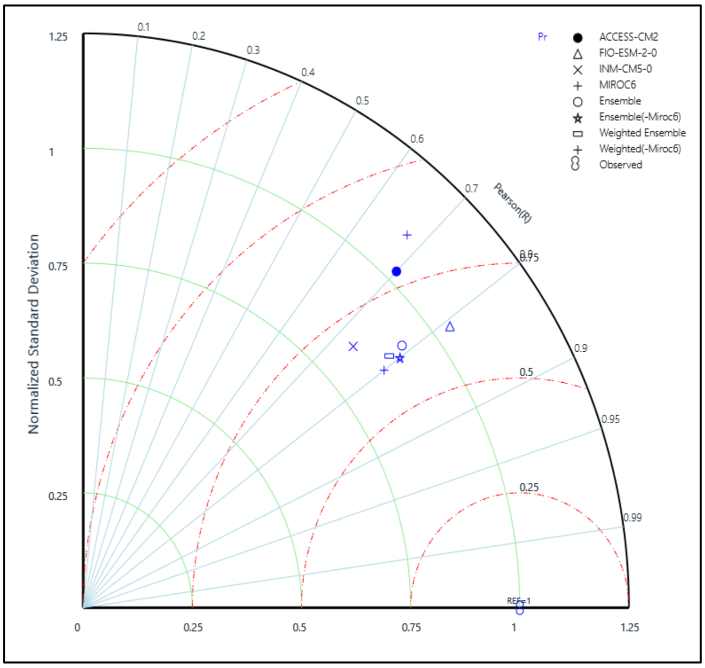

Figure 4.6: Taylor diagram of monthly precipitation.

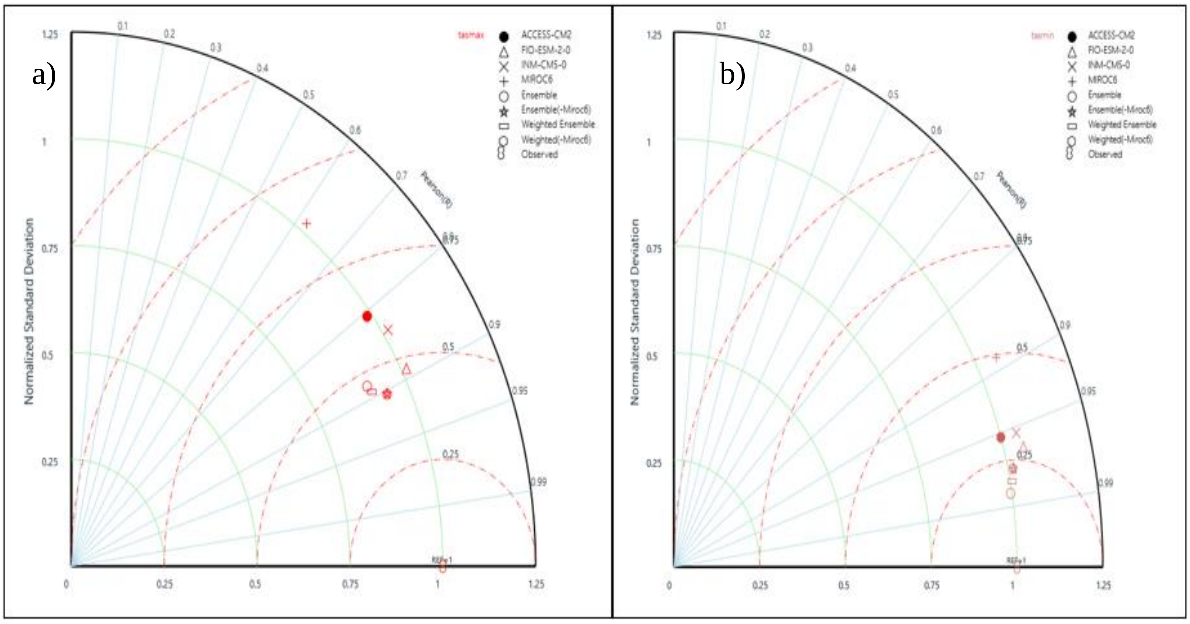

Figure 4.7: Taylor diagram of maximum(a) and minimum(b) temperature.

.

4.2.2 Distribution and Trend

After modelling and projecting for future climate conditions, understanding their distribution and trends is vital before drought assessment can be conducted. As such, charts, tables and maps were created to present these changes. The near-term to mid-century (near future) and mid-century-end century (far future) for each scenario are given the unique suffixes 2021-50, and 2051-80, respectively.

4.2.2.1 Precipitation

The mean monthly rainfall over the study depicts a rise in rainfall in both scenarios during the months of January, February, September, November and December, with areal rainfall surpassing 250mm for January (Figure *4.8*). During the months of March-August and October, a decline in future precipitation values is observed when compared with the current climatic conditions. In the near-term to mid-century, there is a higher increment in monthly precipitation for SSP2-4.5 than in the far future under the same scenario, except for February and March.

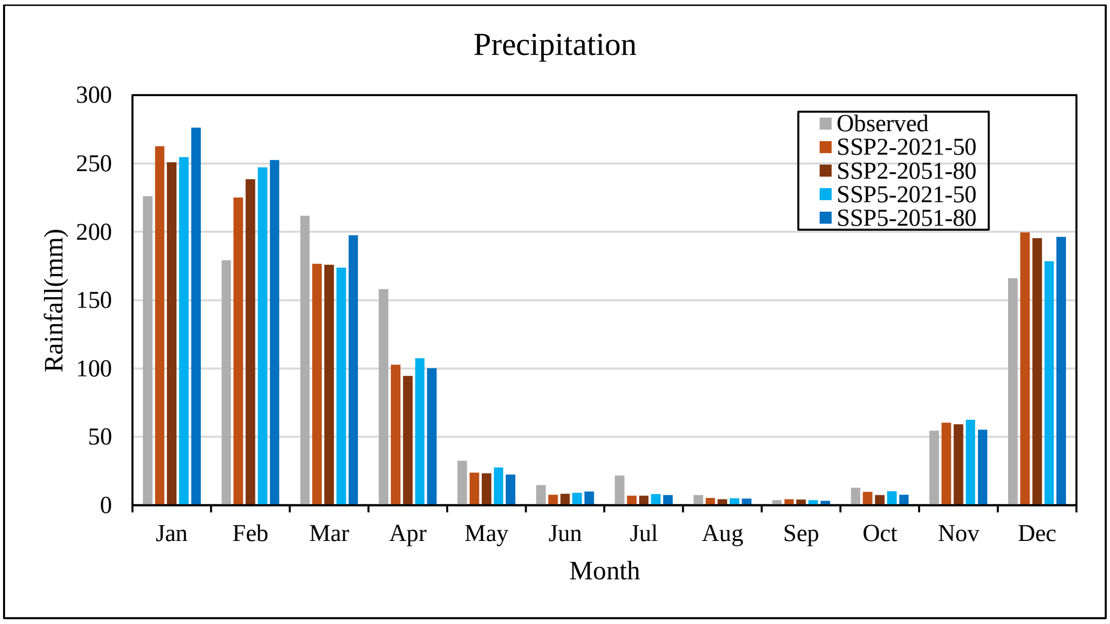

Figure 4.8: Observed and projected monthly mean rainfall over Northern Malawi.

Interestingly, the highest precipitation rise is observed under the SSP5-8.5 scenario whereby the rainfall continues to be greater than the climatic average observed in the other datasets and previous years. For instance, January and February report an increment of greater than 50mm for SSP5-8.5 in the far-future with a lesser increment observed under the other scenarios and periods. The only exceptions to this phenomenon are the months of November and December whereby the far-future SSP2-4.5 has a greater precipitation increment than SSP5-8.5. Existing climatic drivers during this month could be the possible explanation for no scenario superseding the other in all months in terms of areal monthly precipitation over Northern Malawi.

The annual trend of precipitation across the area shows that the only significant trend(rising) in rainfall occurs in the near-term to mid-century at Mzimba, Mzuzu and Nkhatabay under the SSP5-8.5 scenario (Table *4.5*). The only decreasing trends are observed in all stations during the near-term to mid-century SSP2-4.5 scenario. The slope shows a decline of -0.672 to -0.151mm per annum over the time period, with Karonga and Mzimba being the lower and upper limit respectively. The SSP5 shows a rise in precipitation across all time periods with the steepest increase occurring in the far future of 2.05mm to 6.78mm. As opposed to the average monthly precipitation previously discussed, SSP2 shows the highest increasing trend of annual rainfall across the study period of 2.30mm to 7.30mm/year. In all increasing trends and all scenarios, the pattern of lowest to highest value is the same as how the stations are columned in the table below with Mzuzu, Mzimba and Nkhatabay having similar trend patterns but varying trend strength.

Table 4.5:Trend analysis for future annual precipitation

	Metrics	**Bolero**	**Karonga**	**Mzimba**	**Mzuzu**	**Nkhatabay**
SSP2-2021	Kendall's tau	-0.087	-0.066	-0.021	-0.023	-0.021
	p-value	0.329	0.463	0.813	0.804	0.813
	Sen's slope	-0.643	-0.672	-0.151	-0.214	-0.308
SSP2-2051	Kendall's tau	0.232	0.223	0.228	0.228	0.228
	p-value	0.074	0.087	0.080	0.080	0.080
	Sen's slope	2.303	3.426	3.583	5.945	7.298
SSP5-2021	Kendall's tau	0.085	0.186	0.264	0.264	0.264
	p-value	0.521	0.153	**0.042***	**0.042***	**0.042***
	Sen's slope	0.545	2.309	3.296	5.205	6.715
SSP5-2051	Kendall's tau	0.241	0.195	0.218	0.218	0.218
	p-value	0.064	0.134	0.094	0.094	0.094
	Sen's slope	2.055	3.091	3.329	5.620	6.782

* The data showed a significant trend at 95% confidence interval

4.2.2.2 Temperature

The mean monthly maximum temperature over the region is projected to increase across all the scenarios with the temperature range changing from 24-31.5°C to 26-33.6°C, although it is scenario dependent. The temperature ranges for SSP2 and SSP5 are 26.05-32.43°C and 26.05-32.41°C, respectively, in the near-term to mid-century. In the far future, SSP2 will have a maximum temperature range of 26.72-33.05°C whilst under SSP5, the range is from 27.42-

33.6°C. The highest temperature of the year shifts from occurring in November to occurring October in all the scenarios. The monthly temperature rise in the near-term to mid-century is less than 1°C on average across the whole area during most months. SSP5 projects a greater rise in temperature than SSP2 scenario in all the months during each future period. Interestingly, under SSP5 the maximum temperature in the far future is expected to rise by more than 1.5°C all the months with a greater than 2°C increment in January, February, March, April, July and October. This is in contrast with the current observed maximum temperature over the area.

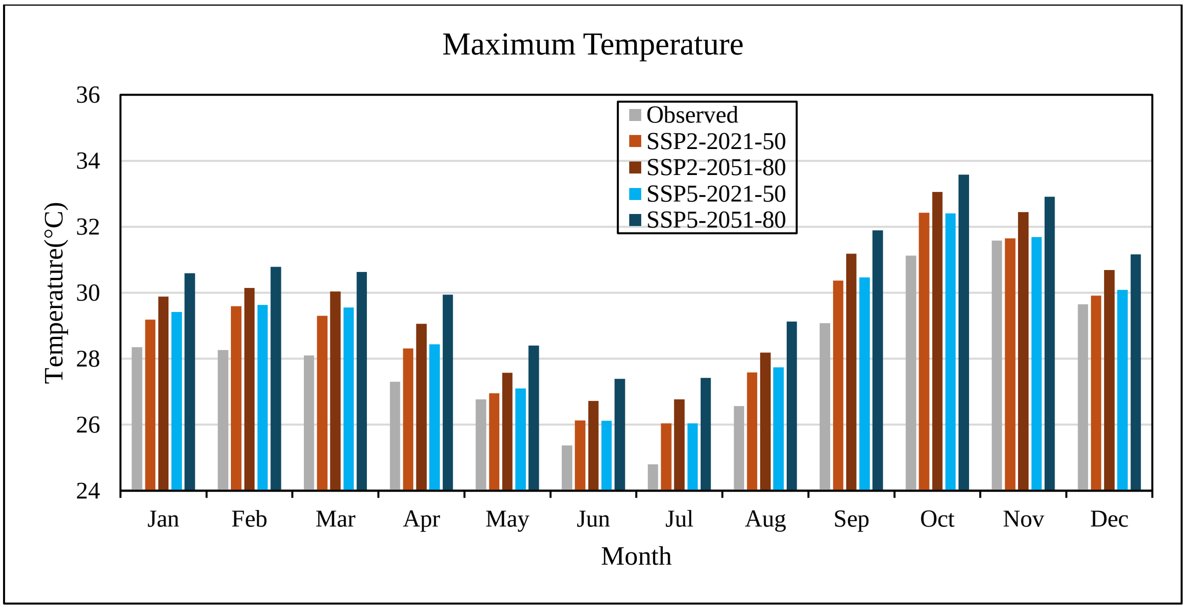

Figure 4.9: Average monthly maximum temperature from 1991-2080.

Table 4.6: Trend analysis for future annual maximum temperature

	Metrics	Bolero	Karonga	Mzimba	Mzuzu	Nkhatabay
SSP2-2021	**Kendall's tau**	0.710	0.680	0.695	0.695	0.694
	p-value	<0.0001*	<0.0001*	<0.0001*	<0.0001*	<0.0001*
	Sen's slope	0.024	0.022	0.021	0.023	0.026
SSP2-2051	**Kendall's tau**	0.287	0.191	0.283	0.237	0.237
	p-value	0.027*	0.143	0.030*	0.069	0.069
	Sen's slope	0.011	0.007	0.011	0.008	0.011
SSP5-2021	**Kendall's tau**	0.641	0.595	0.687	0.729	0.729
	p-value	<0.0001*	<0.0001*	<0.0001*	<0.0001*	<0.0001*
	Sen's slope	0.036	0.028	0.032	0.037	0.040
SSP5-2051	**Kendall's tau**	0.715	0.784	0.747	0.793	0.752
	p-value	<0.0001*	<0.0001*	<0.0001	<0.0001*	<0.0001*
	Sen's slope	0.049	0.045	0.046	0.044	0.056

* The data showed a significant trend at 95% confidence interval

There are significantly increasing trends for annual maximum temperature in all the stations under SSP5 for all future periods whilst for SSP2, an exception to significant trend is observed under the far future period for Karonga, Mzuzu and Nkhatabay (Table *4.6*). Under SSP2, the near-future projects an increment of 0.021-0.0.026°C/year with the rate reducing to 0.008-0.011°C/year in the far future. Meanwhile, for SSP5, the annual increment ranges from 0.028 to 0.040°C in the near-term to mid-century across Northern Malawi. Under the same scenario, the far future portrays a rise in annual maximum temperature of 0.044-0.56°C. The behavior of temperature rise across SSP2 and SSP5 underlies the influence of reducing greenhouse gas emissions as the rate of global warming reduces to 0.1°C per decade as opposed to 0.4°C if left unmitigated.

The monthly minimum temperature bar chart reveals that there is a projected positive change of over 0.5C in the temperature range across the 12 months in all scenarios (Figure *4.10*). The average minimum temperature range changes from 11.08-19.58°C to 12.79-20.18, 13.02-20.16 under SSP2 and SSP5 scenarios respectively, in the near-term to mid-century. This presents a change of 0.6-1.71°C increment in temperature for SSP2 in the near-term to mid-century whilst a rise of 1.1-2.5°C is expected to occur in the far future under a similar scenario when compared to the current climate. Under SSP5, the minimum temperature will increase by 0.58-1.94°C and 1.72-3.61°C in the near and far future respectively. Thus, higher monthly temperatures are expected during the SSP5 scenario than the SSP2 scenario, especially in the far future.

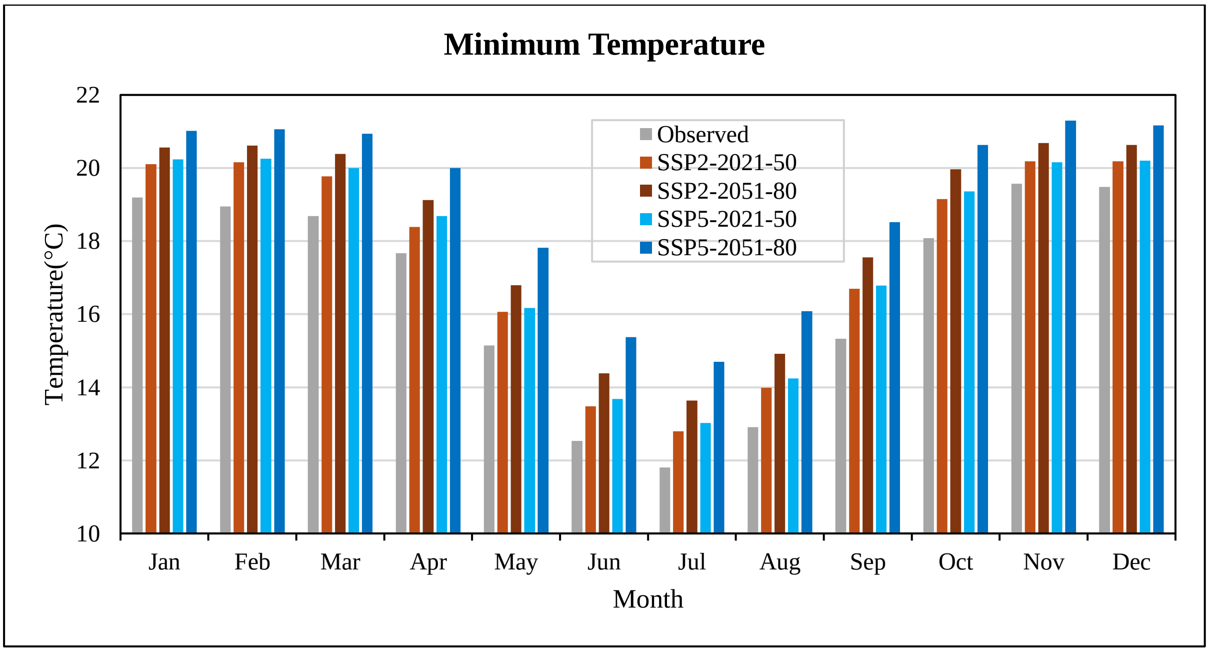

Figure 4.10: Average monthly minimum temperature (1991-2080)

Across all the stations, the projected annual minimum temperature displays significant rising trends in each given scenario and time period. The p-value is observed to be lower than 0.05 in Table *4.7*. There is a 0.02-0.031°C /year increase in minimum temperature under the SSP2 scenario in the near-term to mid-century with a decrease to 0.016-0.030°C /year during 2051-2080. This presents a lower increment in temperature for the far future than in the 2021-2050. SSP5 portrays that the range of temperature trend will increase from 0.029-0.044°C/year to 0.043-0.061°C/year, signifying a higher temperature increment as compared to SSP2. The highest annual minimum temperature trends are observed over Bolero in all time scenarios whilst Mzimba has the lowest trend in the far future in both scenarios.

Table 4.7: Trend analysis for projected minimum temperature

	Metrics	Bolero	Karonga	Mzimba	Mzuzu	Nkhatabay
SSP2-2021	Kendall's tau	0.753	0.753	0.724	0.714	0.736
	p-value	<0.0001*	<0.0001*	<0.0001*	<0.0001*	<0.0001*
	Sen's slope	0.031	0.021	0.020	0.023	0.023
SSP2-2051	Kendall's tau	0.577	0.503	0.522	0.494	0.536
	p-value	8.19E-06*	0.0001*	5.53E-05	0.0001*	3.49E-05*
	Sen's slope	0.030	0.018	0.016	0.021	0.021
SSP5-2021	Kendall's tau	0.641	0.637	0.664	0.655	0.683
	p-value	<0.0001*	<0.0001*	<0.0001	<0.0001*	<0.0001*
	Sen's slope	0.044	0.029	0.031	0.037	0.035
SSP5-2051	Kendall's tau	0.747	0.766	0.761	0.715	0.752
	p-value	<0.0001*	<0.0001*	<0.0001	<0.0001*	<0.0001*
	Sen's slope	0.061	0.042	0.036	0.040	0.043

* The data showed a significant trend at 95% confidence interval

4.2.3 Changes in Climatic Conditions

Figure *4.11* is a map of the spatial distribution of the differences in climatic annual precipitation across the study area. The changes between each 30-year period with the observation dataset ranges from -84.66 to 118.3mm, signifying that there is an increase/decrease in precipitation across the area. In the near-term to mid-century, there will be an overall decline in precipitation across the central and south areas from -3.5mm to -64.4mm with a small area experiencing a decline lower than -65mm under SSP2. Furthermore, the north and eastern side experience a shift in rainfall of -3.5mm to 37.1mm with a moderate zone receiving a 57mm increase in average rainfall. Meanwhile, during the same period, SSP5 shows a similar pattern in terms of rainfall change, although its range is limited to -64.4mm to 57mm with a larger area experiencing a 37-57mm increment than in SSP2. Cutting across to the far-future, the two scenarios depict different changes in rainfall, with SSP2 maintaining a larger area continuing to experience a decline in mean precipitation whilst the opposite is true for SSP5. Under SSP2, only a small area in the eastern side, experiences a rise of 16-37mm in rainfall whilst the average annual precipitation drops by 44.1-84mm in average annual precipitation. The decline in climatic rainfall under SSP2 poses a risk to Northern Malawi's agricultural production and hydrological balance even though a higher increasing trend in annual rainfall is projected over the study area. The difference in direction of trend and accumulative annual precipitation could be due to the occurrence of extreme precipitation. Notably, the same eastern area receives the highest increase in rainfall of 98-118mm under the SSP5 scenario whilst the north and south areas receive 16-98mm rise in annual precipitation mean.

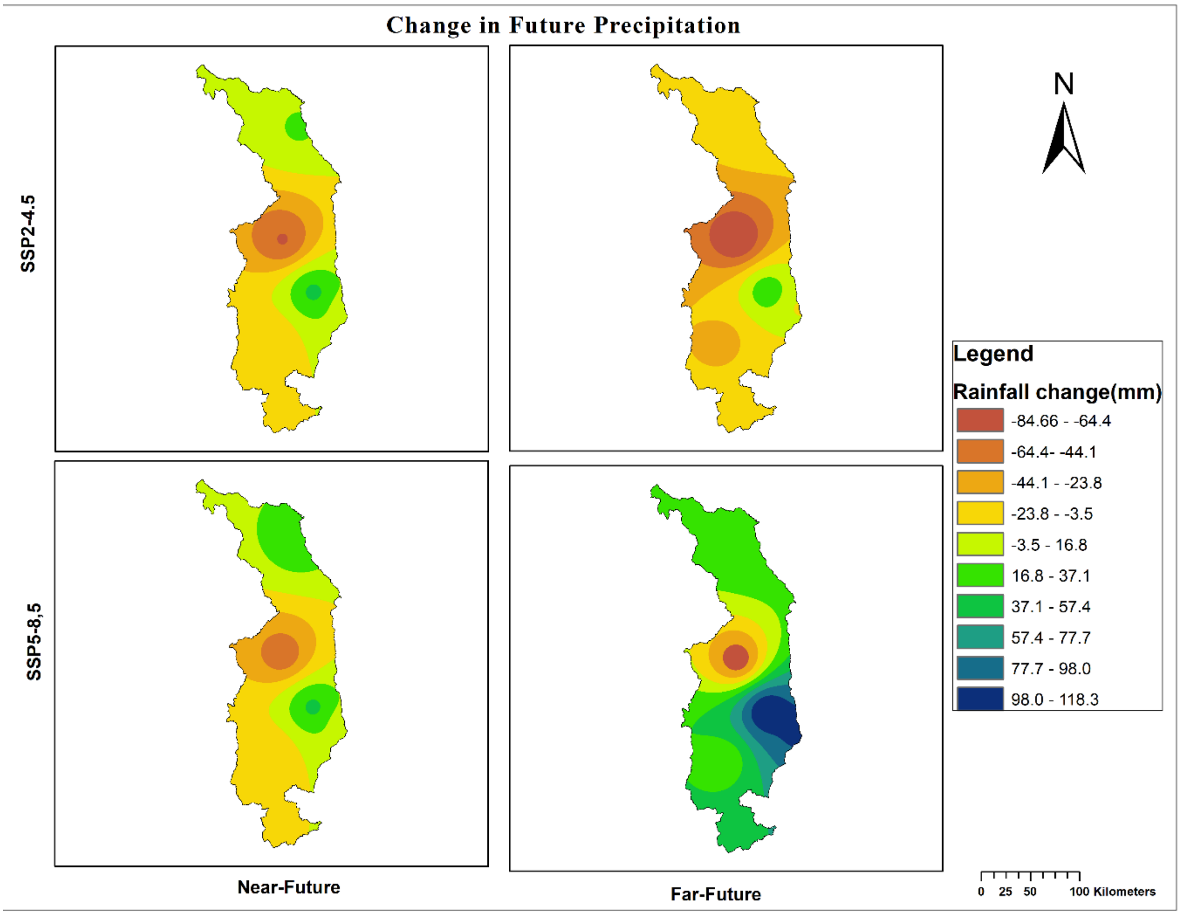

Figure 4.11: Spatial changes in mean annual precipitation.

The average annual maximum temperature over the study period is expected to increase by 0.73-2.51°C between 2021-80 in comparison to 1991-2020(Figure *4.12*). The lower temperature ranges are presented from blue to red with the lower values being in blue. In the near-term to mid-century, Northern Malawi's mean annual maximum temperature will increase by 0.73-0.97°C under SSP2 and 0.85-1.09°C under SSP5. Comparable to a temperature and precipitation projection study over China under SSPs by (Qin, et al., 2021), the temperature change in the far-future is found to be higher 1.32-1.8°C in SSP2 and 1.92-2.51°C in SSP. This signifies that SSP5 leads to a greater shift in temperature than SSP2 and if undertaken, would potentially affect the achievement of limiting temperature increase to below 2°C. In the near-term to mid-century, it can be observed that the northern and southern areas experience the lower shift in mean temperature rise per scenario than the central zone, which experiences the highest shift. During the future period, a similar pattern is also observed in both scenarios with the central area experiencing a rise of 1.56-168°C and 2.27-2.39°C in SSP2 and SSP5 respectively. The temperature shift reduces going to the north and south areas whilst it is highest in a small eastern area. When observing the temperature shift from high to low, a similar spatial pattern is observed in both scenarios with the only difference being that the spatial extent.

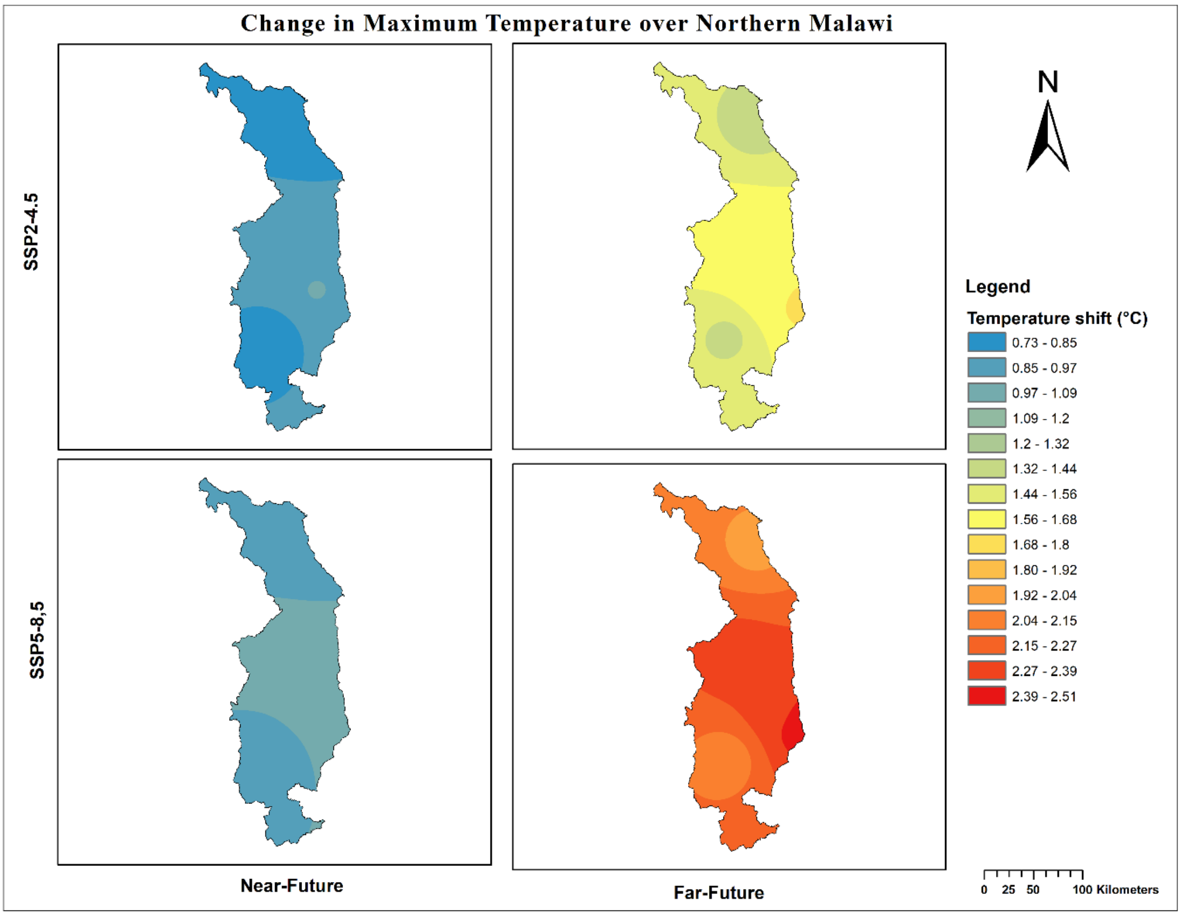

Figure 4.12: Changes in average annual maximum temperature over Northern Malawi

The spatial analysis of the change in average minimum temperature reveals that there is bound to be an increase in minimum temperature in all scenarios ranging from 0.82-3.13°C (Figure *4.13*). The change under SSP2 is 0.82-1.28°C in the near-term to mid-century and 1.28-2.05°C in the far future. In each period, the highest level of change is seen near the central zone whiles the south and north areas experience a low level of change in minimum temperature shift. A large area in the far future is revealed to experience 1.44-1.9°C rise in the climatic minimum temperature. However, under SSP5, the whole northern region is projected to experience a temperature rise of over 2°C with some central areas experiencing a 3.13°C rise in mean minimum temperatures during the same timeframe. This projects a significant increase in minimum temperature in the far future if no greenhouse gas emissions reduction strategies are implemented. Interesting, the distribution of low-high for minimum temperature change follows the same distribution as maximum temperature. This highlights that the regions in the central areas are prone to a greater increment in mean annual average temperature that the outer zones. This could potentially lead to an increase in heatwaves and other temperature extremes as the average temperature would rises.

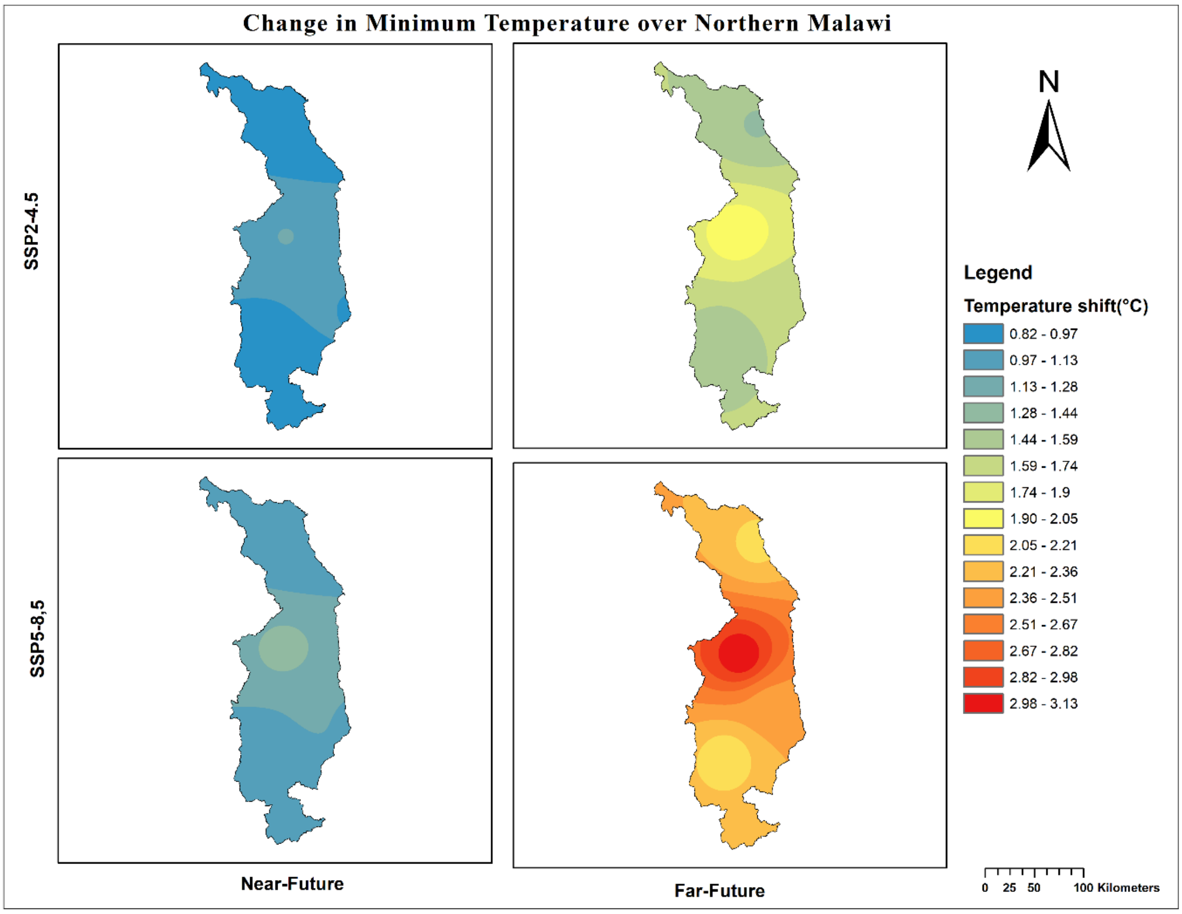

Figure 4.13: Spatial changes in average annual minimum temperature.

4.3 Drought hazard assessment

4.3.1 Historical drought

Seasonal Drought

The values of medium-term drought (SPEI-6) are presented in Figure *4.14*,wherein the red means a dry period, that is occurrence of a climatic water balance below the 0 whilst blue is for wet periods. From this figure and according to the drought classification of -1 means a drought event, it can be observed that Bolero periodically experienced drought from 1992-2017 and that the longest drought runs occurred during 1997-1998 and 2005-06. Interestingly, this period also had extreme drought events occur and the highest extreme drought greater than -4 occurred in 1999. Noteworthy drought cases in Karonga occurred in 1993, 1995,1996, 1998, 1999, 2005, 2007, 2008 with the longest drought happening between 2014-2017. In terms of Mzimba, dry periods occur interchangeably with wet periods but cases of drought of varying intensity can be noted. 1996, 1998, 2005, 2011, 2014, and 2016 mark the years with severe drought cases and runtime longer than 3. Although most areas depict drought cases occurring through 1993-1999, Mzuzu experienced a mostly wet period throughout this timeframe with most of its drought cases coming in the 21st century. This area has experienced 9 drought cases, with 4 severe drought cases, from 2002-2018 as opposed to 2 drought cases in 1991-2001. Notably, the area is experiencing a decrease in annual rainfall which could explain the increase in drought occurrence whilst for Bolero, there is an increment in rainfall which could be the possible factor for occurrence of drought with low severity. Nkhatabay depicts a similar drought pattern to Bolero but with more severe drought cases and longer runtimes. The results capture the 2005/06 and 2016/17 drought cases across the area and also show that the drought run, severity and/or intensity is higher in the 21st century than before, with the only exception being Bolero.

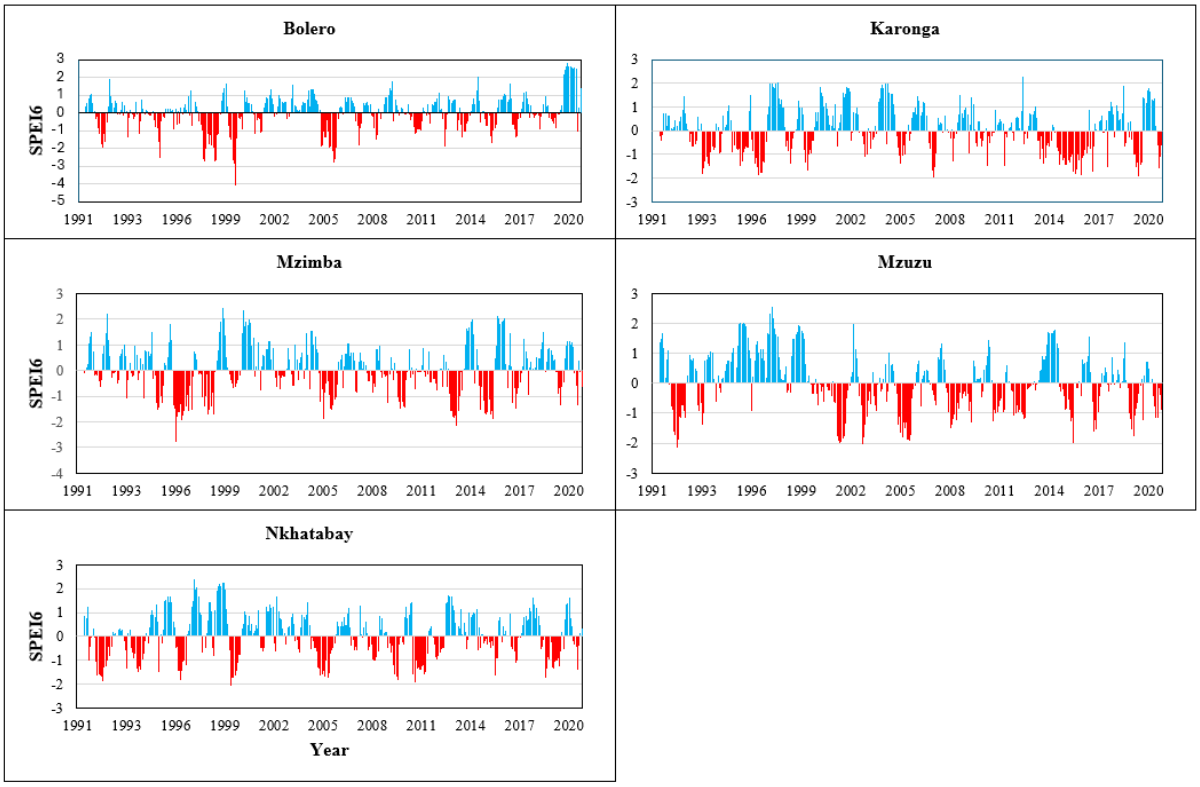

Figure 4.14: Time-series of historical medium-term drought.

In terms of drought runs, Mzimba had the highest number of droughts at 21 whilst Bolero and Karonga had 18 each with Mzuzu and Nkhatabay experiencing 17 and 16 drought events respectively as seen in Table 4.8 below. Although Mzimba had the highest drought cases, its average severity was the lowest at 1.33 with Bolero having the peak severity of 2.19. Notably, the intensity across the region per drought event averages between 0.33-0.53, meaning that severe or moderate cases. From the start to cessation, the drought events over Northern Malawi lasted average period of 3 months per occurrence with Nkhatabay recording the longest drought duration even though it had the lowest drought occurrence.

Table 4.8: Historical drought characteristics (SPEI-6)

Station	**Drought Runs**	**Average Intensity**	**Average Duration**	**Average Severity**
Bolero	18	0.53	3.06	2.19
Karonga	18	0.40	3.44	1.36
Mzimba	21	0.44	2.67	1.33
Mzuzu	17	0.33	3.24	1.47
Nkhatabay	16	0.39	3.94	1.66

Moderate drought occurs more frequently in Northern Malawi than extreme drought as observed from the drought frequency map (Figure *4.15*). Moderate drought has a 0.068-0.114(6-11%) chance of occurring in any given month over the 30-year period whilst extreme drought has the lowest frequency of 0-3.4%. The north and south-east areas have the highest frequency of 10.3-11.4% when it comes to moderate drought with decreases when moving towards south and westward zones. Interestingly when compared to the other areas, the central area has the lowest frequency of 0.068-0.08, and 0.034-0.046 in moderate and severe drought but the highest frequency for extreme drought (0.023-0.034). Such results are similar to the ones obtained in the study by (Lim Kam Sian, et al., 2023). They observed that regions of frequent extreme drought tend to have a lower occurrence of severe and moderate drought occurrence. Although extreme drought cases are of lower occurrence than severe and moderate drought, they nonetheless have a big impact on agriculture, and hydrological balance.

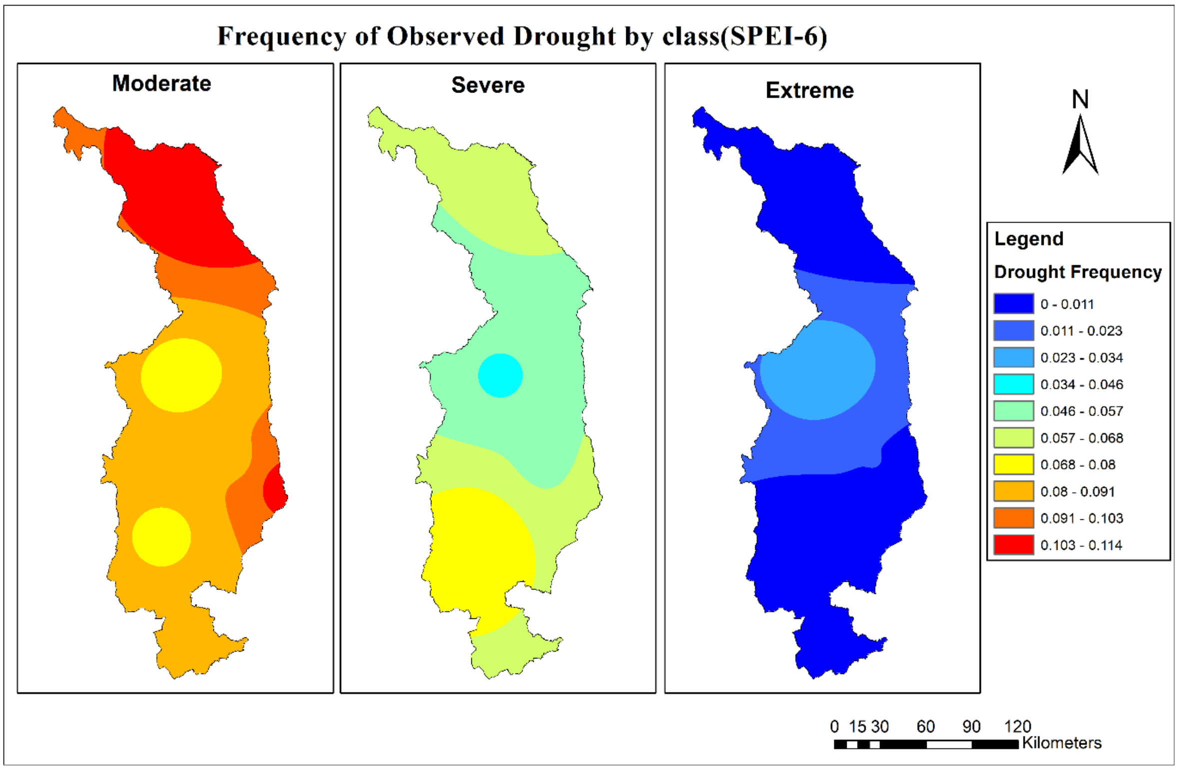

Figure 4.15: Historical medium-term meteorological drought

Long-term drought

It was observed that temporal characteristics of drought differ per station although most stations portray an increment in drought duration during the 21st century except for Bolero as observed in Figure 4.16. Bolero experienced moderate drought in 1993, 2011, 2014, and 2016, and extreme drought coinciding with an extended dry period from 1997-2000, and 2005-2006. The 1997-2000 drought was the longest and severest drought throughout the 1991-2020 period. However, for Karonga, Mzuzu, Nkhatabay and Mzuzu, drought of longer duration occurred in the recent decade(2010s). At Mzuzu, droughts have become commonplace with extended dry periods observed throughout 2000-2020 with 2014-2015 marking the only period with an extended wet period. Extreme drought occurred in the area through 2002-2006 with moderate drought in 2008 and 2011 having the longest runtime and short respite in between. 2014-2017 marked a period of the longest and severest drought case in Karonga which coincides with the 2015/2016 report agricultural drought. From 2005-15, drought occurred frequently over Mzimba with low wet periods observed during this period whilst Nkhatabay also exhibited the same thing but at a lesser severity. Nearly all the stations experiencing longer and/or multiple severe droughts 2005-2016, and this timeframe is the same as the reported major drought cases over the area. Notably, 1996-1999 also marks a period with one or two droughts for all stations except for Mzuzu which experienced an extended wet period from 1993-2000.

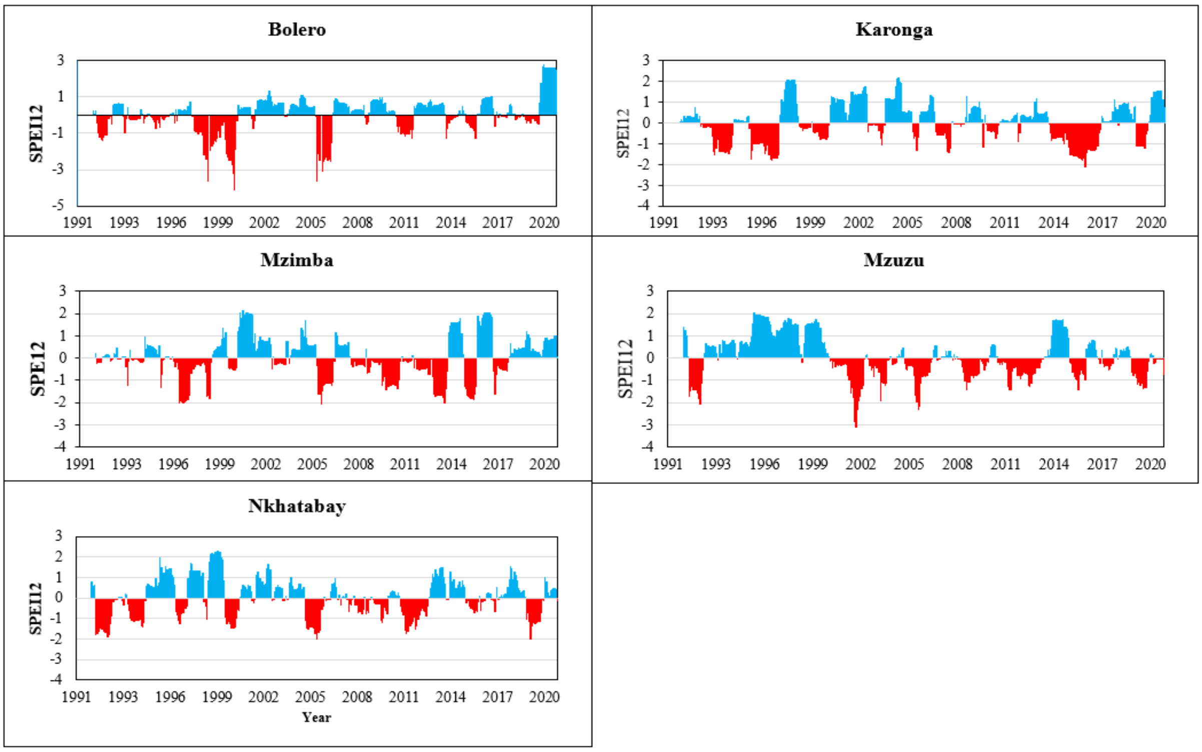

Figure 4.16: Time series of 1991-2020 historical long-term drought.

There is occurrence of 10-13 long-term drought events across Northern Malawi with Bolero recording the highest number of droughts (Table *4.9*). This station, Bolero, also records the highest mean intensity and mean severity per drought even though it has the shortest drought duration. Its mean intensity of 0.74 shows that extreme drought occurred more at Bolero than Mzuzu (0.41), Mzimba (0.51), Karonga (0.29) and Nkhatabay (0.31). Karonga and Nkhatabay, two lakeshore stations, record the highest mean runtime per drought of more than 6 months whilst recording the least drought severity, and intensity. The duration of drought over Mzimba and Mzuzu usually falls within the 5-month period whilst the severity is low at Mzuzu (2.59) and high at Mzimba (3.29). Interestingly, this study found that severity and duration of long-term drought was nearly double that of short-term drought in all the stations, which is similar to the findings over Burundi (Ndayiragije & Li, 2022) and Poland (Kubiak-Wójcicka, Owczarek, Chlost, Olszewska, & Nagy, 2023) .Even though there is a smaller number of droughts occurring the long-term compared to medium-term, the higher drought intensity over Bolero and Mzimba highlights a longer and stronger shift in the climatic water balance over Northern Malawi occurred during long-term drought conditions than medium-term conditions.

Table 4.9: Historical long-term drought characteristics

Station	**Drought Runs**	**Mean Intensity**	**Mean Duration**	**Mean Severity**
Bolero	13	0.74	3.77	3.29
Karonga	11	0.29	6.18	2.44

Mzimba	10	0.51	5.90	3.29
Mzuzu	10	0.41	5.00	2.57
Nkhatabay	11	0.31	6.27	2.53

Across Northern Malawi, moderate and severe long-term drought events were found to be more frequent than severe drought cases, with the only exception being the central area where the extreme drought was more frequent than the severe drought (Figure 4.17). The north and south-western zones areas were found to experience moderate drought at 0.09-0.126(9-12.6%) whilst extreme drought occurred less frequently at 0.002-0.015(0.2-1.5%) during the 1991-2020 period. The Compared to the other zones in Northern Malawi, the south area experiences a moderate chance of severe, moderate and extreme drought at 0.2-9% with extreme drought being the lowest. Areas of high extreme drought occurrence are notably different from those with frequent occurrence of severe and moderate drought. Additionally, the drought frequency pattern of SPEI12 was similar to the one for SPEI6 with the major difference being that the spatial coverage of areas of high extreme drought frequency, and low severe drought frequency are larger in SPEI12.

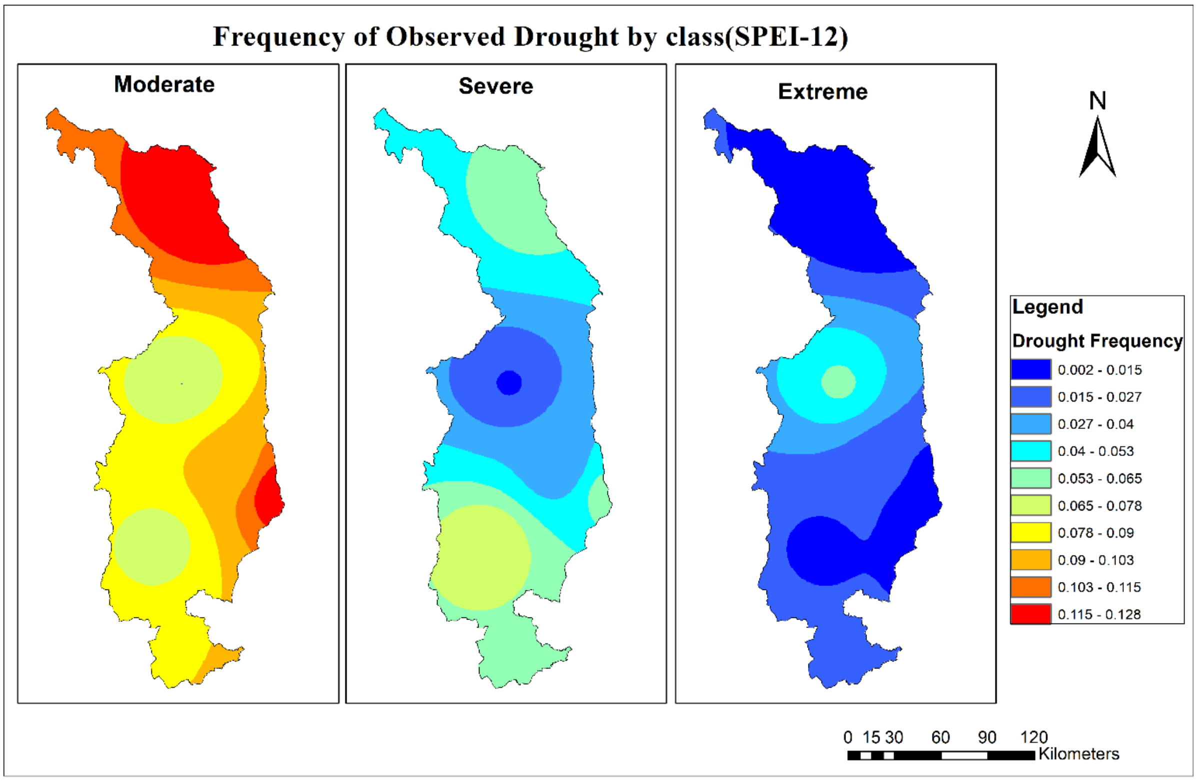

Figure 4.17: Map of historical meteorological drought frequency (SPEI12)

4.3.2 Near-term to mid-century drought

4.3.2.1 Seasonal Drought

The results of near-term to mid-century drought occurrence reveal that seasonal drought (SPEI) is projected to follow a similar pattern across the stations under the SSP2 scenario as seen in Figure *4.18*. Particularly, the major difference was the duration, runtime and severity of each individual drought case. For instance, 2021-2030 was a period of moderate-severe drought occurrence for all the station with each station recording at least one severe drought in 2023, except for Karonga and Bolero which both experience two moderate droughts. Although this period had recurring dry events, longer wet events were observed as opposed to succeeding decades. From 2030-40, it was found that drought increased in occurrence, severity and runtime with severe droughts observed during 2032, 2033, and 2035, and an extreme drought in 2038 across all the station. Interestingly, 2044-47 marks the period with the longest drought occurrence that coincided with periodic dry periods that increased drought severity. Increasing drought severity, occurrence and duration during 2030-50 can be attributed to the decreasing rainfall trend and increasing temperature observed over this time period.

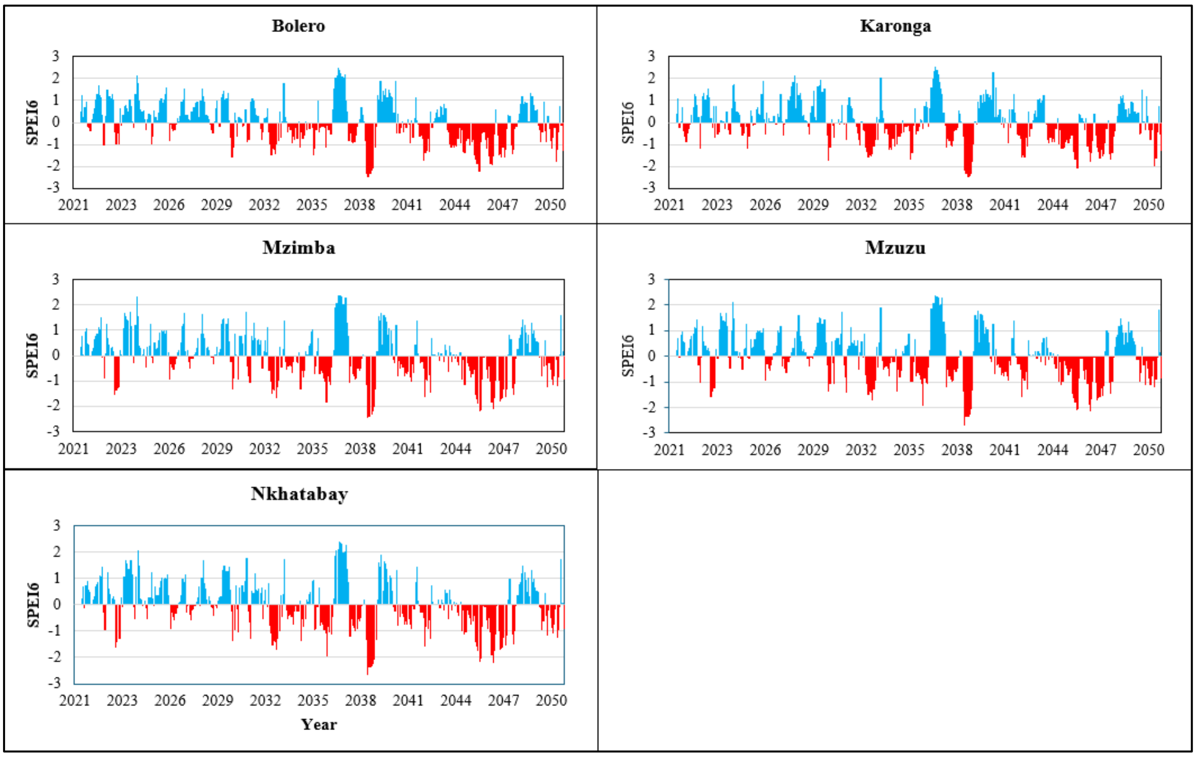

Figure 4.18: Time-series of near-term to mid-century medium-term meteorological drought under SSP2 scenario.

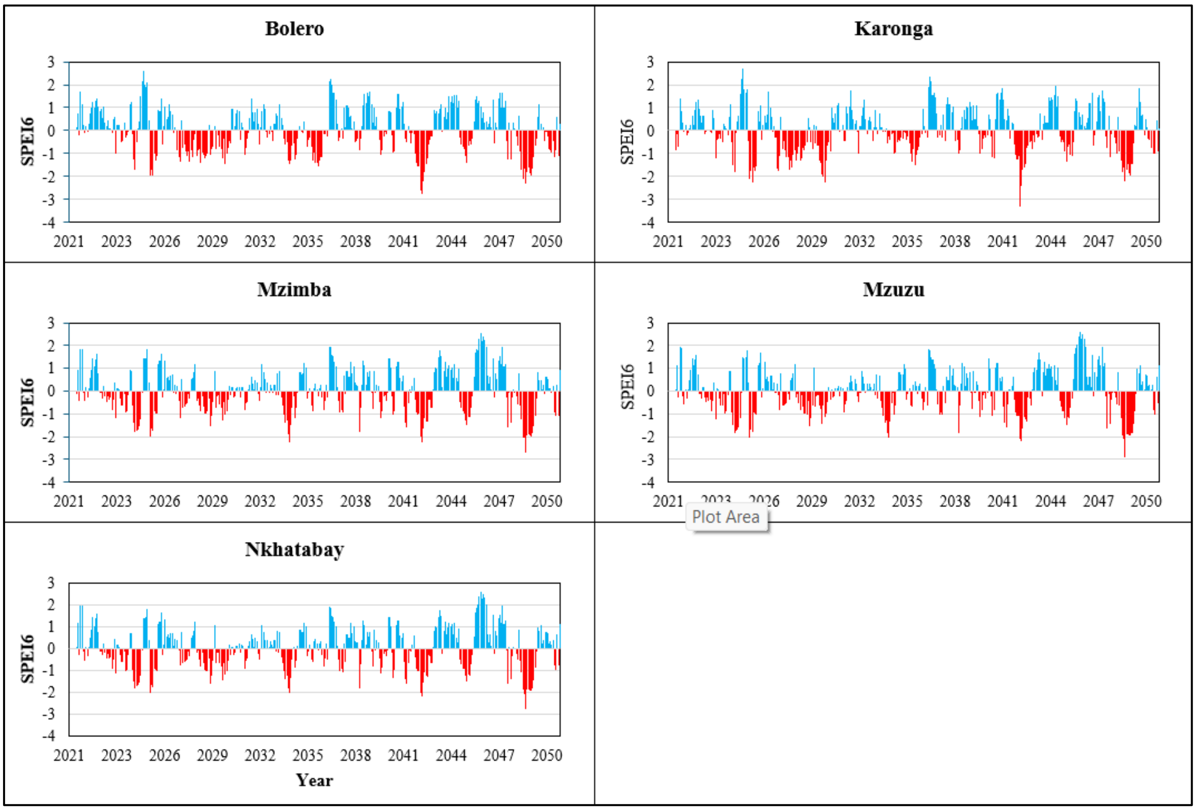

Figure 4.19:Time-series of near-term to mid-century medium-term meteorological drought under SSP5.

Meanwhile, under the SSP5 scenario, the meteorological drought portrays a different scenario of severe and extreme droughts occurring between 2023-2029, and 2041-2050 whilst 2030-40 features moderate droughts across all the stations (Figure *4.19* above). Notably, the longest drought was a moderate drought between 2026-2029 for all the stations with Karonga being the only exception whereby the moderate drought evolved into a severe drought in 2030. The most intense drought is shown to occur in 2041 with values reaching -3.2 at Karonga and -2.8 at Bolero, whilst for Mzuzu, Mzimba and Nkhatabay, 2047 marked the most intense drought event. Thus, showing 2040-50 is the decade with significant drought occurrence in terms of frequency or magnitude under both scenarios. Different to SSP2, dry and wet periods occur interchangeably throughout SSP5 with wet periods greater than 1 being more frequent. Extreme drought runs are found to have occurred more be occurring more than in the historical period over all the stations except for Bolero. There is comparatively a lower drought duration under SSP5 scenario than under SSP2, most likely due to more drought runs under SSP5.

4.3.2.2 Long-term drought

The results of the long-term meteorological drought in Northern Malawi reveals that 2021-30 is a relatively wet period across all the stations with a few minor dry periods but no significant drought case as noted in Figure *4.20*. However, going closer to the mid-century, the drought events would be more frequent and with a longer duration as dry periods become more recurrent than wet events. Results note drought occurrence in 2032, 2035, 2038, 2039, 2042, 2044,2045,2046, 2047, and 2050 for all the stations. With 2044-2047 being the longest dry period, it was observed that one drought extends into another drought case creating a problem in identifying the cessation and starting points resulting in a chain of droughts being observed as one drought. Interestingly, 2038-39 has recuring months of severe and extreme droughts of highest intensity for all station with Karonga portraying the most intense extreme drought. Notably, the droughts during 2032-2050 occur for longer durations with less wet periods between them underpinning the possible influence of decreasing rainfall trend. Additionally, Karonga experiencing the highest drought intensity and severity adds to the notion of declining in rainfall increasing drought severity. As earlier observed, Karonga experienced the highest rate of decline in rainfall of 0.67mm/year when compared to the other stations. Furthermore, compared to the medium-term drought, the longer duration and higher severity of long-term droughts depicts a grim picture for the hydrological sectors as longer long-term meteorological drought correlate with the hydrological drought occurrence (Medeiros & Silva, 2024; Li, et al., 2022).

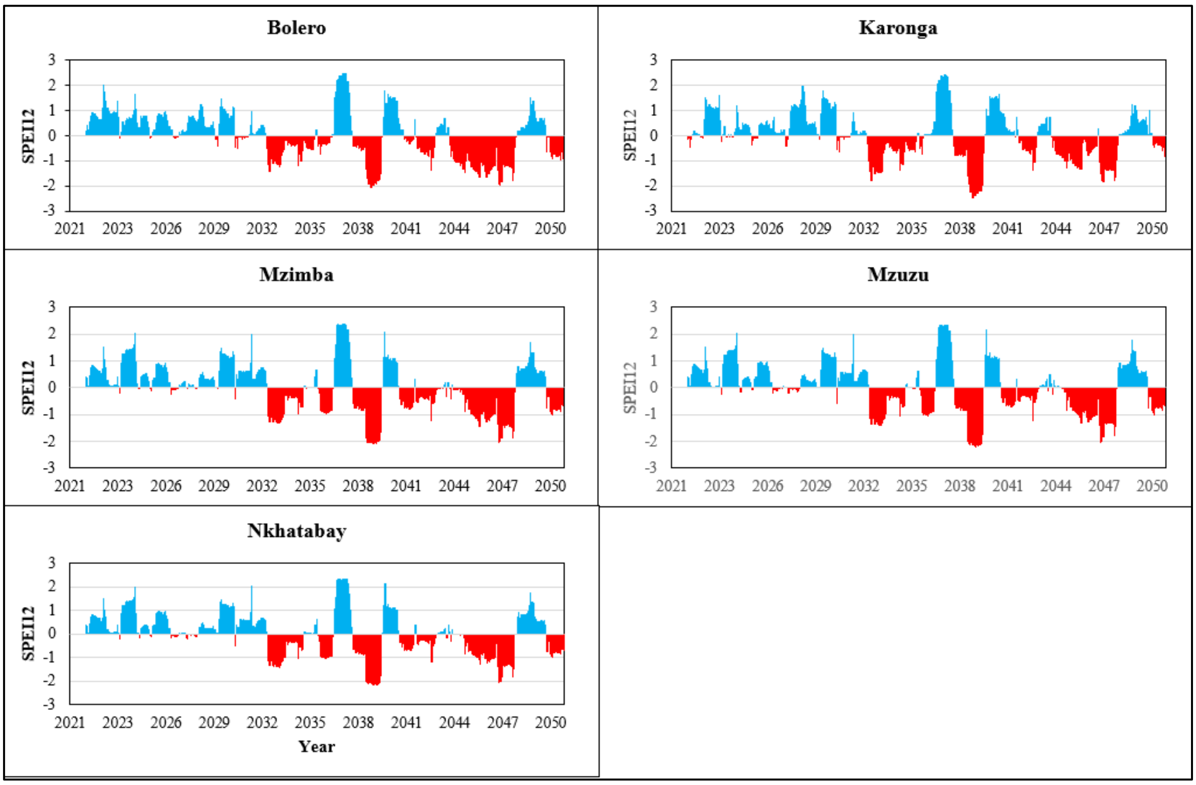

Figure 4.20:Time-series of near-term to mid-century long-term meteorological drought under SSP2 scenario.

Under SSP5 scenario, the near-term to mid-century period displays elongated periods of wet events and dry events with dry events dominating from 2027-2030, 2033-2036, 2041-2044 and

2048-2050 as seen in the Figure 4.21 below. Notably, these drought events recorded some values below -1 and evolved into drought with the 2027-2030 being the longest moderate drought duration across all stations. These results also show that 2048-50 was an extreme drought event of very high severity across all the stations although with varying degrees of intensity. All the stations show a similar drought occurrence pattern with slight differences which could possibly be due to their different temperature and rainfall conditions. For instance, Mzimba, Mzuzu and Nkhatabay are projected to have increased rainfall trend of different magnitude but of a similar ranking distribution which could be the possible factor towards the similar drought occurrence between these stations.

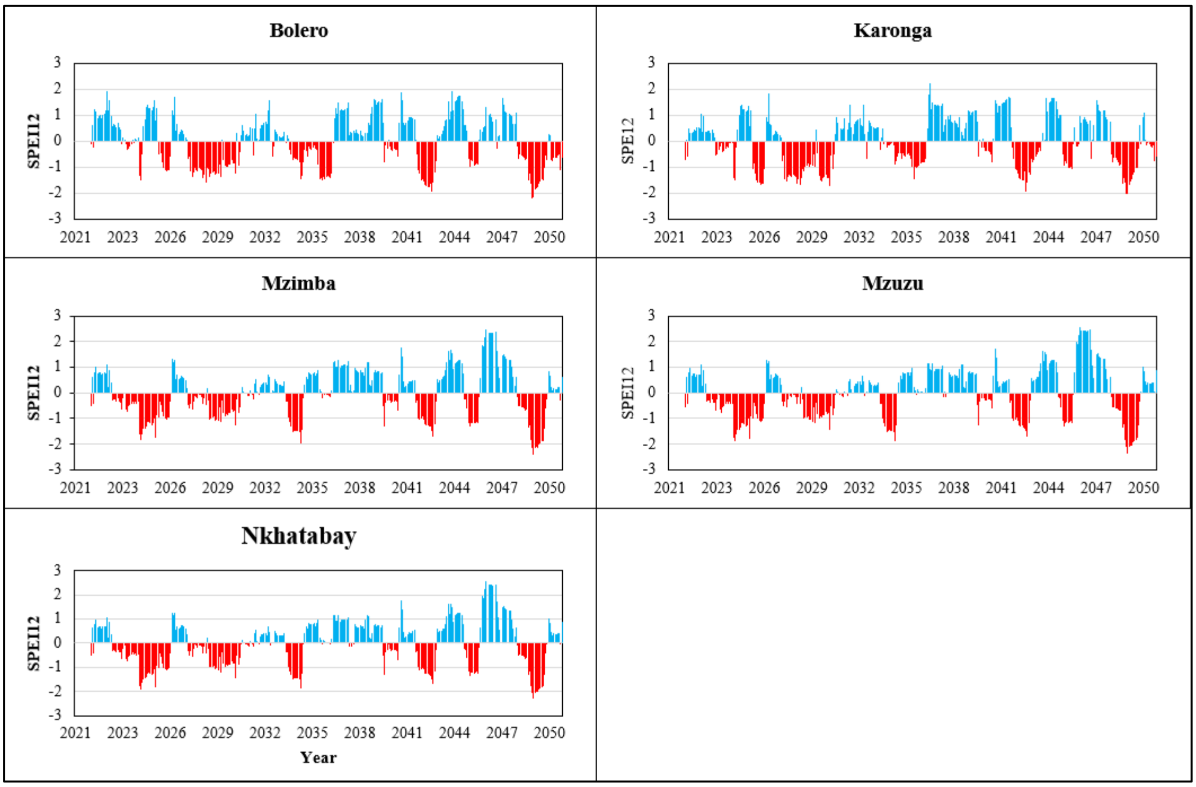

Figure 4.21:Time-series of near-term to mid-century long-term meteorological drought under SSP5 scenario.

4.3.3 Mid-century to End-century drought

4.3.3.1 Seasonal Drought

Across 2051-80, there is an observable decrease in the drought intensity in all the stations when cross-examining drought characteristics between 2051-65 and 2065-2080 periods under the SSP2 scenario (Figure *4.22*). Particularly, extreme droughts are observed to be a rare occurrence during the last 15 years with Bolero and Karonga having no extreme drought occurring after 2065. The decreasing drought intensity and severity could be a product of a slow temperature increase combined with increasing rainfall during this period. The results indicate the 2064 drought as the most intense extreme droughts across all the stations, but subsequent reduction to lower drought levels.

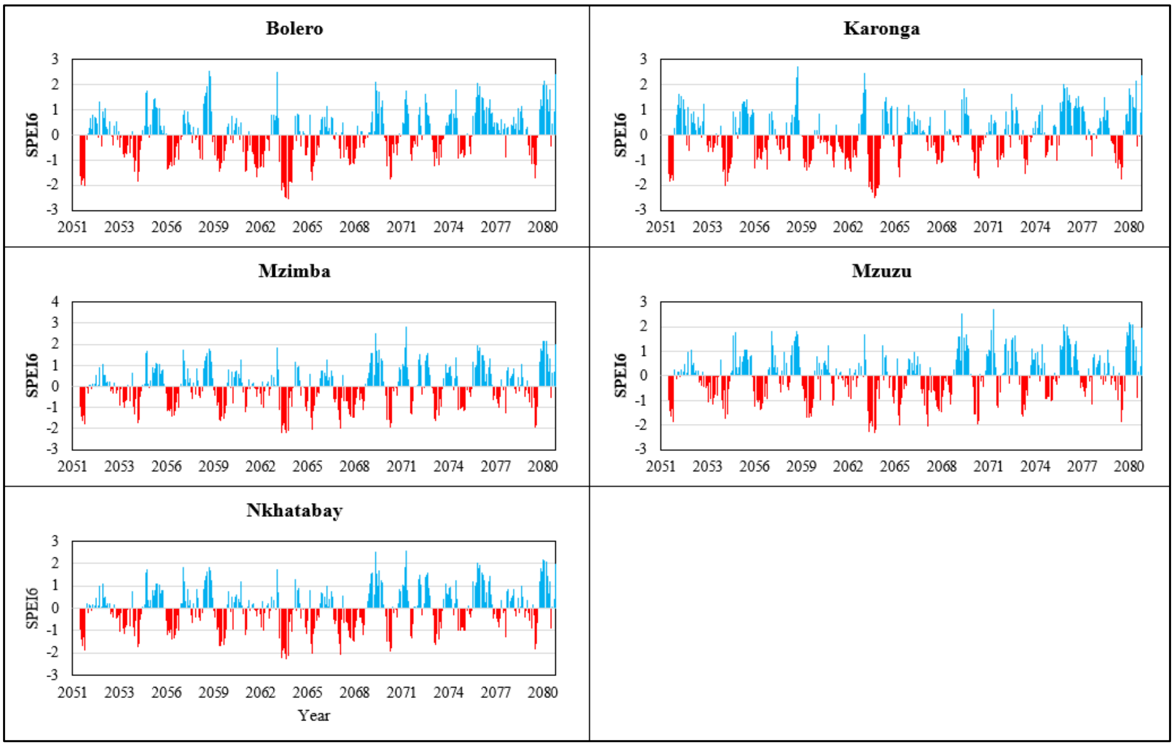

Figure 4.22: Time-series of mid-century to end-century medium meteorological drought under SSP2 scenario.

Interestingly, meteorological droughts under SSP5 scenario (Figure *4.23*) follow a near parabolic drought pattern in terms of intensity as there is an observable decline succeeded by an increase in dry events between 2063-2070 especially for Bolero and Karonga. The mid-century decadal period is observed to contain the most extreme drought with longest severe droughts, particularly over these two stations. Even though Bolero and Karonga display similar drought characteristics, there is a notable lower intensity of drought over Karonga. A possible influence of this could be the higher rate of increment rainfall over Karonga combined with lower temperature increment than Bolero. The 2053 drought is shown to be the most extreme drought with Mzuzu, Nkhatabay and Mzimba having a SPEI value of -2.67. Notably the drought pattern is nearly identical between Mzuzu and Nkhatabay even though the three stations have an identical drought occurrence pattern. This could be due to the presence of similar trend strength between the stations' future precipitation with time even though the rate of precipitation change is different. The stations portray higher drought intensity and severity levels in this scenario than under SSP2, especially in the 2070s.

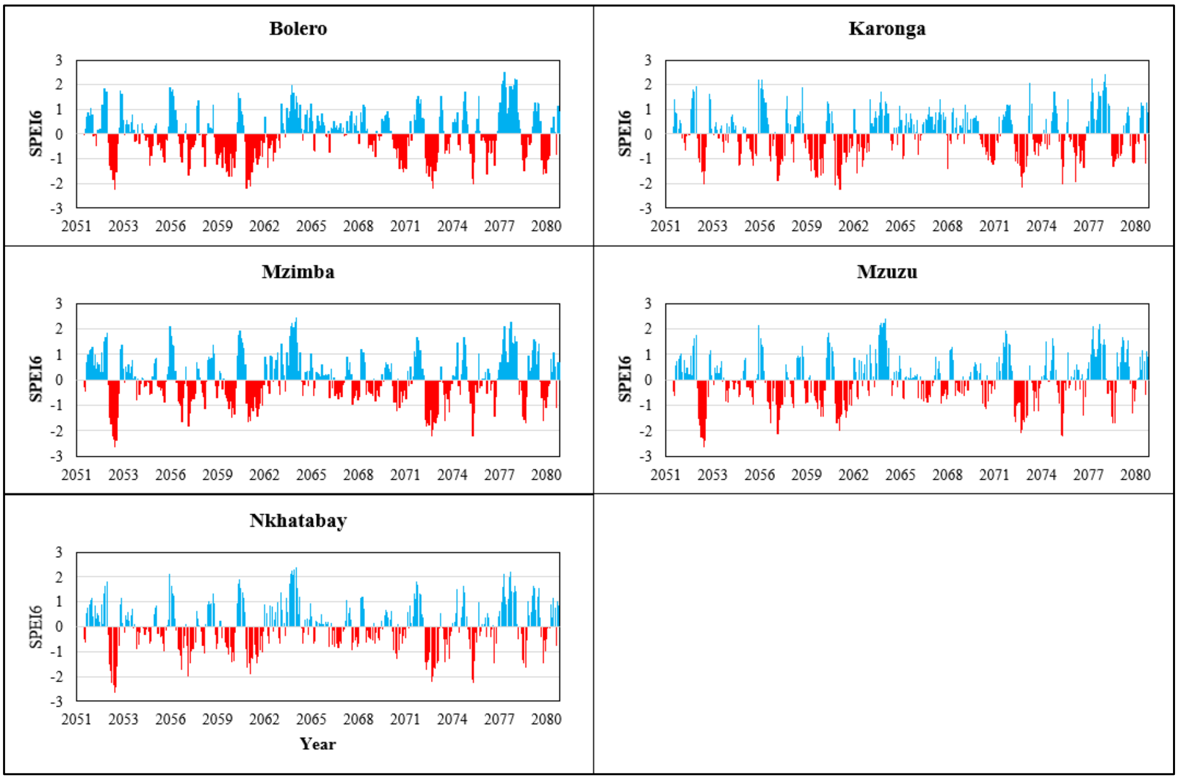

Figure 4.23: Time-series of mid-century to end-century medium-term meteorological drought under SSP5 scenario.

4.3.3.2 Long-term drought

Compared to medium-term drought, the SSP2 long-term meteorological drought analysis(Figure *4.24*) presents a similar decrease in drought intensity, duration and severity towards the 2070s with nearly 2 or 3 moderate droughts occurring in this decade. The decline in extreme drought occurrence and reduction in severity could be due to occurrence of higher precipitation during this time as an increasing trend of rainfall was observed in Table 4.5. Through 2070-80, the dry periods appear sporadic and of a very short duration whilst wet periods dominate. An extreme drought of long duration is observed in all stations between 2064-2065 with Karonga and Bolero having the highest intensity of -2.52. The results indicate the occurrence of moderate and severe droughts is higher than extreme droughts in Mzuzu, Bolero, Mzimba, Nkhatabay and Karonga.

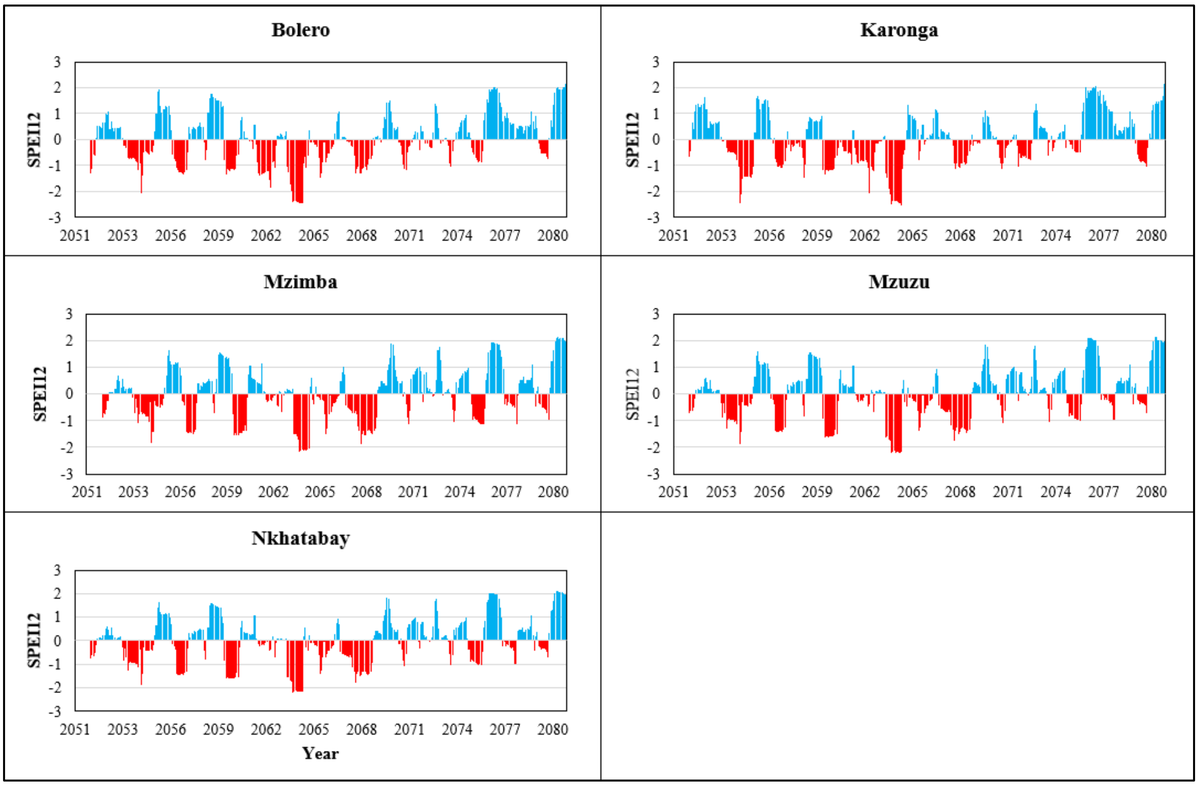

Figure 4.24:Time-series of mid-century to end-century long-term meteorological drought under SSP2 scenario.

However, under SSP5, drought intensity is observed to be nearly the same throughout 2051-80 with the only drought free period being the 2060s in all the stations (Figure *4.25*). Observations indicate that the most extreme drought would occur in 2053 for all stations except for Karonga which shows lower drought intensity compared to the other stations. Notably, Bolero and Karonga portray an increased period of persistent wet events during 2063-68 whilst Mzuzu, Mzimba and Nkhatabay show that dry periods will occur from 2067 that will evolve into 2068 moderate drought. The late 70s are dominated by reduced intensity of dry events with no drought event which is somewhat similar to the SSP2 scenario. Although fewer drought periods were identified during the long-term drought as opposed to the medium-term meteorological drought for all the two scenarios, the droughts tend to occur over a longer duration especially under the SSP2 scenario. Interestingly, the severity of drought is also high in the long-term due to the longer timeframe even though the mean drought intensity is lower. Furthermore, there is a notable increase in drought events over the stations with some shifts in the number of severe, moderate and extreme drought months when compared to SSP2. For instance, Karonga experiences an increase in drought events with declining extreme droughts and increasing severe and moderate drought in the far future SSP5 scenario.

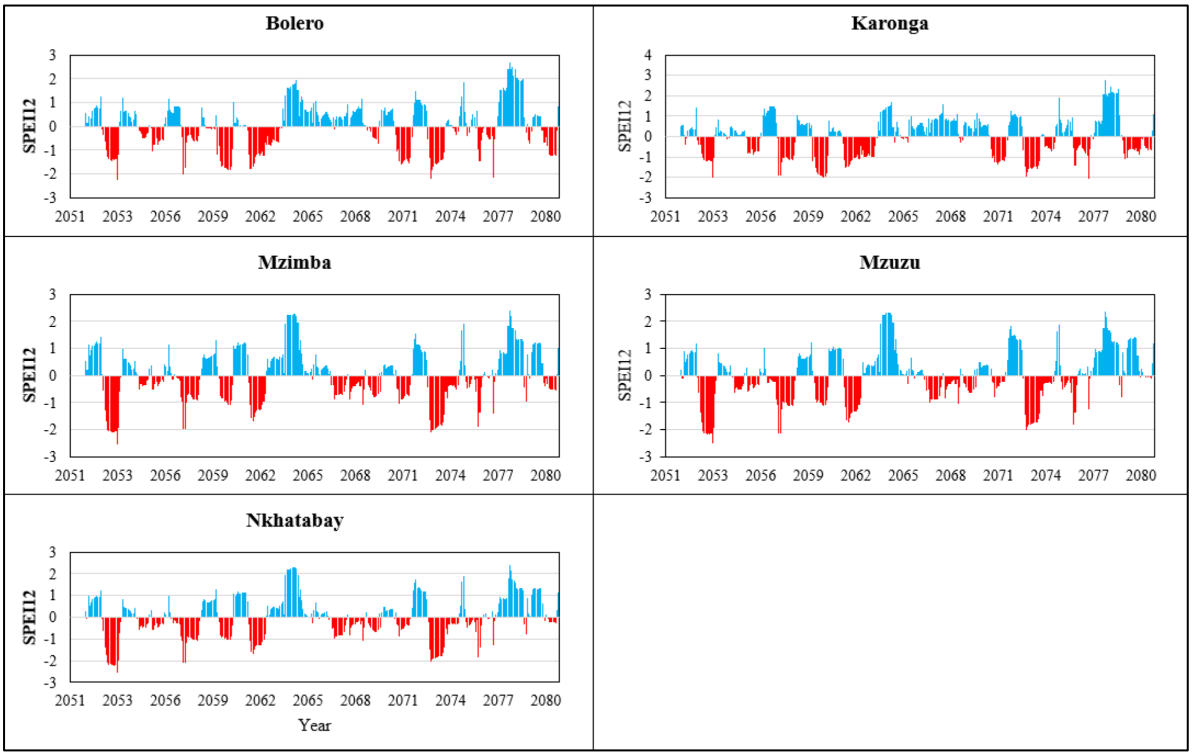

Figure 4.25:Time-series of mid-century to end-century long-term meteorological drought under SSP5 scenario.

4.3.4 Changes in drought characteristics

4.3.4.1 Seasonal drought

A comparative analysis of the future drought characteristics against current drought conditions reveals that the changes in drought differ in magnitude and direction. Table *4.10* shows the changes in the average drought intensity and severity of future drought event for each scenario and period. In the near-term to mid-century, drought would reduce in intensity by 7-36% under SSP2 scenario whilst a greater degree of decline is projected to occur under SSP5 in all the stations except for Mzuzu, Karonga and Nkhatabay. Under SSP5, Mzuzu would experience an increase in drought intensity with a further increase in severity as compared to the SSP2 scenario. The decline in average drought intensity could be due to a reduction in the rate of rainfall change from -16/year to 0.6mm/year. Under SSP2, the mid- to end of century period is predicted to have a higher intensity than 2021-50 but lesser than 1991-2020 even though more rainfall would occur during this period.

Table 4.10: Changes in drought intensity and severity

	Mean Intensity				**Mean Severity**			
Station	**SSP2-2021**	**SSP2-2051**	**SSP5-2021**	**SSP5-2051**	**SSP2-2021**	**SSP2-2051**	**SSP5-2021**	**SSP5-2051**
Bolero	-36%	-33%	-50%	-24%	-42%	-30%	-52%	-42%
Karonga	-14%	-12%	-14%	-18%	-6%	0%	13%	-24%

Mzimba	-16%	-18%	-17%	-9%	3%	-7%	5%	5%
Mzuzu	-7%	9%	5%	26%	-23%	-19%	-31%	1%
Nkhatabay	-11%	-11%	-7%	10%	-21%	-25%	-20%	-6%

The results indicate an increase in drought severity across Mzimba under all the scenarios with the only exception being the far-future SSP2. This portrays the possible impact of a reduced rate of temperature increment combined with the increment in rainfall across this station. However, the highest level of increment in drought severity and intensity is expected in the SSP5 scenario particularly for Mzuzu and Nkhatabay even though there is a greater increment in rainfall under this scenario. Thus, the direct influence of rainfall and temperature change over drought can be argued to be non-linear and area dependent. Furthermore, the highest decrement in all scenarios is observed at Bolero even though it is projected to have increased occurrence of drought in all scenarios except for far-future SSP2(Table *4.11*). Additionally, even though Table *4.11* shows that the average drought duration will be reduced in all scenarios except for Mzimba, it is noted that the occurrence of drought increases, particularly at Nkhatabay. Interestingly, there is a higher increment in drought occurrence for Bolero under SSP5 in both the far and near-term to mid-century whilst for the other stations, it is scenario and period dependent.

Table 4.11: Change in drought duration and number of droughts

Station	**Average Duration**				**Drought Runs**			
	SSP2-2021	**SSP2-2051**	**SSP5-2021**	**SSP5-2051**	**SSP2-2021**	**SSP2-2051**	**SSP5-2021**	**SSP5-2051**
Bolero	-14%	4%	-19%	-14%	3	0	8	4
Karonga	-23%	-20%	-13%	-26%	4	2	1	7
Mzimba	-1%	2%	1%	-6%	-1	1	-1	-1
Mzuzu	-25%	-27%	-21%	-19%	7	6	5	1
Nkhatabay	-35%	-41%	-32%	-28%	5	8	5	1

A spatial map of the changes in drought frequency for all scenarios and periods indicates that an 0.004-0.031(0.4-3%) increase in extreme drought occurrence is projected for a large section of Northern Malawi with the only decline being at the central zone (Figure 4.26). The locations of increased moderate and severe drought match the locations with decreasing rainfall and increased temperatures observed when analyzing for changes in future climatic conditions. The central zone in particular experiences a 0.029-0.048(2.9-4.8%) addition in occurrence1moderate drought.

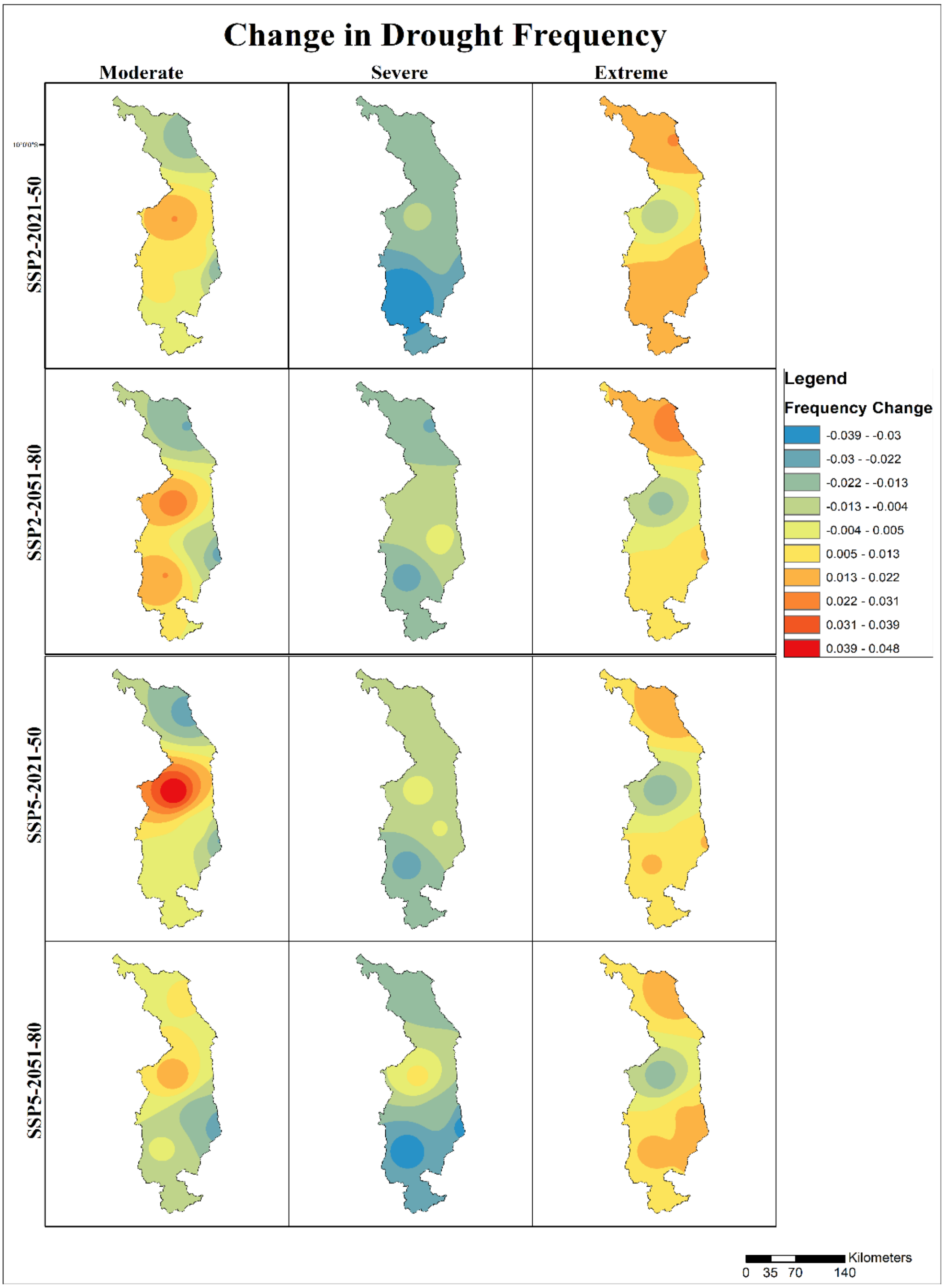

Figure 4.26: Projected changes in medium-term meteorological drought frequency.

Under SSP2, the north area is projected to decrease in moderate drought occurrence with an opposite effect over the south zones. Interestingly, the far-future SSP5 paints a grim picture of increasing moderate drought frequency over the north as opposed to the south. Whilst extreme droughts are projected to occur more frequently in the near-term to mid-century SSP2 than SSP5, possibly due to the reduction in precipitation, the far-future SSP5 shows that a large area will experience values of 0.013-0.022 as compared to SSP2. Severe droughts would occur less in the southern region and more in the central region, especially under the SSP5

4.3.4.2 Long-term drought

SPEI12 reveals a decrease in drought intensity of 9-56% for near-term to mid-century with a further 3-57% decline observed in the far future under the SSP2 scenario (Table 4.12). Karonga is the only exception with Table 4.12 revealing a 47% increase in drought intensity during 2021-50, possibly due to the greater decrease in rainfall than the rest of the stations. Similarly, Nkhatabay, Mzuzu and Karonga experience an increase in drought severity during the near-term to mid-century. Comparative assessment of the change in intensity and severity between SSP2 and SSP5 shows that during 2021-50, there is a greater decline in these characteristics under SSP5 than SSP2. This could be attributed to the projected increment in rainfall under the SSP5 as SSP2 revealed a lower temperature rise than SSP5. Furthermore, in the future SSP2 displays a higher reduction in intensity and severity of 1-57% than SSP5(-8 to -38%). Furthermore, under SSP5.Karonga, Mzuzu and Nkhatabay show increase in drought intensity and/or severity.

Table 4.12: Change in average long-term meteorological drought severity and intensity

Station	Intensity				Severity			
	SSP2-2021	SSP2-2051	SSP5-2021	SSP5-2051	SSP2-2021	SSP2-2051	SSP5-2021	SSP5-2051
Bolero	-56%	-59%	-57%	-38%	-9%	-41%	-25%	-23%
Karonga	47%	-3%	-1%	8%	70%	-7%	-11%	-19%
Mzimba	-37%	-36%	-48%	-10%	-2%	-28%	-32%	-3%
Mzuzu	-30%	-7%	-37%	-7%	13%	12%	-20%	15%
Nkhatabay	-9%	6%	-11%	28%	14%	-4%	-11%	27%

The study found a higher increase in drought duration in the near-term to mid-century under the SSP2 scenario than SSP5 even though there is a decline in number of drought (Table *4.13*). This increase in drought duration could be attributed to the decreasing trend in rainfall combined with an increase in minimum and maximum temperature. However, in the far-future, duration in Nkhatabay, Mzimba and Karonga will be lower than current and SSP5 drought duration. Bolero was found to have a higher duration combined with reduced drought runs, intensity and severity in all scenarios which under further analysis was attributed to a decline in extreme drought occurrence. Meanwhile, the reduction in intensity but increased severity in Mzuzu revealed earlier is attributed to the increase in drought duration as the number of droughts remain unchanged. Compared to the near future, drought will occur more frequently in the far future even though their severity, duration and intensity might reduce more under SSP2.

Table 4.13: Change in long-term meteorological drought duration and number of droughts

Station	Duration				Drought Runs			
	SSP2-2021	**SSP2-2051**	**SSP5-2021**	**SSP5-2051**	**SSP2-2021**	**SSP2-2051**	**SSP5-2021**	**SSP5-2051**
Bolero	92%	20%	69%	44%	-4	0	-2	-1
Karonga	20%	-26%	-11%	-15%	-4	0	1	2
Mzimba	14%	-18%	-11%	-17%	-2	2	2	-1
Mzuzu	27%	8%	5%	8%	-1	0	3	0
Nkhatabay	1%	-28%	-7%	-13%	-2	1	1	-2

The spatial SPE12 analysis of drought frequency shift (Figure 4.27) discloses a nearly 300% increment in the frequency of moderate and severe droughts over the central area of Northern Malawi during SSP5 as the frequency of drought increases by an additional 0.64-0.78 from 0.065-0.078 and 0.002-0.04, respectively. Furthermore, a larger area will experience an increase in moderate drought during the near-future SSP5 scenario than SSP2. The subsequent reduction in area affected by increasing drought frequency could be due to the higher increment in rainfall during the far future SSP5 scenario (Oguntundea, Abiodunc, & Lischeid, 2017). Comparatively, under SSP2 scenario a higher reduction in severe drought frequency is noted in the north and southern areas of Northern Malawi than in SSP5, even though a greater decline in mean annual precipitation is expected. A possible factor for this is the lower temperature increment during SSP2-4.5 than SSP5-8.5. Notably, the study reveals extreme drought conditions become more frequent under the SSP2 scenario in the near-term to mid-century whilst SSP5 portrays a -0.6% -0.8% change in extreme drought occurrence. Moreover, in the far future, areas of increase and decrease in extreme drought frequency are inverted with north and south areas experiencing a decline and increase in SSP5-8.5 and the opposite scenario under SSP2-4.5. Even though the south-east area experiences the highest increase in average annual precipitation, an increase in extreme drought frequency is observed which could impact the region severely. The shift in areas prone to extreme drought towards the north and south areas depict a homogeneous drought hazard risk would occur during the near-future SSP2 over Northern Malawi. Similar observations are noted for the moderate and severe drought cases when compared to Figure 4.17: Map of historical meteorological drought frequency (SPEI12).

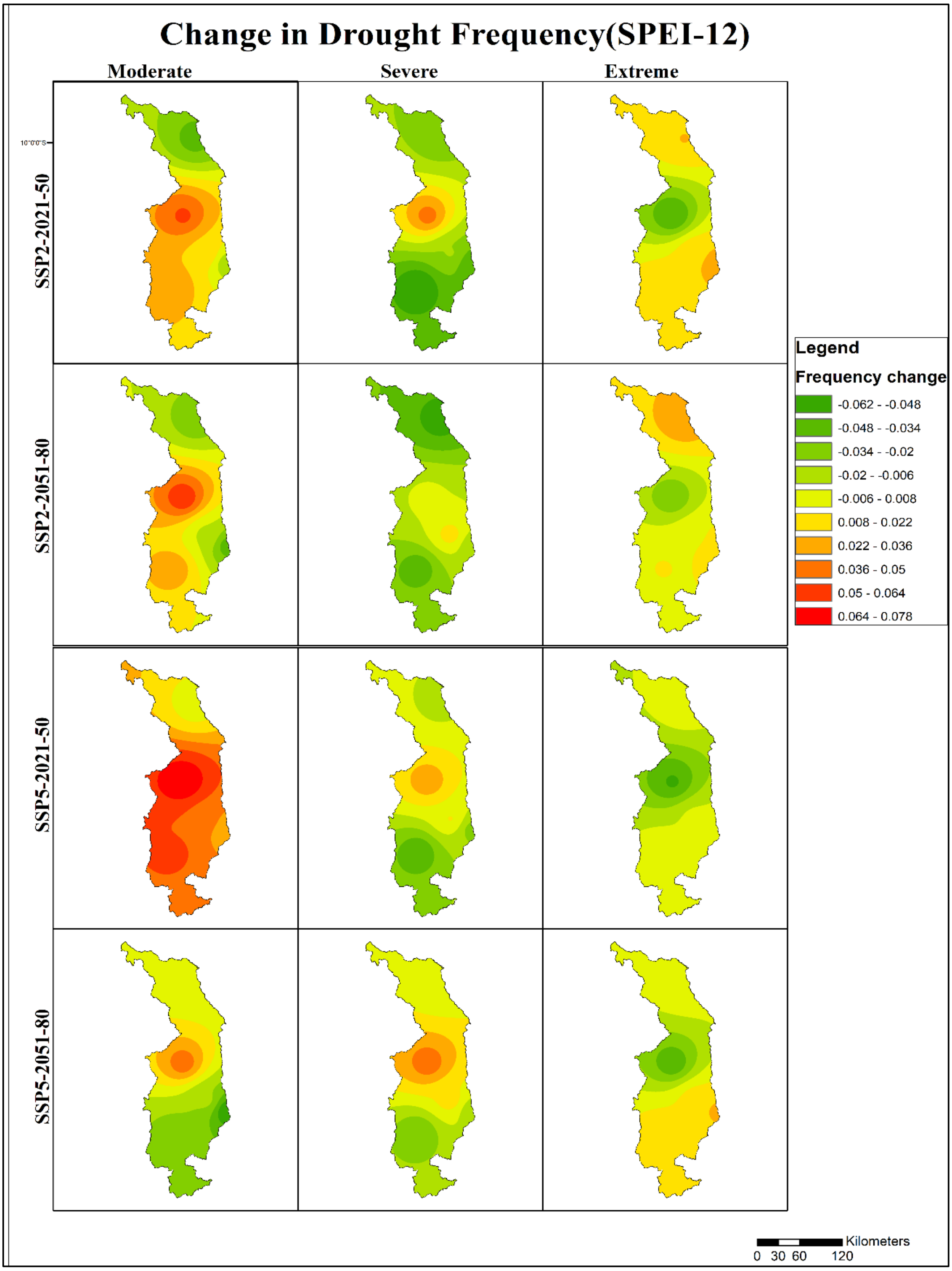

Figure 4.27: Projected changes in long-term meteorological drought frequency.

4.4 Implications of findings

The analysis revealed the spatio-temporal trends of rainfall and temperature over the study area. Interestingly, the areas closer to Lake Malawi exhibit high annual and monthly rainfall values as compared to Bolero and Mzimba which are more inland. This supports the idea that

Lake Malawi has a notable influence on the precipitation pattern via its influence over moisture and atmospheric circulation over Northern Malawi (Diallo, Giorgi, & Stordal, 2018) . The trend over Northern Malawi reveals the regional variability with Mzuzu and Nkhatabay experiencing decreasing rainfall whilst other areas experience an increment in annual rainfall. This depicts a possible impact of other underlying local factors over the climate such as topography or land-use cover change. The higher increment in minimum temperatures observed over the stations could be a possible factor to the decrement in rainfall as this is one of the similar climatic points observed in the two stations. The higher Sen's slope values of minimum temperature compared to maximum temperature underscores warming nighttime regimes, although Karonga portrays cooler night-time conditions due to its decreasing trend. The extremely lower maximum temperature increase over Mzuzu is more likely due to existing local factors as opposed to regional influences.

Futuristically, the rainfall over Northern Malawi is projected to experience increments during the rainy season with exceptions in March and April, although rainfall suppression is expected to occur during the dry season. The SSP5-8.5 scenario exhibits a constant increment in rainfall through near-term until end-century whilst SSP2-4.5 exhibits a near-term decrement in rainfall with an increment occurring in the mid-century to end-century period. Nonetheless, compared to the historical climate records, the mid-century to end-century climatic rainfall over a large expanse of Northern Malawi is projected to decline under SSP2 whilst an increase is expected under SSP5-8.5. This increment is most likely due to the higher temperature increment under the SSP-8.5 scenario, but such conditions pose a threat of recurring heatwaves over Northern Malawi. The higher maximum and minimum temperature noted under the high emissions emphasize the influence of greenhouse gas emissions on global warming trends. Warmer nighttime temperatures are expected to persist under both SSP2 and SSP5 scenarios as the rise in minimum temperatures is higher than the maximum temperature. Additionally, the slower rise in temperature combined with a higher increment in precipitation in the mid-century to end of century underscores the importance of undertaking the middle road scenarios as opposed to the high emissions scenario. Trend analysis reveals that temperature trends are found to be significant as compared to rainfall trends which are found to be insignificant agreeing with (Kambombe, Ngongondo, Eneya, Monjerezi, & Boyce, 2021).

The historical drought obtained from analysis of climate records portrays that drought cases are spatially heterogeneous across the area. Remarkably, even though drought occurrence is found to be highest during the 21st century (2000-2017) across Northern Malawi, Bolero portrays a decrease in drought severity with the most extreme drought occurring in the 20th century. This is possibly an impact of increasing annual rainfall over Bolero combined with a comparatively lower rise in temperature. Notably, in contrast to the 20th century precipitation increment over Northern Malawi, a decline in 21st century precipitation was observed by (Tadeyo, Chen, Ayugi, & Yao, 2020), which supports the increasing drought severity noted in the other stations. The alternating wet to dry episodes observed over Mzimba are likely due to the influence of ENSO over the area leading to variable rainfall conditions. The capturing of the 2005/6 and 2015/16 ENSO drought cases across all the stations portrays the ability of SPEI to capture the influence of climatic drivers on drought.

Interestingly, it can be argued that areas of high precipitation tend to have a lower drought occurrence as high precipitation areas Mzuzu and Nkhatabay record the lowest drought cases of 17 and 16, respectively than Mzimba (21). However, Nkhatabay records the longest duration of drought supporting the idea that humid regions of high temperature and decreasing rainfall trend are prone to droughts of extended duration. The high duration observed with long-term drought when compared to season drought over the area which highlights the areas proneness to hydrological issues. The correlation between meteorological drought and hydrological droughts in semi-arid regions like Northern Malawi is found to be high and more so at timescales of SPEI12 than SPEI6 (Salimi, Asadi, & Darbandi, 2021). Thus, even though the long-term drought occurs lesser than seasonal droughts, their impact of the hydrological balance over Northern Malawi should not be ignored. Similarly to (Hadri, et al., 2024), the areas in the shores of Malawi exhibit a lower drought recurrence when compared to the more inland locations, particular under extreme drought. Opposingly, moderate and severe drought cases follow a different pattern highlighting that regions of prone to extreme drought are not the same ones prone to these drought classes.

In the near-term to mid-century, the findings highlight increasing severity of drought cases particularly during the mid-century under both scenarios, although moderate drought cases are expected to be longer during near-term. Compared to the historical drought, a slightly homogenous future drought occurrence is noted over the area with the major difference being the duration, intensity and severity of said drought. These differences highlight the influence of the temperature and precipitation values over underlying drought conditions whilst the homogeneity is due to the similarity in trend. The mid-century period (2040-2050) depicts an increase in drought severity with longer duration under SSP2-4.5, particularly for long-term drought. The shorter duration of wet periods depicts a possible singular extended drought run as argued by (Kumalioglu, 2020). In their study of drought, they noted that wet periods shorter than 6-months are inadequate for recovery of the climatic water balance and in such scenarios, consecutive drought durations need to be treated as a singular drought run. Notably, drought conditions over SSP5-8.5 occur alternatingly with wet periods, although longer dry duration followed by similarly longer wet episodes are observed during this scenario.

Opposed to the reduction in drought severity under SSP2-4.5 as the end-century approaches, the SSP5 scenario leads to increased drought severity and intensity over the area. This supports the idea (Behzadi, et al., 2024) that precipitation increment is not the only factor that leads to drought severity as rainfall is projected to increase in both scenarios. The only notable difference is the high temperature increment over Northern Malawi under SSP5 as compared to SSP2. Interestingly, the 2061-68 period depicts the highest severity and recurring droughts for Mzuzu, Nkhatabay and Mzimba under the SSP2-4.5 scenario whilst a different scenario of increased wetness is observed under SSP5-8.5. This denotes that drought projections are highly variable, and care must be taken when planning for future drought conditions under climatic projections. Additionally, this results also reveal the impacts of different socio-economic pathways on the climate and indirectly over Northern Malawi drought. The occurrence of severe drought conditions during 2040-2070 calls for a more thorough analysis into its implications over the agricultural and hydrological areas in Northern Malawi. The alternating dry and wet periods observed in future decades also need further assessment of their impact towards the livelihood, development and disaster risk management strategies.

Additionally, the analysis revealed the contrast in drought characteristics of future drought conditions with historical drought cases with more drought runs projected to occur over Northern Malawi. The underlying shifts present the importance of choosing the middle road scenario and undertaking climate mitigation as opposed to continuing high emissions of greenhouse gases (GHG). The shifts in drought severity and increased proneness of drought over Northern Malawi requires localized effort combined with government strategical approach as the drought hotspots shift from a single locale to being widespread. Interestingly, there is an observable heterogeneity in changes of meteorological drought characteristics with some stations experiencing a lower decrement in drought severity and intensity than other stations. This highlights the need for localized approach when undertaking locally focused drought assessment. Furthermore, the differing shifts in drought under seasonal and long-term under each climate scenario depicts the importance of analyzing drought under the Shared Socio-economic pathways. The spatial analysis of climate and drought have portrayed the meteorological drought hotspots under its classification which is a vital consideration in drought risk management. Moreover, the spatial shifts in precipitation, maximum and minimum temperature tend to coincide with the shifts in the moderate and severe drought frequency. Higher drought frequency increments are observable in areas of decreasing precipitation and increasing temperature with some slighter spatial discrepancies.

5 CONCLUSION AND RECOMMENDATIONS

The study focused on assessing the future characteristics of meteorological drought over Northern Malawi under the Shared Socio-economic pathways. Two scenarios, SSP2-4.5 and SSP5-8.5 were the scenarios considered as the portray the middle road and extreme case scenario of zero climate migration efforts. An analysis of 1991-2020 monthly rainfall and temperature revealed that higher temperatures and rainfall tend to occur with the months of November to April whilst lower temperatures and rainfall dominate the months of May – October. Furthermore, the trend slope of annual rainfall over Northern Malawi showed that there was significant and non-significant decreasing and increasing trends dependent on station, implying the influence of local topography and other factors on local precipitation. The trend analysis of annual temperature revealed significant increase in temperature for all stations within Northern Malawi with Karonga being a rare case of decreasing minimum temperature, which highlight increasing evapotranspiration.

The projections from statistically downscaled CMIP6 climate model simulations for 2021-80 climate over Northern Malawi showed that change in rainfall is not heterogenous. Climatic annual precipitation would decrease in some areas, particularly under SSP2-4.5 even though monthly rainfall would increase in some months of the rainy season, such as November – February. Spatially, northern Malawi would experience a higher decrease in rainfall under SSP2 whilst an increase of nearly 119mm would occur under SSP5 depicting changes in the water balance and possible occurrence of water hazards such as floods. Higher increment in average maximum and minimum temperature under SSP5 combined with a steeper rising trend slope, depicts increased evapotranspiration, and potential exposure to heatwaves, particularly over central Northern Malawi. The future maximum and minimum temperature was found to be 0.73-1.8°C, and 0.82-2.05°C under SSP2 and 0.85-2.51°C under SSP5.

The overview of the 1991-2020 historical droughts revealed contrasting results in drought occurrence with some stations revealing 2000-2020 as the period with most droughts and some revealing 1990s. Although the difference was mostly due to the different rainfall and temperature pattern over the area, particularly on the trend direction of rainfall. Long-term drought(12-month) was observed to occur for nearly double the duration of medium-term(6-month) with higher intensity over some areas. Projections of future drought conditions revealed contrasting results depending on the scenario and stations of interest. Temporally, there were observable differences between SSP2 and SSP5 in their drought periods, intensity and severity. SSP5 projected continuous shifting of drought and wet periods throughout each decade whilst

SSP2 displayed that drought would occur predominately during 2040s-2060s across Northern Malawi. Furthermore, the assessment revealed longer duration and intense long-term droughts than medium-term even though their number would continue to be less.

The study concludes that there were notable spatial differences in the drought frequency of moderate, severe and extreme droughts across Northern Malawi with moderate drought being more common, historically. The central zone depicted proneness to extreme droughts whilst the northern and southern areas were found to be more prone to moderate and severe droughts. Futuristically, a shift in frequency was observed with drought prone areas experiencing a decrease in frequency of drought dependent on the drought class with areas prone to moderate becoming prone to extreme droughts. Thus, homogeneity in drought frequency is projected with drought occurrence increasing across the area, especially if no climate mitigation is conducted. Additionally, the shifts in drought severity, intensity and duration were revealed to be vastly different based on scenario and timeframe. However, the SSP2 scenario projected a reduction in drought intensity and severity compared to SSP5, particularly under long-term drought.

Furthermore, the study has shown notably varying interactions of future rainfall, and temperature with meteorological drought across Northern Malawi. The study observed that an increase in drought intensity and severity was discovered under the SSP2 in the near-term to mid-century as a result of the decreasing annual rainfall. Likewise, the higher increase in temperature resulted in increased drought severity under SSP5 but in some stations, a greater reduction in drought severity was observed possibly driven by the rainfall increment. The study was limited to monthly and annual shifts and did not account for potential changes in rainfall and temperature extremes, land-use and land cover change, and water management which can influence meteorological drought.

5.1 Recommendations

The study has depicted the changes in future drought characteristics, temperature and rainfall across the area, including the areas with high drought levels. Thus, it is recommended that a shift in disaster risk management strategies is needed to properly mitigate and reduce their impacts. Disaster relief stakeholders such as the Department of Disaster Management Affairs, have to upscale their projects to consider region-wide responses as the drought frequency has shown propagation. Effort towards mitigating the risk of increasing drought severity and temperature on the agriculture should be considered by the Ministry of Agriculture. High drought exposure combined with high temperatures would result in decreased yields, especially in cereal type crops such as maize. The increase in duration of drought especially, long-term calls for Malawi's government to implement water management strategies that could reduce the impacts of drought on water bodies in the area. The Department of Meteorological and Climate Services in collaboration with other stakeholders needs to increase the number of stations within the Northern Malawi so as to improve the accuracy in drought observations. The level of awareness and early warning systems should be increased as increased temperature would result in higher risk of exposure towards heatwaves. Furthermore, climate mitigation strategies, such as low carbon development plans, should be upscaled and promoted to reduce the occurrence of the SSP5 scenario.

5.2 Future study recommendations

The study assessed the future drought characteristics but there were some limitations to the study that future studies should aim to address. For instance, future studies could analyze the impacts of changes in rainfall and temperature extremes on the meteorological drought. Furthermore, an insight into the influence of daily rainfall and dry spells on meteorological drought could prove vital to assessing other drought types such as flash meteorological droughts. Understanding of the impacts of urbanization and climate change on drought conditions could be another area of focus to help give insight into the relationship between drought, urbanization and climate change. Additionally, projections using other scenarios can be considered to provide a wider range of the plausible drought conditions. As the results found can be argued to be prone to model biases even though measures were taken to minimize them, it is also recommended that future studies consider undertaking comparative studies using additional models and different downscaling techniques, or other methods such as machine learning to predict the future characteristics over Northern Malawi.

6 REFERENCES

Abiodu, B. J., Makhanya, N., Petja, B., Abatan, A. A., & Oguntunde, P. G. (2018). Future projection of droughts over major river basins in Southern Africa at specific global warming levels. *Theoretical and Applied Climatology*.

Almazroui, M., Saeed, F., Saeed, S., Islam, M. N., Ismail, M., Klutse, N. A., & Siddiqui, M. H. (2020). Projected Change in Temperature and Precipitation Over Africa from CMIP6. *Earth Systems and Environment, 4*, 455–475. doi:10.1007/s41748-020-00161-x

Amosi, N., & Anyah, R. (2024). Trends of precipitation and temperature extremes over Malawi and Mozambique during the recent decades from models and observations. *Theoretical and Applied Climatology , 155*, 783–804. doi:10.1007/s00704-023-04659-y

Ayugi, B., Eresanya, E. O., Onyango, A. O., Ogou, F. K., Okoro, E. C., Okoye, C. O., . . . Ongoma, V. (2022). Review of Meteorological Drought in Africa: Historical Trends, Impacts, Mitigation, Measures and Prospects. *Pure and Applied Geophysics, 179*, 1365–1386.

Ayugi, B., Shilenje, Z., Babaousmail, H., Lim Kam Sian, K., Mumo, R., Dike, V., . . . Ongoma, V. (2022). Projected changes in meteorological drought over East Africa inferred from Bias-adjusted CMIP6 models. *Natural Hazards*, 1151-1176. doi:10.1007/s11069-022-05341-8

Beck, H. E., McVicar, T. R., Vergopolan, N., Berg, A., Lutsko, N. J., Dufour, A., . . . Miralles, D. G. (2023). High-resolution (1 km) Köppen-Geiger maps for 1901–2099 based on constrained CMIP6 projections. *Scientific Data , 10*. doi:10.1038/s41597-023-02549-6

Bedair, H., Alghariani, M. S., Omar, E., Anibaba, Q. A., Remon, M., Bornman, C., . . . Alzain, H. M. (2023). Global Warming Status in the African Continent: Sources, Challenges, Policies, and Future Direction. *International Journal of Environmental Research, 17*.

Behrangi, A., Loikith, P. C., Fetzer, E. J., Nguyen, H. M., & Granger, S. L. (2015). Utilizing Humidity and Temperature Data to Advance Monitoring and Prediction of Meteorological Drought. *Climate, 3*, 999-1017. doi:10.3390/cli3040999

Behzadi, F., Javadi, S., Yousefi, H., Shahdany, S. M., Moridi, A., Neshat, A., . . . Maghsoudi, R. (2024). Projections of meteorological drought severity-duration variations based on CMIP6. *Scientific Reports, 14*. doi:10.1038/s41598-024-55340-x

Caretta, M., Mukherji, A., Arfanuzzaman, M., Betts, R., Gelfan, A., Hirabayashi, Y., . . . Supratid, S. (2022). Water. In H.-O. Pörtner, D. Roberts, M. Tignor, E. Poloczanska, K. Mintenbeck, A. Alegría, . . . S. Löschke (Eds.), *Climate Change 2022: Impacts, Adaptation and Vulnerability.Contribution of Working Group II to the Sixth Assessment Report of the Intergovernmental Panel on Climate Change* (pp. 551-712). Cambridge, United Kingdom: Cambridge University Press,.

Chabvungma, S., Mawenda, J., & Kambauwa, G. (2014). Drought Conditions and Management Strategies in Malawi. *Eastern and Southern African Workshop on Capacity Development to support National Drought Management Policy*. Retrieved from https://www.droughtmanagement.info/wp-content/uploads/2016/01/Malawi.pdf

Chauluka, F., Singh, S., & Kumar, R. (2020). Rainfall and streamflow trends of Thuchila River, Southern Malawi. *Materials Today: Proceedings*.

Chen, F.-W., & Liu, C.-W. (2012). Estimation of the spatial rainfall distribution using inverse distance weighting (IDW) in the middle of Taiwan. *Paddy and Water Environment*. doi:10.1007/s10333-012-0319-1.

Chikabvumbwa, S. R., Salehnia, N., Gholami, A., Kolsoumi, S., Mirzadeh, S. J., & Hoogenboom, G. (2024). Characterization of hydro-meteorological droughts based on dynamic future scenarios and effective rainfall over Central Malawi. *Theoretical and Applied Climatology, 155*, 1959–1975.

Chitedze, I., & Chikabvumbwa, S. R. (2021). Assessing the Impact of Spatio-temporal Drought Regimes Using Timescale Standardized Precipitation Index in Malawi. *Journal of Sustainable Development of Energy, Water and Environment Systems, 9*(4).

Choudhury, A., Dutta, D., Bera, D., & Kundu, A. (2021). Regional variation of drought parameters and long-term trends over India using standardized precipitation evapotranspiration index. *Journal of Environmental Management, 296*.

Collados-Lara, A.-J., Gómez-Gómez, J.-d.-D., Pulido-Velazquez, D., & Pardo-Igúzquiza, E. (2022). An approach to identify the best climate models for the assessment of climate change impacts on meteorological and hydrological droughts. *Natural Hazards and Earth System Science, 22*(2), 599-616. doi:10.5194/nhess-22-599-2022

Dai, A. (2013). Increasing drought under global warming in observations and models. *Natural Climate, 3,* 52-58.

Demissie, T., & Gebrechorkos, S. H. (2024). Spatio-Temporal Trends in Precipitation, Temperature, and Extremes: A Study of Malawi and Zambia (1981–2021). *Sustainability, 16*, 3885-3893. doi:10.3390/su16103885

Diallo, I., Giorgi, F., & Stordal, F. (2018). Influence of Lake Malawi on regional climate from a double-nested regional climate model experiment. *Climate Dynamics, 50,* 3397–3411. doi:10.1007/s00382-017-3811-x

Dinku, M. B., & Gibre, A. M. (2024). Comparison of bias correction methods to regional climate model simulations for climate change projection in Muger Subbasin, Upper Blue Nile Basin, Ethiopia. *Journal of Water and Climate Change, 15*(6), 2612–2627. doi:10.2166/wcc.2024.591

Dione, P. M., Faye, C., & Sadio, C. A. (2023). Hydrological Impacts of Climate Change(Rainfall and Temperature) and Characterization of Future Drought in the Aga Foua Dijas Watershed. *Indonesian Journal of Socila and Environmental Issues, 4*(3), 353-375.

Dix, M., Bi, D., Dobrohotoff, P., Fiedler, R., Harman, I., Law, R., . . . Williams. (2019). CSIRO-ARCCSS ACCESS-CM2 model output prepared for CMIP6 ScenarioMIP. *Earth System Grid Federation*. doi:10.22033/ESGF/CMIP6.2285

Ebedi-Nding, D., Tamoffo, A., & Mouassom, F. (2024). Extremes events and socio-economic impacts in central Africa: a CMIP6-based analysis of projections. *Modeling Earth Systems and Environment, 10*, 6575–6598.

En-Nagre, K., Aqnouy, M., Ouarka, A., Naqvi, S. A., Bouizrou, I., Messari, J. E., . . . El-Askary, H. (2024). Assessment and prediction of meteorological drought using machine learning algorithms and climate data. *Climate Risk Management*. doi:10.1016/j.crm.2024.100630

Feyissa, G., Zeleke, G., Bewket, W., & Gebremariam, E. (2018). Downscaling of Future Temperature and Precipitation Extremes in Addis Ababa under Climate Change. *Climate, 6*(3). doi:10.3390/cli6030058

Gama, A. C., Mapemba, L. D., Masikat, P., Tui, S. H.-K., Crespo, O., & Bandason, E. (2014, September). Modeling potential impacts of future climate change in Mzimba District Malawi, 2040-2070. *IFPRI Working Paper 08*.

Gan, T., Ito, M., Hulsmann, S., Qin, X., Lin, X. X., Liong, S. Y., . . . Koivusalo, H. (2016). Possible climate change/variability and human impacts, vulnerability of drought-prone regions, water resources and capacity building for Africa. *Hydrological Sciences, 2016*.

GFDRR. (2019). *Disaster Risk Profile: Malawi.* Washington: The World Bank.

Gizaw, M. S., & Gan, T. Y. (2017). Impact of climate change and El Niño episodes on droughts in sub-Saharan Africa. *Climate Dynamics, 49*, 665–682.

Gondwe, M. F., Chirwa, P. W., & Geldenhuys, C. J. (2019). Land use land cover change and the comparative impact of co-management and government-management on the forest cover in Malawi (1999-2018). *https://www.tandfonline.com/journals/tlus20, 14*(4).

Government of Malawi. (2019). *2018 Population and Housing Census.* National Statistics Office.

Hadri, A., Ndiaye, A. S., Khadir, L., Jaffar, O., Zamzami, H. A., El Khalki, E. M., . . . Chehbouni, A. (2024). Spatio-temporal analysis of meteorological drought return periods in a Mediterranean arid region, the center of Morocco. *Journal of Water and Climate Change, 15*(9), 4573-4595.

Hargreaves, G. (1994). Defining and Using the Reference Evapotranspiration. *Journal of Irrigation and Drainage Engineering, 120*(6), 1132–1139. doi:10.1061/(asce)0733-9437(1994)120:6(1132)

Hellwig, J., Stahl, K., Ziese, M., & Becker, A. (2018). The impact of the resolution of meteorological data sets on catchment-scale precipitation and drought studies. *International Journal of Climatology*.

Henchiri, M., Igbawua, T., Javed, T., Bai, Y., Zhang, S., Essifi, B., . . . Zhang, J. (2021). Meteorological Drought Analysis and Return Periods over North and West Africa and Linkage with El Niño–Southern Oscillation (ENSO). *Remote Sensing, 13*(23). doi:10.3390/rs13234730

Hoell, A., Gaughan, A. E., Magadzire, T., & Harrison, L. (2021). The Modulation of Daily Southern Africa Precipitation by El Niño–Southern Oscillation across the Summertime Wet Season. *Journal of Climate, 34*(3), 1115–1134. doi:10.1175/JCLI-D-20-0379.1

Huang, S., Zhang, H., Liu, Y., Liu, W., Wei, F., Yang, C., . . . Chen, Y. (2024). Assessment of Hydrological and Meteorological Composite Drought Characteristics Based on Baseflow and Precipitation. *Water, 16*. doi:10.3390/w16111466

IDMP. (2022). *Drought and Water Scarcity.* Geneva, Switzerland: Global Water Partnership and World Meteorological Organization.

IPCC. (2022). Annex II: Glossary. In V. Möller, R. van Diemen, J. Matthews, C. Méndez, S. Semenov, & J. Fuglestvedt (Eds.), *Climate Change 2022: Impacts, Adaptation and Vulnerability. Contribution of Working Group II to the Sixth Assessment Report of the Intergovernmental Panel on Climate Change* (pp. 2897–2930). Cambridge, UK: Cambridge University Press. doi:10.1017/9781009325844.029

IPCC. (2023a). Glossary. In H. Lee, & J. Romero (Eds.), *Climate Change 2023: Synthesis Report. Contribution of Working Groups I, II and III to the Sixth Assessment Report of the Intergovernmental Panel on Climate Change.* Geneva, Switzerland: IPCC.

IPCC. (2023b). Sections. In H. Lee, & J. Romero (Eds.), *Climate Change 2023: Synthesis Report. Contribution of Working Groups I, II and III to the Sixth Assessment Report of the Intergovernmental Panel on Climate Change* (pp. 35-115). Geneva, Switzerland: IPCC. doi:10.59327/IPCC/AR6-9789291691647

Irish Aid. (2017). *Malawi Climate Action Report 2016.* Resilience and Economic Inclusion Team. Irish Aid.

Jaya, M., Ruchjana, B. N., Abdullah, A. S., & Andriyana, Y. (2021). Comparison of IDW and GP models with application to spatiotemporal interpolation of rainfall in Bali

Province, Indonesia. *Journal of Physics: Conference Series*. doi:10.1088/1742-6596/1722/1/012080
Kamal, A. S., Hossain, F., & Shahid, S. (2021). Spatiotemporal changes in rainfall and droughts of Bangladesh for1.5 and 2 °C temperature rise scenarios of CMIP6 models. *Theoretical and Applied Climatology*. doi:10.1007/s00704-021-03735-5
Kamanga, T. F., Tantanee, S., Mwale, F. D., & Buranajarukorn, P. (2020). A Multi Hazard Perspective In Flood And Drought Vulnerability: Case Study Of Malawi. *Geographia Technica, 15*(1), 132-142.
Kambombe, O., Ngongondo, C., Eneya, L., Monjerezi, M., & Boyce, C. (2021). Spatio-temporal analysis of droughts in the Lake Chilwa Basin, Malawi. *Theoretical and Appiled Climatology, 144*, 1219–1231.
Kocsis, T., Kovács-Székely, I., & Anda, A. (2020). Homogeneity tests and non-parametric analyses of tendencies in precipitation time series in Keszthely, Western Hungary. *Theoretical and Applied Climatology, 139*, 849-859. doi:10.1007/s00704-019-03014-4
Kubiak-Wójcicka, K., Owczarek, M., Chlost, I., Olszewska, A., & Nagy, P. (2023). Assessment of Meteorological Drought Trends in a Selected Coastal Basin Area in Poland—A Case Study. *Water, 15*(15). doi:10.3390/w15152836
Kumalioglu, A. A. (2020). Characterizing meteorological and hydrological drought droughts:A case study of the Gediz River Basin, Turkey. *Meteorological Applications, 27*(1). doi:10.1002/met.1857
Kumbuyo, C. P., Yasuda, H., Kitamura, Y., & Shimizu, K. (2014). Fluctuation of rainfall time series in Malawi: An analysis of selected areas. *Geofikiza, 31*.
Kumwenda, L., Kumambala, P. G., Fiwa, L., Chipula, G., Phiri, S., Kachali, R., & Mfune, S. M. (2024). Projected Drought Prevalence in Malawi's Lufilya Catchment: A Study Using Regional Climate Models and the SPI Method. *Water, 16*(24). doi:10.3390/w16243548
Lee, J.-Y., Marotzke, J., Bala, G., Cao, L., Corti, S., Dunne, J., . . . Maycock, A. (2021). Future Global Climate: Scenario-based Projections and Near-term Information. In *Climate Change 2021: The Physical Science Basis. Contribution of Working Group I to the Sixth Assessment Report of the Intergovernmental Panel on Climate Change* (pp. 553–672). Cambridge: Cambridge University Press. doi:10.1017/9781009157896.006.
Lehner, F., Coats, S., Stocker, T. F., Pendergrass, A. G., Sanderson, B. M., Raible, C. C., & Smerdon, J. E. (2017). Projected drought risk in 1.5°C and 2°C warmer climate. *Geophysical Research Letters*, 7419-7425. doi:10.1002/2017GL074117
Li, J., Wang, Y., Li, Y., Ming, W., Long, Y., & Zhang, M. (2022). Relationship between meteorological and hydrological droughts in the upstream regions of the Lancang–Mekong River. *Journal of Water and Climate Change , 13* (2), 421–433.
Li, Y., Huang, Y., Li, Y., Zhang, H., Fan, J., Deng, Q., & Wang, X. (2024). Spatiotemporal heterogeneity in meteorological and hydrological drought patterns and propagations influenced by climatic variability, LULC change, and human regulations. *Scientific Reports , 14*.
Libanda, B., & Nkolola, N. B. (2019). Skill of CMIP5 models in simulating rainfall over Malawi. *Modeling Earth Systems and Environment*.
Likoya, E., Birch, C. E., Chapman, S., & Dougill, A. J. (2023). Austral summer droughts and their driving mechanisms in observations and present-day climate simulations over Malawi. *International Journal of Climatology, 43*(11), 5154-5176. doi:10.1002/joc.8137

Lim Kam Sian, K. T., Zhi, X., Ayugi, B. O., Onyutha, C., Shilenje, Z. W., & Ongoma, V. (2023). Meteorological Drought Variability over Africa from Multisource Datasets. *Atmosphere, 14*(6). doi:10.3390/atmos14061052

Lombe, P., Carvalho, E., & Rosa-Santos, P. (2024). Drought Dynamics in Sub-Saharan Africa: Impacts and Adaptation Strategies. *Sustainability, 16*(22). doi:10.3390/su16229902

Lu, J., Carbone, G. J., & Grego, J. M. (2019). Uncertainty and hotspots in 21st century projections of agricultural drought from CMIP5 models. *Scientific Reports*.

Mahesh, W., & Shahapure, S. (2023). Stastistical Downscaling for Evaluating Precipitation and Extremes for Bhima River Basin. *Journal of Harbin Engineering University, 44*(10), 152-164.

Maure, G., Pinto, I., Ndebele-Murisa, M., Muthige, M., Lennard, C., Nikulin, G., . . . Meque, A. (2018). The southern African climate under 1.5C and 2C of global warming as simulated by CORDEX regional climate models. *Environmental Research Letters, 13*.

Medeiros, G. C., & Silva, S. M. (2024). Propagation from Meteorological Drought to Hydrological Drought Using SPI and SPEI Combined with the Adapted Threshold Level Method. *EGUsphere*. doi:10.5194/egusphere-2024-813

Mehr, A. D., Sorman, A. U., Kahya, E., & Afshar, M. H. (2020). Climate change impacts on meteorological drought using SPI and SPEI: case study of Ankara, Turkey. *Hydrological Sciences Journal, 65*(2), 254-268. doi:https://doi.org/10.1080/02626667.2019.1691218

Mendez, M., Maathuis, B., Hein-Griggs, D., & Alvarado-Gamboa, L.-F. (2020). Performance Evaluation of Bias Correction Methods for Climate Change Monthly Precipitation Projections over Costa Rica. *Water, 12*(2). doi:10.3390/w12020482

Ministry of Natural Resources and Climate Change. (2023). *State of Malawi Climate in 2023.* Department of Climate Chnage and Meteorological Services. Blantyre: Department of Climate Chnage and Meteorological Services.

Mmame, B., & Ngongodo, C. (2024). Evaluation of CMIP6 model skills in simulating tropical climate extremes over Malawi, Southern Africa. *Modelling Eath Systems and Environment, 10*, 1695-1709.

Mohammed, R., & Scholz, M. (2023). Quality Control and Homogeneity Analysis of Precipitation Time Series in the Climatic Region of Iraq. *Atmosphere, 14*(197). doi:10.3390/atmos14020197

Mohammed, Y., Yimer, F., Tadesse, M., & Tesfaye, K. (2018). Meteorological drought assessment in north east highlands of Ethiopia. *International Journal of Climate Change Strategies and Management, 10*(1), 142-160. doi:10.1108/IJCCSM-12-2016-0179

Mtilatila, L., Bronstert, A., & Vormoor, K. (2022). Temporal evaluation and projections of meteorological droughts in the Greater Lake Malawi Basin, Southeast Africa. *Frontiers in Water*. doi:10.3389/frwa.2022.1041452

Mtilatila, L., Bronstert, A., Bürgera, G., & Vormoor, K. (2020). Meteorological and hydrological drought assessment in Lake Malawi and Shire River basins (1970–2013). *Hydrological Sciences Journal, 65*(16). doi:10.1080/02626667.2020.1837384

Muse, N. M., Tayfur, G., & Safari, M. J. (2023). Meteorological Drought Assessment and Trend Analysis in Puntland Region of Somalia. *Sustainability, 15*. doi:10.3390/su151310652

Muthiah, M., Sivarajan, S., Madasamy, N., Natarajan, A., & Ayyavoo, R. (2024). Exploring short- and long-term meteorological drought parameters in the Vaippar Basin of Southern India. *Scientific Reports, 14*.

Naik, M., & J., A. B. (2020). Projected changes in drought characteristics over the Western Cape, South Africa. *Meteorological Applications, 27*(1).

National Drought Mitigation Center. (n.d.). *Types of Drought*. Retrieved September 10th, 2024 , from National Drought Mitigation Center: https://drought.unl.edu/Education/DroughtIn-depth/TypesofDrought.aspx

Ndayiragije, J. M., & Li, F. (2022). Monitoring and Analysis of Drought Characteristics Based on Climate Change in Burundi Using Standardized Precipitation Evapotranspiration Index. *Water, 14*. doi:10.3390/w14162511

Ngwenya, M., & Simatele, M. D. (2024). Modeling future (2021–2050) meteorological drought characteristics using CMIP6 climate scenarios in the Western Cape Province, South Africa. *Modeling Earth Systems and Environment, 10*, 2957–2975.

O'Neill, B., Tebaldi, C., Vuuren, D., Eyring, V., Friedlingstein, P., Hurtt, G., . . . Sanderson, B. M. (2016). The Scenario Model Intercomparison Project (ScenarioMIP) for CMIP6. *Geoscientific Model Development, 9* , 3461–3482. doi:10.5194/gmd-9-3461-2016

Oguntundea, P. G., Abiodunc, B. J., & Lischeid, G. (2017). Impacts of climate change on hydro-meteorological drought over the Volta Basin, West Africa. *Global and Planetary Change, 155*, 121–132. doi:10.1016/j.gloplacha.2017.07.003

Onyeuwaoma, N., Sivakumar, V., & Bade, M. (2024). Modelling drought in South Africa: meteorological insights and predictive parameters. *Environmental Monitoring and Assessment, 196*. doi:10.1007/s10661-024-13009-y

Price, J., Warren, R., Forstenhäusler, N., Wallace, C., Jenkins, R., Osborn, T. J., & Vuuren, D. P. (2022). Quantification of meteorological drought risks between 1.5 °C and 4 °C of global warming in six countries. *Climate Change*. doi:10.1007/s10584-022-03359-2

Promping, T., & Tingsanchali, T. (2020). Meteorological Drought Hazard Assessment under Future Climate Change Projection for Agriculture Area in Songkhram River Basin, Thailand. *2020 International Conference and Utility Exhibition on Energy, Environment and Climate Change (ICUE)*, 1-7.

Qin, J., Su, B., Tao, H., Wang, Y., Huang, J., & Jiang, T. (2021). Projection of temperature and precipitation under SSPs-RCPs Scenarios over northwest China. *Frontier Earth Science, 15*(1), 23–37. doi:10.1007/s11707-020-0847-8

Salah, M., Mourst, F., Soliman, E., & Gamal, G. (2023). Assessing the potential impacts of climate change on droughts in East Africa using CORDEX-CORE regional climate models' simulations: A focus on Tanzania. *Geophysics and Geology, 53*(3), 271-300.

Salimi, H., Asadi, E., & Darbandi, S. (2021). Meteorological and hydrological drought monitoring using several drought indices. *Applied Water Science, 11*(11).

Samantaray, A. K., Ramadas, M., & Panda, R. K. (2020). Assessment Of Impacts Of Potential Climate Change On Meteorological Drought Characteristics At Regional Scales . *International Journal of Climatology*. doi:10.1002/joc.6687

Shiogama, H., Abe, M., & Tatebe, H. (2019). MIROC MIROC6 model output prepared for CMIP6 ScenarioMIP. *Earth System Grid Federation*. doi:10.22033/ESGF/CMIP6.898

Sidiqi, M., Kasiviswanathan, K., Scheytt, T., & Devaraj, S. (2023). Assessment of Meteorological Drought under the Climate Change in the Kabul River Basin, Afghanistan. *Atmosphere, 14*(570).

Song, Z., Q. F., Bao, Y., Shu, Q., Song, Y., & Yang, X. (2019). FIO-QLNM FIO-ESM2.0 model output prepared for CMIP6 CMIP. . *Earth System Grid Federation*. doi:10.22033/ESGF/CMIP6.9047

Spinoni, J. M., Bucchignani, E., Cassano, J., Cavazos, T., Christensen, J., Christensen, O., . . . K, L. (2020, May). Future global meteorological drought hotspots: a study based on CORDEX data. *Journal of Climate, 33*, 3635-3661. doi:10.1175/JCLI-D-19-0084.1

Sreeparvathy, V., & Srinivas, V. V. (2022). Meteorological flash droughts risk projections based on CMIP6 climate change scenarios. *npj Climate and Atmospheric Science, 5*.

Su, B., Huang, J., Mondal, S. K., Zhai, J., Wang, Y., Wen, S., . . . Aiwei, L. (2021). Insight from CMIP6 SSP-RCP scenarios for future drought characteristics in China. *Atmospheric Research, 250*.

Tadeyo, E., Chen, D., Ayugi, B., & Yao, C. (2020). Characterization of Spatio-Temporal Trends and Periodicity of Precipitation over Malawi during 1979–2015. *Atmosphere, 11*. doi:10.3390/atmos11090891

Tamura, M., Kumano, N., & Yokoki, H. (2019). Global assessment of the effectiveness of adaptation in coastal areas based on RCP/SSP scenarios. *Climate Change, 152*, 363-377.

Trisos, C., Adelekan, I., Totin, E., Ayanlade, A., Efitre, J., Gemeda, A., . . . Zakieldeen, S. (2022). Africa. In *limate Change 2022: Impacts, Adaptation and Vulnerability. Contribution of Working Group II to the Sixth Assessment Report of the Intergovernmental Panel on Climate Change* (pp. 1285–1455). Cambridge, United Kingdom: Cambridge University Press. doi:10.1017/9781009325844.011

Ukkola, A. M., Kauwe, M. G., Roderick, M. L., Abramowitz, G., & Pitman, A. J. (2020). Robust Future Changes in Meteorological Drought in CMIP6 Projections Despite Uncertainity in Precipitation. *Geophysical Research Letters, 47*(11).

Umwali, E. D., Chen, X., Ayugi, B. O., Mumo, R., Babaousmail, H., Mbigi, D., & Izere, D. (2024). Estimating the Effects of Climate Fluctuations on Precipitation and Temperature in East Africa. *Atmosphere, 15*. doi:10.3390/atmos15121455

UNDRR. (2021). *Global Assessment Report on Disaster Risk Reduction: Special Report on Drought 2021*. Geneva: United Nations Office for Disaster Risk Reduction.

USAID. (2019, March). Climate Risks in Food for Peace Geographies. *Climate Risk Profile*.

Vicente-Serrano, S. M., Begueria, S., & López-Moreno, J. I. (2010). A Multiscalar Drought Index Sensitive to Global Warming: The Standardized Precipitation Evapotranspiration Index. *Journal of Climate, 23*, 1696-1718.

Volodin, E., Mortikov, E., Gritsun, A., Lykossov, V., Galin, V., Diansky, N., . . . Emelina, S. (n.d.). INM INM-CM5-0 model output prepared for CMIP6 ScenarioMIP. *Earth System Grid Federation*. doi:10.22033/ESGF/CMIP6.12322

Wang, T., Tu, X., Singh, V. P., Chen, X., & Lun, K. (2021). Global data assessment and drought analysis of drought charactertistics based on CMIP6. *Journal of Hydrology, 596*.

Wang, Zhang, Q., Wang, J., Liu, Y., & Zhang, Y. (2021). Relationship between Drought and Precipitation Heterogeneity: An Analysis across Rain-Fed Agricultural Regions in Eastern Gansu, China. *Atmosphere, 12*(1274). doi:10.3390/atmos12101274

Wang, Zhang, X., Wang, S., Salahou, M. k., & Fang, Y. (2020). Analysi and Application if Drought Characteristics Based on Theory if Runs and Copula in Yunnan, Southwest China. *International Jourbak of Environment Resources Public Health, 17*(13). doi:10.3390/ijerph17134654

Warnatzsch, E. A., & Reay, D. S. (2019). Temperature and precipitation change in Malawi: Evaluation of CORDEX-Africa climate simulations for climate change impact assessments and adaptation planning. *Science of the Total Environment*, 378-392.

WMO & Global Water Partnership(GWP). (2016). Handbook of Drought Indicators and Indices. (M. Svoboda, & B. Fuchs, Eds.) *Integrated Drought Management Programme (IDMP),Integrated Drought Management Tools and Guidelines Series 2*.

WMO. (2023). *Guildelines on the Definition and Characterization of Extreme Weather and Climate Events* (2023 edition ed., Vol. 1310). Geneva, Switzerland: WMO.

World Meteorological Organization . (2021). *WMO Atlas of Mortality and Economic Losses from Weather, Climate and Water Extremes(1970-2019)* (Vol. 1267). Geneva, Switzerland: World Meteorological Organisation.

Yang, C., Liu, C., Wang, Y., Gu, Y., & Ma, X. (2023). Assessment of the spatiotemporal evolution and driving forces of meteorological drought in the North China Plain. *International Journal of Climatology*.

Yılmaz, B., Aras, E., & Nacar, S. (2024). A CMIP6-ensemble-based evaluation of precipitation and temperature projections. *Theoretical and Applied Climatology, 155,* 7377–7401.

Zhan, W., Guan, K., Sheffield, J., & Wood, E. F. (2016). Depiction of drought over sub-Saharan Africa using reanalyses precipitation data sets. *Journal of Geophysical Research: Atmospheres*. doi:10.1002/2016JD024858

Zhang, B., & Zhou, W. (2021). Spatial–Temporal Characteristics of Precipitation and Its Relationship with Land Use/Cover Change on the Qinghai-Tibet Plateau, China. *Land, 10,* 269. doi:10.3390/land10030269

Zhang, G., Zhang, Z., Li, X., Zheng, B., & Zhang, X. (2023). Evolution Characteristics of Meteorological Drought under Future Climate Change in the Middle Reaches of the Yellow River Basin Based on the Copula Function. *Water, 15*(2265). doi:10.3390/w15122265

Zuzani, P. N. (2019). Examining Trends of Hydro-Meteorological Extremes in the Shire River Basin in Malawi. *Physics and Chemistry*, 91-102.

7 Appendix

7.1 Homogeneity test

Precipitation

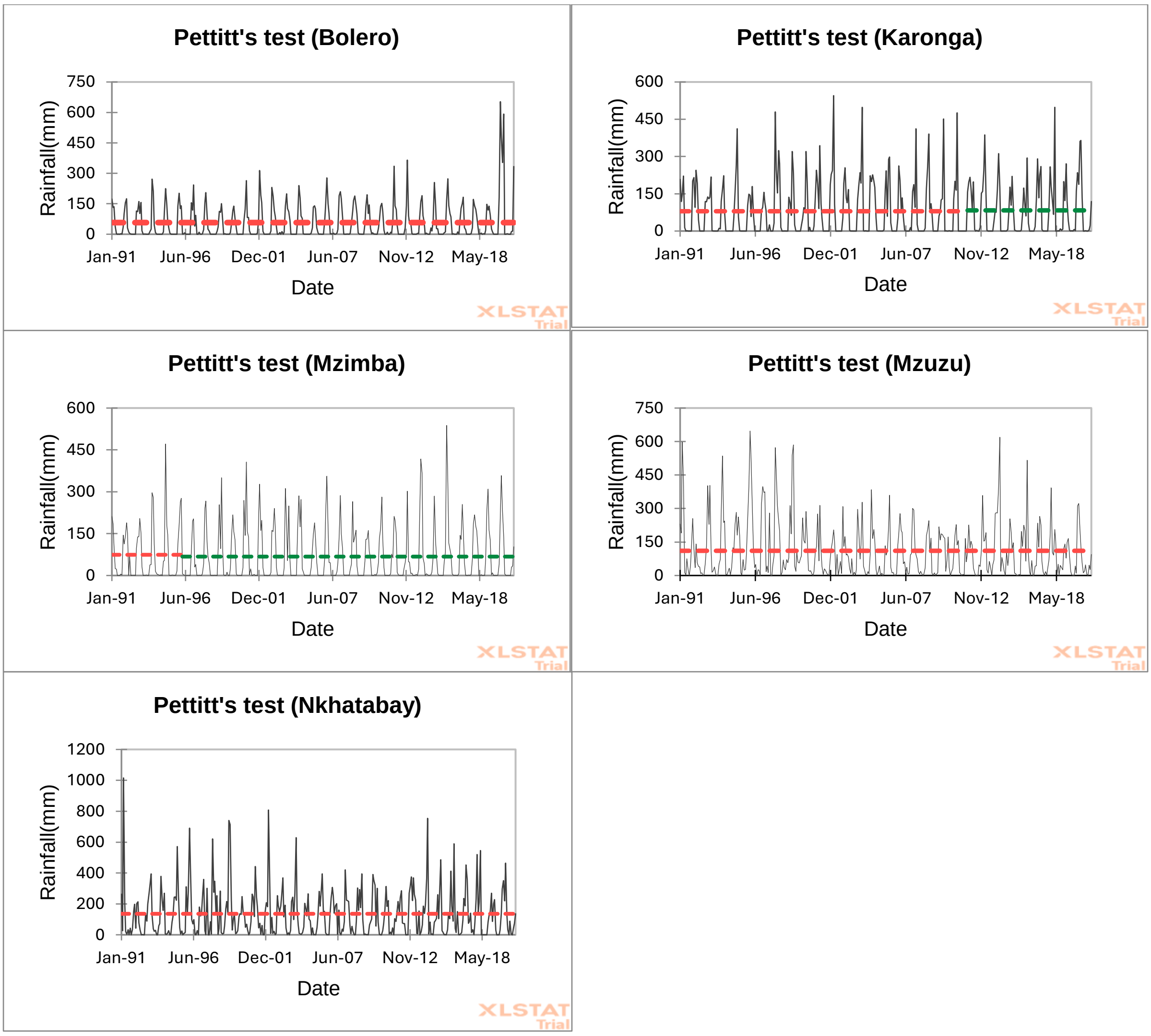

Figure 7.1: Pettitt test result for inter-month rainfall over Northern Malawi

Table 7.1: Pettit test results for 1991-2020 annual precipitation for each station

Station	P-value	Break point
Bolero	0.137	
Karonga	0.947	
Mzimba	0.667	
Mzuzu	0.033*	1999*
Nkhatabay	0.351	

* The data failed to be homogeneous at a 95% confidence interval

7.2 Downscaling method selection

	Access-CM5			FIOESM2=0			INM-CM5			MIROC6		
	D	E	Q	D	E	Q	D	E	Q	D	E	Q
Bolero												
Pr	7*	1	0	7*	1	1	8*	0	1	7*	1	0
Tasmax	2	2	5*	2	7*	2	2	7*	2	3	4	5*
Tasmin	8*	0	5	2	1	6*	7*	2	2	2	6*	2
Karonga												
Pr	7*	1	0	8*	1	1	7*	1	0	6*	2	0
Tasmax	3	7*	4	3	7*	3	2	2	7*	2	1	7*
Tasmin	2	1	8*	3	1	8*	3	1	8*	2	7*	2
Mzimba												
Pr	6*	2	1	8*	1	1	8*	1	1	7*	1	0
Tasmax	1	2	6*	3	3	7*	2	6*	3	3	2	7*
Tasmin	2	5*	4	2	1	7*	3	1	8*	2	6*	2
Mzuzu												
Pr	7*	1	0	2	1	7*	8*	1	1	1	0	7*
Tasmax	3	7*	2	2	6*	3	3	6*	2	3	2	7*
Tasmin	2	7*	2	2	7*	2	3	5*	2	2	7*	2
Nkhatabay												
Pr	6*	1	1	6*	0	3	8*	0	1	1	2	5*
Tasmax	7*	3	4	3	2	7*	2	6*	2	3	1	8*
Tasmin	4	5	7*	5	7*	2	2	6*	2	2	7*	2

Temperature

Table 7.2: Homogeneity of monthly maximum and minimum temperature (1991-2020)

	Max Temperature		Min Temperature	
Station	**P-value**	**Breakpoint**	**P-value**	**Breakpoint**
Bolero	0.116		0.273	
Karonga	0.072		0.029*	Apr-11
Mzimba	0.010*	Aug-02	0.003*	Sep-02
Mzuzu	0.008*	Aug-96	0.104	
Nkhatabay	0.043*	Aug-09	0.083	

* The data failed to be homogeneous at a 95% confidence interval

Table 7.3: 1991-2020 Annual maximum and minimum temperature's homogeneity results

	Max Temperature		Min Temperature	
Station	**P-value**	**Breakpoint**	**P-value**	**Breakpoint**
Bolero	0.000*	2004	<0.0001*	2008
Karonga	0.007*	2009	0.0002*	2011

Mzimba	<0.0001*	2002	<0.000*	2004
Mzuzu	0.086		0.0002*	2005
Nkhatabay	0.001*	2004	0.003*	2002

* The data failed to be homogeneous at a 95% confidence interval

7.3 Model bias correlation

Table 7.4: Pearson's coefficient of modelled against observed datasets.

Set	Pr	Tasmax	Tasmin
Observed	1	1	1
ACCESS-CM2	0.700	0.806	0.953
FIOESM2-0	0.808	0.890	0.964
INM-CM5-0	0.736	0.839	0.954
MIROC6	0.675	0.620	0.887
Ensemble	0.788	0.884	0.985
Ensemble (No MIROC6)	0.800	0.903	0.974
Weighted Ensemble	0.800	0.893	0.980
Weighted (No MIROC)	0.788	0.904	0.974